Accepted Manuscript

Alkyl indole-based cannabinoid type 2 receptor tools: Exploration of linker and fluorophore attachment

Anna G. Cooper, Christa Macdonald, Michelle Glass, Sarah Hook, Joel D.A. Tyndall, Andrea J. Vernall

PII: S0223-5234(17)30978-9

DOI: 10.1016/j.ejmech.2017.11.076

Reference: EJMECH 9951

To appear in: *European Journal of Medicinal Chemistry*

Received Date: 23 September 2017

Revised Date: 23 November 2017

Accepted Date: 26 November 2017

Please cite this article as: A.G. Cooper, C. Macdonald, M. Glass, S. Hook, J.D.A. Tyndall, A.J. Vernall, Alkyl indole-based cannabinoid type 2 receptor tools: Exploration of linker and fluorophore attachment, *European Journal of Medicinal Chemistry* (2017), doi: 10.1016/j.ejmech.2017.11.076.

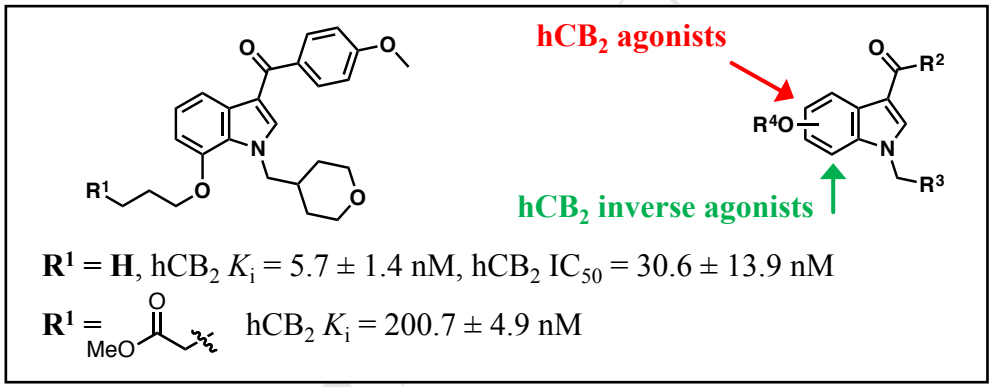

R¹ = H, hCB_2 K_i = 5.7 ± 1.4 nM, hCB_2 IC_{50} = 30.6 ± 13.9 nM

R¹ = MeO O ~ hCB_2 K_i = 200.7 ± 4.9 nM

Alkyl indole-based cannabinoid type 2 receptor tools: Exploration of linker and fluorophore attachment

Anna G. Cooper,[†] Christa Macdonald,[‡] Michelle Glass,[‡] Sarah Hook,[†] Joel D. A. Tyndall,[†] Andrea J. Vernall[†]*

[†] School of Pharmacy, University of Otago, Dunedin, New Zealand

[‡] Department of Pharmacology and Clinical Pharmacology, University of Auckland, Auckland, New Zealand

* School of Pharmacy, 18 Frederick Street, Dunedin 9054, New Zealand.

Ph: 64 3 479 4518

Email: andrea.vernall@otago.ac.nz

Abbreviations: BODIPY 630/650-X-OSu, 6-(((4,4-difluoro-5-(2-thienyl)-4-bora-3a,4a-diaza-s-indacene-3-yl)styryloxy)acetyl) aminohexanoic acid, succinimidyl ester; PEG, polyethylene glycol.

ABSTRACT

Cannabinoid type 2 (CB_2) receptor continues to emerge as a promising drug target for many diseases and conditions. New tools for studying CB_2 receptor are required to further inform how this receptor functions in healthy and diseased states. The alkyl indole scaffold is a well-recognised ligand for cannabinoid receptors, and in this study the indole C5-7 positions were explored for linker and fluorophore attachment. A new high affinity, CB_2 receptor selective inverse agonist was identified (**16b**) along with a general trend of C5-substituted indoles acting as agonists versus C7-substituted indoles acting as inverse agonists. The indole C7 position was found to be the most tolerant to linker extension and resulted in a high affinity inverse agonist with a medium length linker (**19**). Although a high affinity fluorescent ligand for CB_2 receptor was not identified in this study, the indole C7 position shows great promise for fluorophore or probe attachment.

KEYWORDS

Cannabinoid type 2 receptor

Cannabinoid

Fluorescent probe

Alkyl indole

G protein-coupled receptor

1. INTRODUCTION

Cannabinoid type 2 (CB_2) receptor is a member of the G protein-coupled receptor (GPCR) superfamily. GPCRs are the largest family of transmembrane signalling proteins in the human genome and a major therapeutic target [1]. CB_2 receptor, cannabinoid type 1 (CB_1) receptor, endocannabinoids and associated regulatory enzymes comprise the endocannabinoid system, which plays a key role in the regulation of various neurotransmitter systems [2]. CB_1 receptor is one of the most abundant receptors in the brain and plays a significant role in motivation and cognition [3]. In contrast, CB_2 receptor is mostly expressed on cells of the immune system and in lymphatic tissues, spleen and tonsils [4] and only at low levels in the central nervous system [5]. CB_2 receptor is crucial to immune system function, including modulation of cytokine release and immune cell migration [6, 7].

The cannabinoid (CB) receptors are potential drug targets in multiple pathologies, including CNS diseases (e.g. Alzheimer's disease), cancer, cardiovascular disease, drug addiction, pain, obesity and inflammatory disorders [8]. In particular, CB_2 receptor has been implicated in cancer [9] and inflammatory diseases such as neurodegenerative disorders [10], atherosclerosis [11] and inflammatory bowel disease [12]. In order to realise the potential of CB_2 receptor as a drug target to treat these conditions there is a need for more detailed knowledge of how this receptor functions in healthy and diseased states. Current tools available for studying CB_2 receptor include radioligands, covalent ligands and antibodies and whilst these have been used to study receptor localisation, structure and function, they all possess significant limitations in their utility [13]. Fluorescent ligands are powerful tools for studying receptor localisation, structure, dynamics and function in whole live cells [14]. Fluorescent ligands are adaptable to different assay and imaging systems, including high throughput screening [15], fluorescent resonance energy transfer [16], confocal microscopy, scanning confocal microscopy, flow cytometry and fluorescence correlation spectroscopy [17].

Whilst fluorescent ligands have been successfully designed for some other GPCRs [18], attempts at developing high affinity, selective CB_2 receptor fluorescent ligands for use in high resolution confocal imaging studies have been thwarted by high non-specific binding, limiting their utility as imaging tools [19-24]. A number of these fluorescent ligands for CB_2 receptor have been developed by conjugating varying fluorophores to a pharmacophore-

linker (mbc94) derived from SR144528 and of these, NIR760-mbc94 has been shown to identify CB_2 receptor mediated inflammation in a mouse model [25]. The challenge of developing a high affinity, selective CB_2 receptor fluorescent ligand with little non-specific membrane binding is increased further by the lipophilic nature of cannabinoids and many fluorescent dyes. Conjugation of a fluorescent dye to a pharmacophore introduces a large amount of steric bulk to the ligand, which can significantly alter the pharmacology and physicochemical properties compared to the unconjugated pharmacophore. Variation of site of linker attachment, linker length, linker composition and fluorescent dye choice can all influence affinity and efficacy of the probe and the overall physicochemical properties.

It is necessary to select a region of the pharmacophore for linker attachment that is amenable to change and the introduction of steric bulk/length. The aim of this study was to locate a suitable linker position on the alkyl indole scaffold and use this for the development of a high affinity, selective fluorescent CB_2 receptor antagonist or inverse agonist.

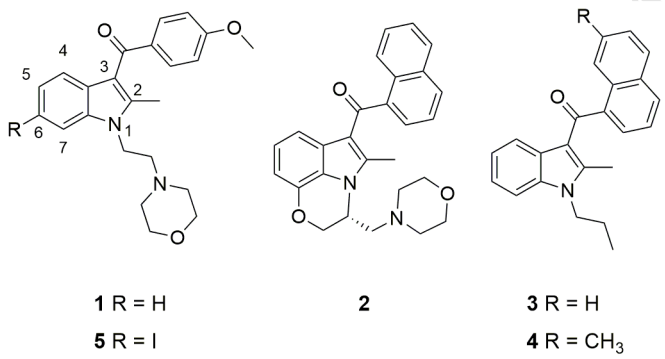

Figure 1: CB receptor agonists WIN-48,098 (pravadoline) (**1)** and WIN-55,212-2 (**2**). CB_2 receptor agonists JWH-015 (**3**) and JWH-046 (**4**). CB_2 receptor inverse agonist AM630 (**5)**.

Development of the indole class of cannabinoids was spearheaded by the development of CB receptor agonists WIN-48,098 (pravadoline) **1** [26] and WIN-55,212-2 **2** [27] (Figure 1). These were followed by variations to the scaffold to give CB_2 receptor selective agonists such as JWH-015 **3** [28] and JWH-046 **4** [29], and inverse agonists such as AM630 **5** (iodopravadoline; hCB_2 K_i = 31.2 nM, hCB_1 K_i = 5152 nM) [30]. Many CB_2 receptor

selective indoles have subsequently been reported [31, 32]. In this project, linker attachment via indole C5-C7 was explored for a variety of reasons. Firstly, the presence of the bulky C6 iodine group in AM630 **5** demonstrates that CB_2 receptor binding is still possible with steric bulk at this side of the indole ring. Secondly, a number of other studies have shown that a variety of bulky groups at the C5, C6 and C7 positions, for example *O*-benzyl [33] and furan [34], maintain high affinity and selectivity for CB_2 receptor and give varying function as either agonists or inverse agonists. Thirdly, other studies that attached linkers and fluorescent dyes at the C3 acyl position of the alkyl indole scaffold were unsuccessful and resulted in a >250 fold loss in affinity for CB_2 receptor compared to the parent pharmacophore and implied that there is a strict size limitation on the C3 acyl substituent in order to retain affinity [35]. In addition, established structure activity relationships (SAR) dictate that the indole scaffold is highly sensitive to variation of N1 substituents and that alkyl chains longer than hexyl at this position are not tolerated [29]. In this project, the N1-alkyl and C3-acyl groups were selected based on optimal affinity and selectivity reported previously by others [36, 37] and a C2-H was used instead of the C2-methyl as present in AM630 **5** for synthetic ease since the latter is not essential for CB_2 receptor binding affinity [38].

2. RESULTS AND DISCUSSION

2.1 Chemistry

All compounds were synthesised from a commercially available 5-, 6- or 7-*O*-benzyl substituted indole (**6a-c**) (Scheme 1). Indoles **6a-c** were *N*-alkylated with R^1-mesylate using sodium hydride to give **7a-e** in good yield. *N*-Alkyl indoles **7a-e** were acylated at C3 with different R^2-nitriles in the presence of catalytic [(Phen)Pd$(OAc)_2$] using a recently reported adapted procedure [39, 40] to give **8a-h**. The palladium-ligand catalytic complex was pre-formed rather than generated *in situ* as this gave superior product yields. Previously, Friedel-Crafts acylation has commonly been used for C3 acylation of this indole class [37], however, this palladium-catalysed reaction provides a cleaner and safer procedure with robust yield. The benzyl ether of **8a-h** was cleaved using Pd/C and hydrogen to reveal hydroxyindoles **9a-h**. Although these compounds were all evaluated for CB_2 receptor binding (Table 1), not all combinations of R^1 and R^2 were progressed through further derivatisations.

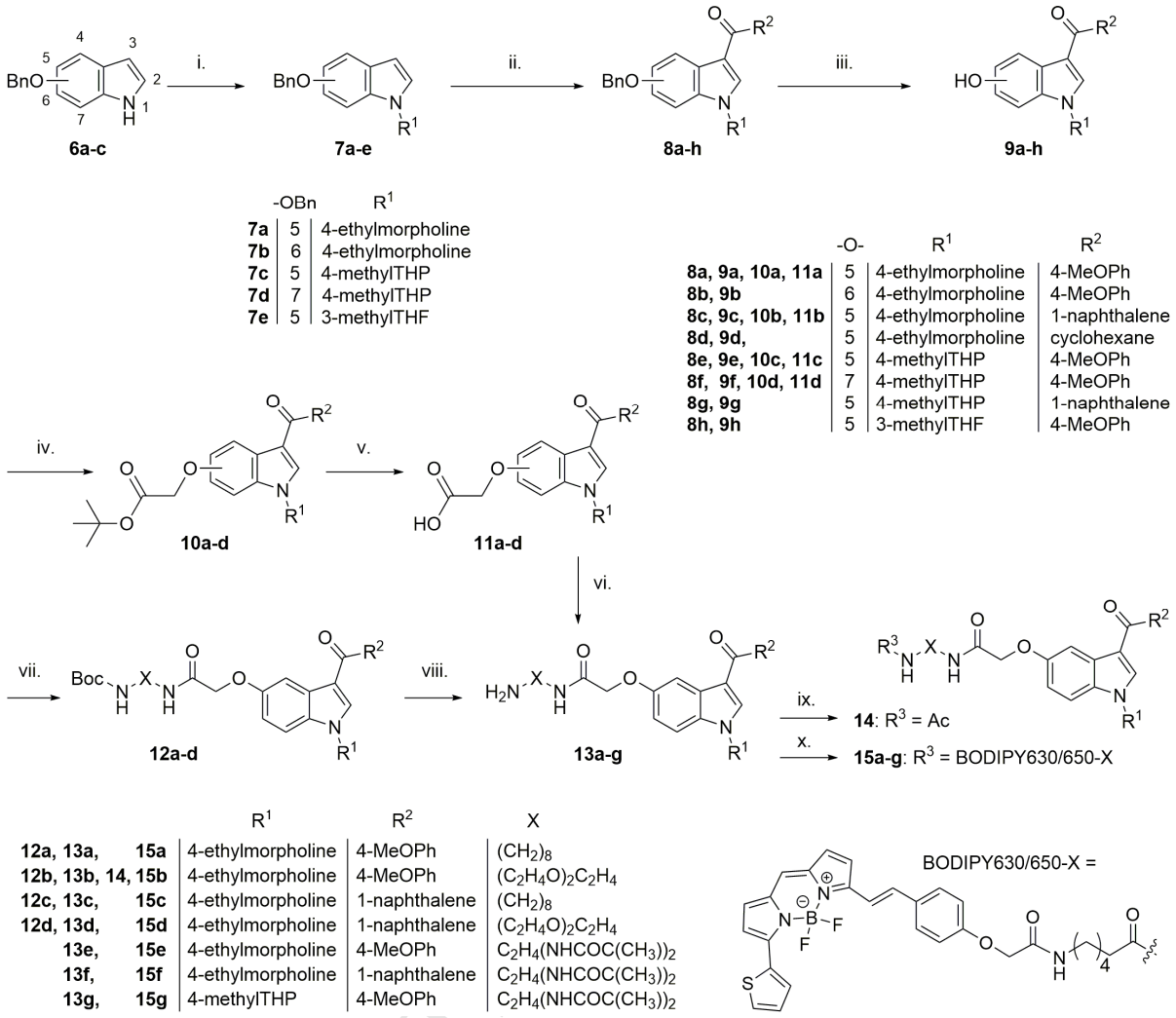

	-OBn	R^1
7a	5	4-ethylmorpholine
7b	6	4-ethylmorpholine
7c	5	4-methylTHP
7d	7	4-methylTHP
7e	5	3-methylTHF

	-O-	R^1	R^2
8a, 9a, 10a, 11a	5	4-ethylmorpholine	4-MeOPh
8b, 9b	6	4-ethylmorpholine	4-MeOPh
8c, 9c, 10b, 11b	5	4-ethylmorpholine	1-naphthalene
8d, 9d,	5	4-ethylmorpholine	cyclohexane
8e, 9e, 10c, 11c	5	4-methylTHP	4-MeOPh
8f, 9f, 10d, 11d	7	4-methylTHP	4-MeOPh
8g, 9g	5	4-methylTHP	1-naphthalene
8h, 9h	5	3-methylTHF	4-MeOPh

		R^1	R^2	X
12a, 13a,	**15a**	4-ethylmorpholine	4-MeOPh	$(CH_2)_8$
12b, 13b, 14,	**15b**	4-ethylmorpholine	4-MeOPh	$(C_2H_4O)_2C_2H_4$
12c, 13c,	**15c**	4-ethylmorpholine	1-naphthalene	$(CH_2)_8$
12d, 13d,	**15d**	4-ethylmorpholine	1-naphthalene	$(C_2H_4O)_2C_2H_4$
13e,	**15e**	4-ethylmorpholine	4-MeOPh	$C_2H_4(NHCOC(CH_3))_2$
13f,	**15f**	4-ethylmorpholine	1-naphthalene	$C_2H_4(NHCOC(CH_3))_2$
13g,	**15g**	4-methylTHP	4-MeOPh	$C_2H_4(NHCOC(CH_3))_2$

Scheme 1. Reagents and Conditions: (i) R^1-OMs, NaH, DMF, 45°C, 2 h, 54 - 87%; (ii) R^2-nitrile, $[(Phen)Pd(OAc)_2]$, H_2O, CH_3COOH, 1,4-dioxane, 140°C, 24 h, 18 - 81%; (iii) Pd/C, H_2, EtOH, EA, rt, 20 h, 8 - 67%; (iv) *tert*-butylbromoacetate, NaH, DMF, 60°C, 3 h, 45 - 61%; (v) TFA, DCM, rt, 1 h; (vi) 1. Fmoc-Ala-Ala-trityl resin (prepared by SPPS*), piperidine, DMF, 2. HATU, DIPEA, DMF, 3. Resin cleavage (TFA, DCM, rt, 1 h), 19 - 26%; (vii) H_2N-$(CH_2)_8$-NHBoc or H_2N-$(C_2H_4O)_2C_2H_4$-NHBoc, HATU, DIPEA, DMF, rt, 12 h, 50 - 94%; (viii) TFA, DCM, rt, 1 h, 27 - 77%; (ix.) Ac_2O, DCM, r.t, 1 h, 97%; (x) BODIPY 630/650-X-OSu, DIPEA, DMF, rt, 12 h, 36 - 88%. * 1. 1,2-diaminoethane trityl resin, Fmoc-Ala-OH, HBTU, DIPEA, DMF, 2. Ac_2O, DIPEA, DMF, 3. piperidine, DMF, 4. Fmoc-Ala-OH, HBTU, DIPEA, DMF.

Hydroxyindoles **9a**, **9c** and **9e-f** were alkylated using *tert*-butylbromoacetate to install a short spacer (**10a-d**), followed by cleavage of the *tert*-butyl group to give carboxylic acids **11a-d**.

These carboxylic acids were coupled to three different linkers, either *N*-Boc-1,8-octanediamine, *N*-Boc-2,2'-(ethylenedioxy)diethylamine (polyethylene glycol (PEG) linker) or Ala-Ala-ethylene-resin-bound (synthesised by solid phase peptide synthesis, then the product cleaved from the resin) to give Boc-protected **12a** and **12c**, **12b** and **12d** or primary amines **13e-g** respectively. Linkers were chosen to give a range of polarity and functionality, from the hydrophobic 'benign' alkyl chain to a more hydrophilic short peptide, with the goal in mind to create a fluorescent probe with suitable physicochemical properties and little non-specific-membrane binding and also to generate tools for studying CB_2 receptor with varied polarity. Boc-deprotection of **12a-d** yielded primary amines **13a-d**, which along with **13e-g** were then coupled to BODIPY 630/650-X-OSu (6-(((4,4-difluoro-5-(2-thienyl)-4-bora-3a,4a-diaza-s-indacene-3-yl)styryloxy)acetyl) aminohexanoic acid, succinimidyl ester) to give **15a-g**. BODIPY 630/650-X was chosen as a fluorophore due to success with other Class A GPCR fluorescent probes [18, 41, 42] and due to its high photo and chemical stability, intense absorption and good fluorescence quantum yield, and red-emitting wavelength meaning minimal detection interference from cellular autofluorescence. The amine **13b** was also acylated to give **14**.

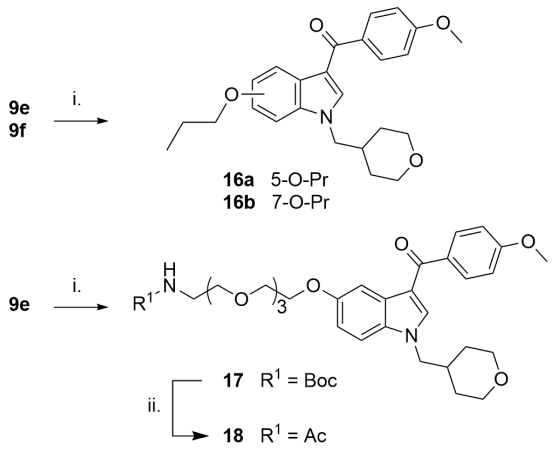

Scheme 2. Reagents and Conditions: (i) 1-bromopropane or $BocNH(C_2H_4O)_3C_2H_4Br$, NaH, DMF, rt, 20 h, 31 - 83%; (ii) 1. TFA, DCM, rt, 1 h, 2. Ac_2O, DCM, r.t, 1.5 h, 71%.

Initial biological characterisation of compounds described thus far indicated the polar carbonyl group/amide bond installed via the short 5- or 7-linker in close proximity to the pharmacophore core may be detrimental to CB_2 receptor binding. Therefore, hydroxyindoles **9e-f** were reacted by Williamson ether procedure with either a short alkyl bromide or a longer

PEG-alkyl bromide to give **16a-b** or **17** respectively (Scheme 2). Once in hand, **17** was Boc-deprotected and acetylated to give **18**. Attachment of a PEG-amine alcohol to **9e** was initially attempted using Mitsunobu conditions however, this did not give a satisfactory yield of **17**.

Biological characterization (described in detail in sections 2.2 and 2.3 below) revealed 7-*O*-propyl substituted **16b** as a lead compound, therefore 7-position linker derivatives of **16b** maintaining the same R^1 and R^2 groups were explored (Scheme 3). Alkylation of **9f** with methyl 5-bromovalerate or *N*-Boc-bromohexylamine afforded **19** or **24** respectively. Methyl ester hydrolysis of **19** gave carboxylic acid **20**, which underwent an amide coupling with *N*-Boc-2,2'-(ethylenedioxy)diethylamine to yield **21**. Boc-deprotection of **21** followed by coupling to BODIPY 630/650-X-OSu afforded **23**. In a separate reaction, this amine intermediate was also acetylated to give **22**. In an analogous manner, **24** was converted to the corresponding BODIPY 630/650-X (**26**) or acetylated (**25**) conjugate.

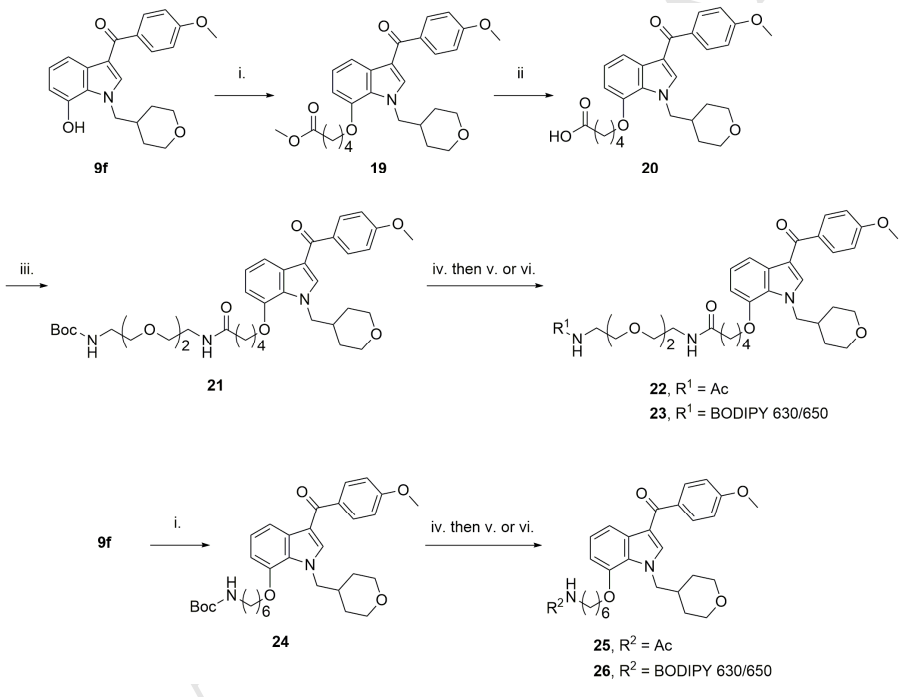

Scheme 3. Reagents and Conditions: (i) methyl 5-bromovalerate or 6-(Boc-amino)hexyl bromide, NaH, DMF, rt, 20 h, 33 - 79%; (ii) 0.2 M aq. $LiOH.H_2O$, THF, 0°C, 1 h, 95%; (iii) *N*-Boc-1,8-diamino-3,6-dioxaoctane, HATU, DIPEA, DMF, rt, 12 h, 82%; (iv) TFA, DCM, rt, 1 h, 92 - 95%; (v) Ac_2O, DIPEA, DCM, rt, 1 h, 95-96%; (vi) BODIPY 630/650-X-OSu, DIPEA, DMF, rt, 12 h, 77 - 93%.

2.2. Radioligand binding assays

Key smaller alkyl indoles and indole-linker conjugates along with all fluorescent compounds were subjected to a competition radioligand binding assay screen, using [^{3}H]CP-55,940 as the competing radioligand and human embryonic kidney 293 (HEK) cells over-expressing human (h) CB_2 receptor chimerized with three *N*-terminal haemagglutinin (HA) tags (3HA-hCB_2) [43]. For compounds that displaced [^{3}H]CP55,940 by more than 50% at hCB_2 receptor, concentration response curves were obtained at hCB_2 receptor to determine K_i values (Table 1). Compounds that showed high affinity for hCB_2 receptor were then subjected to a competition binding assay screen in HEK cells over-expressing 3HA-hCB_1 receptor [44]. CB receptor inverse agonist SR144528 was analysed in the binding assays as a literature comparison control. In this study, SR144528 displayed a K_i = 51.0 ± 3.0 nM at hCB_2 and K_i = 5682 ± 2890 nM at hCB_1 receptor with a CB_2:CB_1 selectivity of 110. This is comparable to the recently reported SR144528 pK_i = 7.88 ± 0.06 at hCB_2 (K_i = 13.2 nM) and pK_i = 5.77 ± 0.09 at hCB_1 receptor (K_i = 1698.2 nM; using [^{3}H]CP55,940 K_d = 0.33 at hCB_2 and 0.1 at hCB_1), with a CB_2:CB_1 selectivity of 129 [45].

Table 1. Affinity of pharmacophore and pharmacophore-linker conjugates for hCB_2 and hCB_1 receptors.

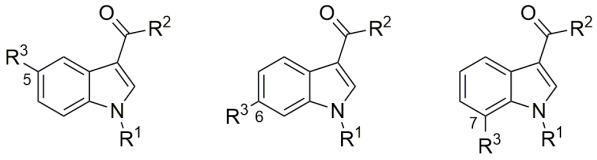

Compound	R^1	R^2	R^3 position	K_i hCB_2 (nM ± SEM) [a]	K_i hCB_1 (nM ± SEM) [a]	Selectivity fold hCB_2 / hCB_1
9a	Et-morpholino	MeOPh	5	746.6 ± 139.8 [b]	>10000	> 13
9b	Et-morpholino	MeOPh	6	>10000	no binding [c]	-
9c	Et-morpholino	naphthalene	5	169.0 ± 16.7	2838 ±705.3 [b]	17
9d	Et-morpholino	cyclohexane	5	895.3 ± 332.2 [b]	>10000	> 11
9e	Me-THP	MeOPh	5	120.1 ± 23.4	1406 ±463.6 [d]	12
9f	Me-THP	MeOPh	7	53.9 ± 7.6 [d]	3583 ± 427	66
9g	Me-THP	naphthalene	5	275.4 ± 82.7 [d]	823.8 ±214.6 [d]	3
9h	Me-THF	MeOPh	5	>10000	no binding	-
11a	Et-morpholino	MeOPh	5	>10000	>10000	-
11b	Et-morpholino	naphthalene	5	>10000	>10000	-
11c	Me-THP	MeOPh	5	1660 ± 114.2	>10000	> 6
11d	Me-THP	MeOPh	7	581.8 ± 70.8	>10000	> 17
16a	Me-THP	MeOPh	5	1350 ± 399.3 [d]	4527 ± 676	3
16b	Me-THP	MeOPh	7	5.7 ± 1.4 [b]	504.6 ± 148.2 [b]	89
19	Me-THP	MeOPh	7	200.7 ± 4.9	1583 ± 242.7	8
20	Me-THP	MeOPh	7	1307 ± 302.5 [b]	>10000	> 7
13a	Et-morpholino	MeOPh	5	>10000	n.d.[e]	-
13b	Et-morpholino	MeOPh	5	>10000	n.d.	-
14	Et-morpholino	MeOPh	5	>10000	n.d.	-
13c	Et-morpholino	naphthalene	5	>10000	n.d.	-
13d	Et-morpholino	naphthalene	5	>10000	n.d.	-
18	Me-THP	MeOPh	5	>10000 [d]	no binding [b]	-
22	Me-THP	MeOPh	7	>10000	>10000	-
13e	Et-morpholino	MeOPh	5	no binding	n.d.	-
13f	Et-morpholino	naphthalene	5	no binding	n.d.	-
13g	Me-THP	MeOPh	5	no binding	n.d.	-
25	Me-THP	MeOPh	7	1969 ± 351.9	3918 ± 800.4	2
SR144528				51.0 ± 3.0	5628 ± 2890	110

[a] K_i obtained by radioligand binding assay, using 2.5 nM [^{3}H]CP55,940 (calculated with a K_d = 3 nM for hCB_2 receptor or K_d = 2 nM for hCB_1 receptor) and transfected HEK 293 3HA cells. SEM = standard error of the mean. Data is the mean of three individual experiments performed in triplicate, except [b] which is four individual experiments performed in triplicate and [d] which is five individual experiments performed in triplicate. Low affinity compounds that passed D'Agostino & Pearson normality test and showed significant competition with

[^{3}H]CP55,940 (as determined by a one sample t-test) were determined to have a K_i value >10000 nM. [c] no significant binding was detected, where compounds showed no significant competition with [^{3}H]CP55,940 as determined by a one sample t-test. [e] n.d. = value was not determined.

Comparison between the hydroxyindole compound series (**9a-h**, Scheme 1) revealed 7-hydroxy **9f** to have the highest affinity for hCB_2 receptor and the greatest selectivity (approx. 66-fold selective) over hCB_1 receptor. With the same R^1 and R^2 groups present in each pair, the 7-hydroxy position gave better hCB_2 receptor affinity than the 5-hydroxy (compare **9f** to **9e**) and the 5-hydroxy position better than the 6-hydroxy (compare **9a** to **9b**). The three derivatives with the 5-hydroxy and 4-methoxyphenol R^2 groups held constant, but with varying R^1 groups revealed 4-methyl tetrahydropyran (THP) (**9e**) to have higher affinity for hCB_2 receptor compared to 4-ethylmorpholino (**9a**) and 3-methyl tetrahydrofuran (THF) (**9h**), the latter of which showed no appreciable binding to either hCB_1 or hCB_2 receptor. The optimal R^2 group was determined by comparing 5-hydroxy and the same R^1 group and it was found that either 1-napthalene (compare **9c** to **9a** and **9d**) or 4-methoxyphenyl (compare **9e** to **9g**) afforded higher hCB_2 receptor affinity. Therefore, the 6-hydroxy, 3-methylTHF R^1 and cyclohexane R^2 groups were not included in further derivatisations. Frost *et al* also found that for 5-hydroxyindole compounds 4-methylTHP at R^1 provides a higher K_i than ethylmorpholino (when in combination with a tetramethylcyclopropyl group) [33]. However, Frost *et al* also found 5-hydroxy substitution conferred higher affinity than 7-hydroxy substitution (R^1 = 4-methylTHP, R^2 = tetramethylcyclopropyl) indicating that the preferred position of 7-hydroxy found in our study is specific to the R^1 and R^2 groups utilised.

Evaluation of the six derivatives (**11a-d** and **16a-b**, Schemes 1 and 2) with a 4-atom linker/linear group revealed that the 7-indole-linked position conferred higher hCB_2 receptor affinity than the 5-position. The 7-substituted **11d** had a 3-fold higher affinity than 5-substituted **11c**, and 7-substituted **16b** around 230-fold higher affinity for CB_2 receptor than **16a** (Table 1, Figure 2a). The weak binding of **11a** and **11b** compared to **11c** indicated a preference for R^1 group 4-methylTHP and R^2 group 4-methoxyphenyl. Of all the compounds analysed, 7-*O*-propyl **16b** (hCB_2 K_i = 5.7 ± 1.4 nM, hCB_1 K_i = 504.6 ± 148.2) had the highest hCB_2 receptor affinity and had the most pronounced subtype selectivity (89 fold hCB_2 over hCB_1 receptor) of the new compounds reported in this study.

Derivatives **19** and **20** were evaluated to see if linker extension from the propyl-chain of lead compound **16b** was tolerated. Despite having a 35-fold reduction in hCB_2 receptor affinity compared to **16b**, **19** still retained reasonable hCB_2 receptor affinity (hCB_2 K_i = 200.7 ± 4.9 nM) (Figure 2a) and was considered a promising lead for a fluorescent conjugate. The carboxylic acid **20** showed approximately a 6-fold loss in affinity for hCB_2 receptor compared to the methyl ester analogue **19**, which indicated it was unlikely the methyl ester was hydrolysed during the assay.

Conjugation of longer linkers onto pharmacophore-short linker scaffolds was generally not well tolerated. The longest linked derivative to show appreciable hCB_2 receptor binding was alkyl-ether-acetylated-**25**. Alkyl, or PEG linkers introduced to derivatives **11a-b**, **9e** and **20** to give **13a-d**, **18** and **22** showed minimal affinity (hCB_2 receptor K_i >10000 nM). The lack of binding of acetylated analogue **14** compared with the corresponding primary amine **13b** demonstrated the primary amine of **13b** is not solely responsible for the lack of affinity. There was no detectable hCB_2 receptor binding observed for compounds containing a dipeptide linker (**13e-g**). Unfortunately, conjugation of BODIPY630/650-X did not furnish high affinity hCB_2 receptor ligands, even when the fluorescent dye was conjugated to the most promising pharmacophore-linker conjugate **19**. The alkyl linker containing fluorescent ligands showed no discernible binding, whilst the PEG and dipeptide-linked fluorescent ligands showed very minimal affinity (hCB_2 receptor K_i = >10000 nM; Supplementary Table 1).

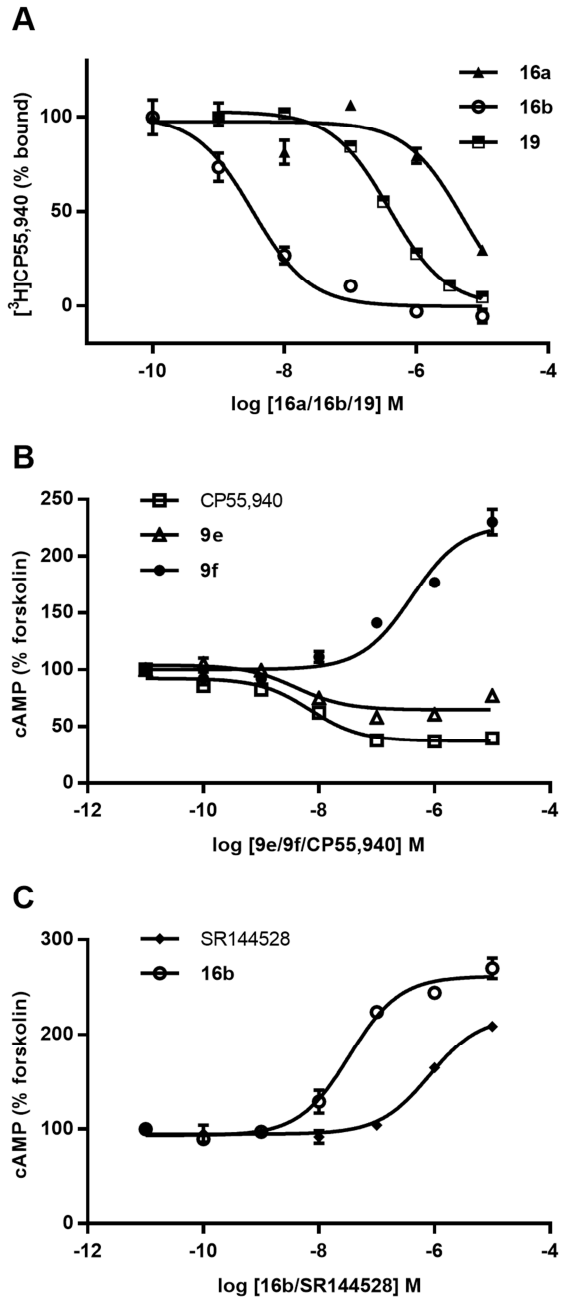

Figure 2: (A) Binding affinity of **16a**, **16b** and **19** at hCB_2 receptor, determined using competition binding curves against [^{3}H]CP55,940. [^{3}H]CP55,940 bound (ccpm) values are normalised to the specific binding window (%). Data shown is representative of a single experiment performed in triplicate, with error bars indicating ± SEM. (B) Concentration response curve of **9e**, **9f** and CP55,940, measuring forskolin-stimulated cAMP (5µM). Area under the curve values are normalised so that forskolin only response = 100% and basal response = 0%. Data shown is representative of a single experiment, with data points conducted in duplicate. (C) Concentration response curve of **16b** and SR144528, measuring forskolin-stimulated cAMP. Area under the curve values are normalised so that forskolin only response = 100% and basal response = 0%. Data shown is representative of a single experiment, with data points conducted in duplicate.

2.3. cAMP assays

Compounds that showed micromolar or nanomolar affinity for hCB_2 receptor were also analysed for functional activity using a bioluminescence resonance energy transfer (BRET) sensor to measure modulation of forskolin-stimulated cyclic adenosine monophosphate (cAMP) at hCB_2 and hCB_1 receptors. Initially compounds were tested at 10 μM in the presence and absence of CP 55,940. Since both CB_1 and CB_2 receptor are G_i coupled, agonists cause a decrease in cellular cAMP, antagonists can prevent the inhibition produced by an EC_{90} concentration of a full agonist (i.e. CP 55,940) and inverse agonists lead to an increase in cellular cAMP. Compounds that demonstrated a functional response were then subjected to a concentration response assay at CB_2 receptor and the three highest CB_2 receptor affinity compounds, **9e**, **9f** and **16b** were also analysed for potency at CB_1 receptor (Table 2).

The five indoles with a 5-hydroxyl but varying R^1 and R^2 groups (**9a, 9c-e, 9g**) all behaved as hCB_2 receptor agonists in the cAMP assay. The compound with the highest affinity for CB_2 receptor (**9e**) was also the most potent agonist. 5-Hydroxy-**9e** had the highest hCB_2 receptor agonist potency of all compounds tested (hCB_2 EC_{50} = 4.4 ± 0.35 nM) but also showed agonist activity at hCB_1 receptor at a lower potency (hCB_1 EC_{50} = 62.9 ± 29.7 nM). Extension of the 5-hydroxy position with a short chain either retained agonist activity (**11c**) or resulted in no response (**16a**).

In contrast to the 5-substituted agonists, derivatisation of the alkyl indole scaffold in the 7-position led to inverse agonist activity at hCB_2 receptor in five (**9f, 16b, 19, 20, 25**) out of six compounds analysed. Of note is the dramatic difference in function between the regioisomers 5-hyroxy-**9e** and 7-hydroxy-**9f**, which showed agonism or inverse agonism at hCB_2 receptor respectively (Figure 2b). These two compounds were also analysed for function at hCB_1 receptor and both behaved as agonists, with **9e** having the highest potency (hCB_1 EC_{50} = 62.9 ± 29.7 nM).

Table 2: Functional data at hCB_2 and hCB_1 receptor.

	hCB_2 receptor			hCB_1 receptor		
Compound	EC_{50} [a] or IC_{50} [b] (nM ± SEM)	E_{max} (% ± SEM) [e]	Function	EC_{50} [a] or IC_{50} [b] (nM ± SEM)	E_{max} (% ± SEM) [e]	Function
9a	5.4 ± 2.7 [a]	67.5 ± 2.9	Agonist	n.d.	70.4 ± 4.6	Agonist
9c	8.7 ± 1.6 [a]	77.4 ± 6.1	Agonist	n.d.	54.6 ± 5.4	Agonist
9d	18.6 ± 5.1 [a]	74.1 ± 1.2	Agonist	n.d.	74.3 ± 4.2	Agonist
9e	4.4 ± 0.35 [a]	65.7 ± 3.7	Agonist	62.9 ± 29.7 [a]	62.2 ±3.4	Agonist
9g	14.7 ± 5.3 [a]	64.4 ± 1.5	Agonist	n.d.	52.4 ± 1.9	Agonist
11c	70.2 ± 6.2 [a]	57.4 ± 3.2	Agonist	n.d.	60.4 ± 1.2	Agonist
16a	-	-	No response	-	-	No response
9f	271.7 ± 130.7 [b]	189.8 ± 13.8	Inverse agonist	632.5 ± 315.1 [a]	64.3 ± 8.1	Agonist
16b	30.6 ± 13.9 [b]	263.3 ± 14.4	Inverse agonist	-	-	No response
11d	>10000 [a,]	84.9 ± 3.3	Agonist	n.d.	80.5 ± 5.5	Agonist
19	>10000 [b, c]	165.8 ± 7.1	Inverse agonist	n.d.	77.8 ± 3.6	Agonist
20	>10000 [b, c]	123.6 ± 7.7	Inverse agonist	n.d.	82.5 ± 1.6	Agonist
25	>10000 [b, c]	150.9 ± 10.7	Inverse agonist	n.d.	74.3 ± 4.9	Agonist
CP-55,940	5.6 ± 2.3 [a]	41.0 ± 1.4	Agonist	n.d.	56.5 ± 1.4	Agonist
SR144528	760 ± 61.7 [b,d]	212.2 ± 2.5	Inverse agonist	-	-	No response

Potency was determined by concentration response BRET assays measuring forskolin-stimulated cAMP. [a] EC_{50} for compounds showing agonist activity. [b] IC_{50} for compounds showing inverse agonist activity. [c] Compounds did not reach a plateau for maximum efficacy. Data is the mean of at least three individual experiments performed in duplicate, except [d] which is two individual experiments performed in duplicate. SEM = standard error of the mean. [e] Area under the curve (AUC) analysis was used to determine E_{max} as a percentage of normalised forskolin only response (100%) and vehicle (0%). A t-tests was used to determine if the E_{max} observed was significantly different from the forskolin only response and if no significant difference was found, the compounds were deemed to show no response. n.d. = value was not determined.

It remains to be determined if this regioisomer functional switch between 5- and 7-substituted indoles is a more robust trend as there is no additional SAR available in the literature directly comparing the function of 5- and 7-substituted analogues with regards to cAMP signalling. Pasquini *et al* identified 5-aryl-substituted indoles that displayed inverse agonism with cAMP signalling, however with very different N1 and C3 indole substituents than those utilised in our study [34]. In an interesting study by Frost *et al* [33] using 4-, 5-, 6- and 7-hydroxyl, *O*-benzyl and methoxy substituted indoles, the 7-substituted analogues failed to show agonism in a fluorescence imaging plate reader (FLIPR) calcium flux assay (but were not tested for

antagonism or inverse agonism), whilst two out of three 5-substituted analogues did display agonism.

It is important to note that we only analysed the G_i pathway via cAMP production in this study and no other CB receptor signalling pathways such as β-arrestin recruitment, G_q coupling (intracellular calcium release), or G_s coupling (adenyl cyclase stimulation). GPCR ligands are well known to exhibit signalling bias [46, 47], and therefore the new ligands reported herein could possess varying functions via signalling pathways other than cAMP. The compound with the highest affinity for CB_2 receptor, **16b**, also showed the highest hCB_2 receptor potency (hCB_2 receptor IC_{50} = 30.6 ± 13.9 nM) amongst the inverse agonists in this series, and a higher potency and E_{max} than the control inverse agonist SR144528 (Figure 2c). **16b** was also analysed for hCB_1 receptor potency but failed to produce a significant response at concentrations up to 10 µM. In comparison to previously reported alkyl indole scaffolds, **16b** showed improved hCB_2 receptor affinity over AM630 **5** (hCB_2 *K*i = 32.1 nM, hCB_2/hCB_1 165-fold) [30] but with less subtype selectivity. There are a very few higher affinity alkyl indoles that have been reported as CB_2 receptor inverse agonists, for example an inverse agonist (hCB_2 K_i = 0.37 nM, hCB_1 K_i = 344.9 nM, calculated using [^{3}H]CP55,940 hCB_2 K_d = 0.31 nM, hCB_1 K_d = 0.18 nM) reported by Pasquini *et al* [34]. In contrast, there are many higher affinity CB_2 receptor indole-based agonists reported, which could be attributed to the increased interest in CB receptor agonists driven by drug discovery efforts [48]. **16b** also showed a higher affinity than diarylpyrazole inverse agonist SR144528 in this study.

Compound **19** was the highest affinity pharmacophore-linker conjugate, and **25** was the longest linked derivative to show appreciable hCB_2 receptor binding, however despite both behaving as an inverse agonist at CB_2 receptor, an IC_{50} could not be estimated for either as a maximal response plateau was not reached at 10 µM.

All the compounds analysed for potency in the cAMP BRET assay were also tested at 10 µM and 1 µM in wild type (WT) HEK 293 cells to verify that the observed effects at hCB_2 and hCB_1 receptors were receptor mediated (Supplementary Table 2). **9c**, **9f**, **16a-b**, and **20** all invoked a small but significant response at 10 µM but not at 1 µM and as these compounds all demonstrated a response in HEK293-hCB_2 cells at 1 µM, it can be concluded that the WT HEK cell response is not large enough to have significantly affected the calculated hCB_1 and

hCB_1 receptor potencies. **19** and **25** showed a significant response in WT HEK cells at both 10 μM and 1 μM, but as both compounds demonstrated very weak potency at hCB_2 receptor (IC_{50} >10000nM) the potential effect of non-receptor mediated activity on the measured CB receptor response is of limited concern.

2.4. Molecular Modelling

GPCRs have proved difficult to crystallise due to the inherent insolubility of membrane bound proteins, low expression levels, conformational flexibility and lack of stability in detergents [49]. However, recent technological advances such as protein engineering and lipid-based crystallisation have led to a rapid increase in the numbers of GPCR crystal structures obtained [50]. A crystal structure of CB_2 receptor has not yet been reported, however three structures were recently determined for CB_1 receptor [51-53]. A homology model of CB_2 receptor based on the crystal structure of inverse-agonist-bound CB_1 receptor (PDB ID: 5TGZ) [51] was constructed. The secondary structure of a homology model is heavily influenced by the template structure. CB_2 receptor homology models reported prior to the determination of CB_1 crystal structures have utilised other, less closely related crystal structures, such as β2-adrenoceptor, A_{2A} adenosine receptor or rhodopsin and therefore will differ slightly to the model reported here [54-56].

Ligand docking studies were carried out in an attempt to rationalise the hCB_2 receptor affinity of the inverse agonist pharmacophore-linker conjugate **19**. Docking poses were clustered into two groups, with the most consistent pose showing the methyl valerate linker oriented out of the binding pocket between TM1 and TM7, into the lipid bilayer (Figure 3). It has previously been proposed that ligands may enter CB_1 and CB_2 receptors via the lipid membrane [57] and molecular dynamics simulations have shown a likely entry route between TM1 and TM7 for tetrahydrocannabinol and anandamide binding to CB_1 receptor [58]. A similar exit pathway from the orthosteric binding site of CB_2 receptor between TM1 and TM7 to that postulated here for **19** has been proposed for a biotin-containing CB_2 receptor probe [59]. In this pose, the 7-ether demonstrates hydrogen bonding with S285, whilst the THP oxygen and the ester carbonyl hydrogen bonds with the extracellular loop. The phenyl is positioned in a hydrophobic pocket between TM3-6 and the indole core and phenyl are able to engage in van der Waals interactions with multiple nearby aromatic residues (F183, W194, W258 and F281). This linker pose reinforces that the indole C7 position holds promise for linker and

fluorescent dye conjugation. The other, smaller cluster of poses (three out of ten) showed the linker exiting through the extracellular loops, however the flexibility of extracellular loops makes docking in this region difficult.

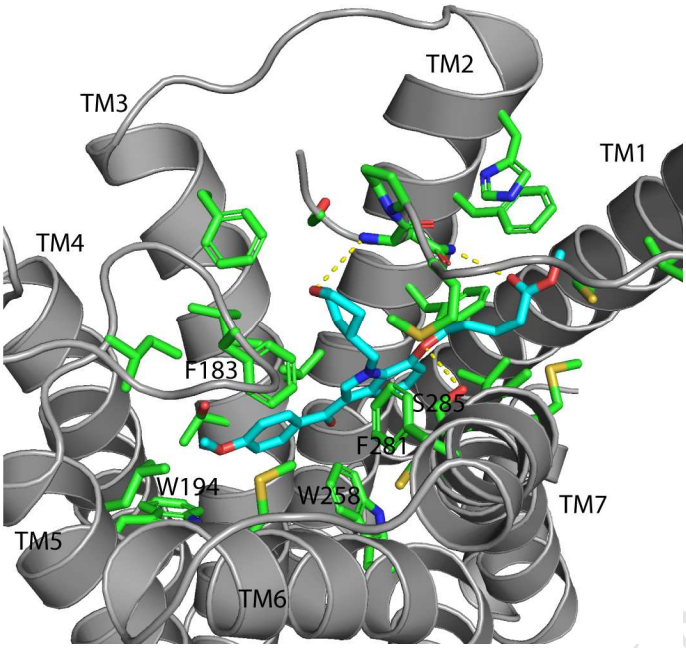

Figure 3: Inverse agonist **19** (cyan carbon atoms) docked into hCB_2 receptor homology model (grey ribbon). The methyl valerate linker is orientated out of the binding pocket between helices 1 (TM1) and 7 (TM7). Hydrogen bonding (yellow dotted lines) is shown between the 7-ether and S285 (shown as sticks) as well as the THP ether and the ester carbonyl with the extracellular loop. Side chains of residues within 4 Å of the ligand **19** are shown as sticks (green).

2.5. Off target activity

Compounds **8e-h**, **9e-g** and **16a** were accepted into the Eli Lilly and Company Open Innovation Drug Discovery Program and the Tres Cantos Open Lab Foundation and did not show significant proprotein convertase subtilisin kexin type 9 (PCSK9) inhibition, GPR120 agonism, disruption to IL-17 protein-protein interaction, *Leishmania donovani* growth inhibition, voltage-gated potassium channel KCNQ2/3 agonism or nicotinamide N-methyltransferase (NNMT) inhibition.

3. CONCLUSIONS

In this study, the C5-C7 positions of CB_2 receptor alkyl indole ligands were explored for tolerability of linker attachment, with the aim to develop a high affinity, selective CB_2 receptor fluorescent ligand. Substitution of short linkers at the indole C7 resulted in higher affinity and selectivity for hCB_2 receptor compared to the analogous C5 compounds. These C7 substituted compounds also showed inverse agonism in contrast to the C5-substituted agonists in nearly all examples. C7-Short alkyl-linked indole **16b** (hCB_2 K_i = 5.7 ± 1.4 nM, hCB_1 K_i = 504.6 ± 148.2, hCB_2/hCB_1 88-fold) was identified as a new high affinity hCB_2 receptor inverse agonist.

The pharmacophore-linker conjugate **19** that retained CB_2 receptor affinity demonstrated that a linker is tolerated in this indole C7 position and molecular modelling suggests this would be amenable to further extension and fluorophore conjugation. Unfortunately, conjugation of a fluorescent dye, including extension of **19**, failed to produce a high affinity CB_2 receptor fluorescent ligand in this study. However, **19** remains a promising pharmacophore-linker lead and future studies could explore extension of **19** with other linker lengths and types in addition to different fluorescent dyes. In the context of this study that investigated C5-C7 indole positions and in light of previous efforts of linker conjugation via the C3 acyl group [35] or extension of the N1 substituent [29] the search for an indole-based fluorescent ligand for CB_2 receptor remains elusive.

EXPERIMENTAL PRODECURES

Material and Methods

Chemistry

Chemicals and solvents were purchased from Sigma Aldrich, Merck or AK Scientific and were used without further purification. BODIPY 630/650-X-OSu was obtained from Life Technologies. Anhydrous grade solvents were used when a dry atmosphere was required. Unless stated, all reactions were carried out at room temperature (rt) and under atmospheric pressure. 1,2-diaminoethane trityl resin (200-400 mesh) was purchased from Merck.

Thin layer chromatography was carried out on 0.2 mm aluminium-backed silica gel plates 60 F_{254} and visualised under UV light at λ = 254 nM and 365 nM and then with potassium permanganate dip. Flash column chromatography was carried out using 40-63 µm silica. Reverse phase high performance liquid chromatography (RP-HPLC) was carried out on an Agilent 1260 Infinity system, using an YMC C8 5 µm (150 × 10 mm) column for semi-preparative RP-HPLC and an YMC C8 5 µm (150 × 4.6 mm) column for analytical RP-HPLC. The mobile phases used were A: H_2O (0.05% TFA) and B: 9:1 ACN:H_2O (0.05% TFA). Analytical RP-HPLC retention times quoted below were determined with a standard method - 5% A for 1 min, then a linear gradient of 5-95% B from 1-27 min (followed by 1 min at 95% B, 2 min linear gradient 95-5% B and then 4 min re-equilibration at 5% A). All compounds analysed for biological activity were > 95% purity by UV detection at 254 and 380 nm (and 550 nm for fluorescent compounds) by analytical RP-HPLC. All compounds HPLC purified as the trifluoroacetic acid (TFA) salt were neutralised using an Amberlyst A21 ion exchange resin before biological testing.

High resolution electrospray ionization mass spectra (HRMS-ESI) were obtained on a microTOF$_Q$ mass spectrometer. Proton and carbon nuclear magnetic resonance (NMR) spectra were obtained on either a 400 MHz or a 500 MHz Varian MR spectrometer. Two-dimensional NMR experiments, including COSY, HSQC, HMBC and NOESY were used to assign spectra. Chemical shifts are listed on the δ scale in ppm, referenced to $CDCl_3$, MeOD-d_4 or DMSO-d_6 with residual solvent as the internal standard and coupling constants (*J*) recorded in hertz (Hz). Signal multiplicities are assigned as: s, singlet; d, doublet; t, triplet; q, quartet; quint, quintet; dd, doublet of doublets; dt, doublet of triplets; td, triplet of doublets; br, broad; or m, multiplet.

5□(Benzyloxy)□1□[2□(morpholin□4□yl)ethyl]□1*H*□indole (7a)

Preparation of 2-(morpholin-4-yl)ethyl methanesulfonate. A stirred solution of 4-(2-hydroxyethyl)-morpholine (2.5 mL, 20.7 mmol) and Et_3N (8.6 mL, 62.0 mmol) in anhydrous DCM (48 mL) under N_2 was cooled to 0°C and then methanesulfonyl chloride (2.4 mL, 31.0 mmol) was added dropwise. The mixture was stirred at rt for 2 h, filtered, the solid washed with minimal DCM and this filtrate combined with the original filtrate was evaporated under reduced pressure to give a yellow oil (10.24 g) as a mixture of the desired product 2-(morpholin-4-yl)ethyl methanesulfonate and a salt ($Et_3NH^+Cl^+$). This material was used

without further purification. A stirred solution of 5-benzyloxyindole (600 mg, 2.7 mmol) in anhydrous DMF (11 mL) under N_2 was cooled to 0°C, and then NaH (60% by mass dispersion in mineral oil; 358 mg, 9.0 mmol) was added. The mixture was stirred at 0°C for 10 min and then at rt for 30 min. The reaction mixture was cooled to 0°C and a solution of 2-(morpholin-4-yl)ethyl methanesulfonate (1.13 g, 5.4 mmol) in anhydrous DMF (5 mL) was added. The mixture was stirred at 45°C for 2 h, cooled to rt, diluted with EA (20 mL) and quenched with sat. aq. NH_4Cl (20 mL) and H_2O (10 mL). The layers were separated and the aqueous layer extracted with EA (3 × 20 mL). The combined organics were washed with H_2O (4 × 70 mL), dried over $MgSO_4$, filtered and evaporated under reduced pressure. The crude product was purified using flash silica column chromatography (2:1 PE:EA) to yield the desired **7a** (690 mg, 2.1 mmol, 76%) as a light brown wax (R_f 0.13, 2:1 PE:EA). ^{1}H NMR (400 MHz, $CDCl_3$): δ 7.52 – 7.46 (m, 2H, ArH Bn), 7.43 – 7.37 (m, 2H, ArH Bn), 7.37 – 7.30 (m, 1H, ArH Bn), 7.26 (d, *J* = 8.8 Hz, 1H, ArH indole), 7.18 (d, *J* = 2.3 Hz, 1H, ArH indole), 7.13 (d, *J* = 3.1 Hz, 1H, ArH indole), 6.98 (dd, *J* = 8.9, 2.2 Hz, 1H ArH indole), 6.41 (dd, *J* = 3.2, 1.1 Hz, 1H, ArH indole), 5.12 (s, 2H, CH_2 Bn), 4.22 (t, *J* = 6.9 Hz, 2H, N1-CH_2), 3.72 (t, *J* = 4.6 Hz, 4H, O-CH_2 morpholino), 2.75 (t, *J* = 6.9 Hz, 2H, N1-$CH_2C\underline{H_2}$), 2.49 (t, *J* = 4.6 Hz, 4H, N-CH_2 morpholino). ^{13}C NMR (101 MHz, $CDCl_3$) δ 153.33, 137.86, 131.56, 128.98, 128.69, 128.61, 127.85, 127.64, 112.69, 110.03, 104.38, 101.03, 71.01, 67.03, 58.36, 53.99, 44.29. HRMS-ESI calculated for $C_{21}H_{25}N_2O_2$ $[M+H]^+$ 337.1911, found *m/z* 337.1884.

6-(Benzyloxy)-1-[2-(morpholin-4-yl) ethyl]-1*H* indole (7b)

6-Benzyloxyindole (1.34 g, 6.0 mmol), NaH (732 mg, 18.3 mmol), and 2-(morpholin-4-yl)ethyl methanesulfonate (2.51 g, 12.0 mmol) in DMF (48 mL) were reacted as described in the procedure for **7a**. The crude product was purified using flash silica column chromatography (2:1 hexane:EA) to yield the desired **7b** (1.10 g, 3.3 mmol, 54%) as a brown solid (R_f 0.13, 2:1 PE (petroleum ether):EA). ^{1}H NMR (400 MHz, $CDCl_3$) δ 7.55 – 7.44 (m, 3H, ArH Bn & ArH indole), 7.44 – 7.36 (m, 2H, ArH Bn), 7.36 – 7.29 (m, 1H, ArH Bn), 7.04 (d, *J* = 3.2 Hz, 1H, ArH indole), 6.95 – 6.83 (m, 2H, ArH indole), 6.42 (dd, *J* = 3.2, 0.7 Hz, 1H, ArH indole), 5.14 (s, 2H, CH_2 Bn), 4.32 – 4.04 (br m, 2H, N1-CH_2), 3.82 – 3.57 (br m, 4H, O-CH_2 morpholino), 2.83 – 2.62 (br m, 2H, N1-$CH_2C\underline{H_2}$), 2.60 – 2.29 (br m, 4H, N-CH_2 morpholino). ^{13}C NMR (101 MHz, $CDCl_3$) δ 155.44, 137.60, 136.67, 128.67, 127.97, 127.63, 127.26, 123.27, 121.68, 109.95, 101.38, 94.83, 70.94, 67.02, 58.08, 53.99, 44.10. HRMS-ESI calculated for $C_{21}H_{25}N_2O_2$ $[M+H]^+$ 337.1911, found *m/z* 337.1880.

5-(Benzyloxy)-1-[(oxan-4-yl) methyl]-1*H*-indole (7c)

Preparation of (oxan□4□yl)methyl methanesulfonate. 4-(Hydroxymethyl) tetrahydropyran (2.9 mL, 25.0 mmol), Et_3N (10.4 mL, 74.9 mmol) and methanesulfonyl chloride (2.9 mL, 37.5 mmol) in DCM (50 mL) were reacted as described in the procedure for 2-(morpholin-4-yl)ethyl methanesulfonate to give an orange oil (7.77 g) as a mixture of the desired (oxan□4□yl)methyl methanesulfonate and a salt. This material was used without further purification. 5-Benzyloxyindole (600 mg, 2.7 mmol), NaH (481 mg, 12.0 mmol) and (oxan□4□yl)methyl methanesulfonate (1.04 g, 5.4 mmol) in DMF (17 mL) were reacted as described in the procedure for **7a**. The crude product was purified using flash silica column chromatography (2:1 PE:EA) to yield the desired **7c** (570 mg, 1.8 mmol, 66%) as a light brown oil (R_f 0.44, 2:1 PE:EA). ^{1}H NMR (400 MHz, $CDCl_3$) δ 7.52 – 7.44 (m, 2H, ArH Bn), 7.43 – 7.36 (m, 2H, ArH Bn), 7.35 – 7.29 (m, 1H, ArH Bn), 7.23 (d, *J* = 8.9 Hz, 1H, ArH indole), 7.17 (d, *J* = 2.4 Hz, 1H, ArH indole), 7.03 (d, *J* = 2.4 Hz, 1H, ArH indole), 6.96 (dd, *J* = 8.9, 2.4 Hz, 1H, ArH indole), 6.40 (d, *J* = 3.0 Hz, 1H, ArH indole), 5.11 (s, 2H, CH_2 Bn), 3.99 – 3.91 (m, 4H, N-CH_2 & O-CH_2 tetrahydropyran (THP)), 3.31 (td, *J* = 11.7, 2.3 Hz, 2H, O-CH_2 THP), 2.16 – 2.02 (m, 1H, CH THP), 1.53 – 1.32 (m, 4H, O-$CH_2C\underline{H_2}$ THP). ^{13}C NMR (101 MHz, $CDCl_3$) δ 153.29, 137.85, 131.77, 129.02, 128.96, 128.61, 127.85, 127.64, 112.68, 110.25, 104.24, 100.72, 70.97, 67.58, 52.65, 36.40, 30.98. HRMS-ESI calculated for $C_{21}H_{24}NO_2$ $[M+H]^+$ 322.1802, found *m/z* 322.1778.

7-(Benzyloxy)-1-[(oxan-4-yl) methyl]-1*H*-indole (7d)

7-Benzyloxyindole (335 mg, 1.5 mmol), NaH (268 mg, 6.7 mmol) and (oxan□4□yl)methyl methanesulfonate (582 mg, 3.0 mmol) in DMF (14 mL) were reacted as described in the procedure for **7a**. The crude product was purified using flash silica column chromatography (4:1 hexane:EA) to yield the desired **7d** (418 mg, 1.3 mmol, 87%), as a pale violet wax (R_f 0.63, 2:1 PE:EA). ^{1}H NMR (400 MHz, $CDCl_3$) δ 7.51 – 7.44 (m, 2H, ArH Bn), 7.44 – 7.33 (m, 3H, ArH Bn), 7.24 (dt, *J* = 8.0, 0.7 Hz, 1H, ArH indole), 7.00 (t, *J* = 7.8 Hz, 1H, ArH indole), 6.91 (d, *J* = 2.9 Hz, 1H, ArH indole), 6.73 (dd, *J* = 7.8, 0.8 Hz, 1H, ArH indole), 6.40 (d, *J* = 3.0 Hz, 1H, ArH indole), 5.14 (s, 2H, CH_2 Bn), 4.08 (d, *J* = 7.2 Hz, 2H, N-CH_2), 3.87 – 3.76 (m, 2H, O-CH_2 THP), 3.13 (td, *J* = 11.6, 2.5 Hz, 2H, O-CH_2 THP), 2.11 – 1.92 (m, 1H, CH THP), 1.26 – 1.03 (m, 4H, O-$CH_2C\underline{H_2}$ THP). ^{13}C NMR (101 MHz, $CDCl_3$) δ 146.85, 136.98, 131.35, 130.02, 128.71, 128.56, 128.41, 125.57, 119.87, 114.12, 103.02, 100.83,

70.60, 67.70, 55.41, 37.68, 30.43. HRMS-ESI calculated for $C_{21}H_{23}NNaO_2$ $[M+Na]^+$ 344.1621, found *m/z* 344.1591.

5-(Benzyloxy)-1-[(oxolan-3-yl) methyl]-1*H*-indole (7e)

Preparation of (oxolan-3-yl)methyl methanesulfonate. Tetrahydro-3-furanmethanol (0.86 mL, 9.0 mmol), Et_3N (3.7 mL, 26.9 mmol) and methanesulfonyl chloride (1.0 mL, 13.4 mmol) in DCM (21 mL) were reacted as described in the procedure for 2-(morpholin-4-yl)ethyl methanesulfonate to give a yellow oil (3.29 g) as a mixture of the desired (oxolan□3□yl)methyl methanesulfonate and a salt. This material was used without further purification. 5-Benzyloxyindole (600 mg, 2.7 mmol), NaH (322 mg, 8.1 mmol) and (oxolan□3□yl)methyl methanesulfonate (969 mg, 5.4 mmol) in DMF (16 mL) were reacted as described in the procedure for **7a**. The crude product was purified using flash silica column chromatography (2:1 PE:EA) to yield the desired **7e** (582 mg, 1.9 mmol, 70%), as a red-orange oil (R_f 0.63, 2:1 EA:PE). ^{1}H NMR (400 MHz, $CDCl_3$) δ 7.55 – 7.46 (m, 2H, ArH Bn), 7.44 – 7.37 (m, 2H, ArH Bn), 7.37 – 7.30 (m, 1H, ArH Bn), 7.27 (d, *J* = 8.9 Hz, 1H, ArH indole), 7.19 (d, *J* = 2.5 Hz, 1H, ArH indole), 7.08 (d, *J* = 3.1 Hz, 1H, ArH indole), 6.98 (dd, *J* = 8.9, 2.4 Hz, 1H, ArH indole), 6.43 (dd, *J* = 3.1, 0.8 Hz, 1H, ArH indole), 5.12 (s, 2H, CH_2 Bn), 4.06 (d, *J* = 7.8 Hz, 2H, N-CH_2), 3.97 (td, *J* = 8.3, 5.5 Hz, 1H, O-CH_2 tetrahydrofuran (THF)), 3.82 – 3.67 (m, 2H, O-CH_2 THF), 3.61 (dd, *J* = 8.9, 4.7 Hz, 1H, O-CH_2 THF), 2.90 – 2.75 (m, 1H, CH THF), 2.10 – 1.94 (m, 1H, CH_2 THF), 1.73 – 1.57 (m, 1H, CH_2 THF). ^{13}C NMR (101 MHz, $CDCl_3$) δ 153.39, 137.84, 131.69, 129.02, 128.63, 128.43, 127.87, 127.65, 112.84, 110.11, 104.36, 101.14, 71.13, 71.01, 67.68, 49.22, 40.16, 29.97. HRMS-ESI calculated for $C_{20}H_{21}NNaO_2$ $[M+Na]^+$ 330.1464, found *m/z* 330.1441.

5-(Benzyloxy)-3-(4-methoxybenzoyl)-1-[2-(morpholin-4-yl)ethyl]-1*H*-indole (8a)

Formation of [(Phen)Pd(OAc)$_2$] complex. Palladium (II) acetate (324 mg, 1.5 mmol) was dissolved in acetone (28 mL) and left unstirred for 30 min at rt, after which, undissolved solid $Pd(OAc)_2$ was removed by filtration with fine filter paper. 1,10-Phenanthroline (313 mg, 1.7 mmol) was added to the reddish-brown filtrate, the solution swirled for 1 min in which time a precipitate started to form. The solution was left to sit unstirred for 30 min, the precipitate was filtered, washed with cold acetone and vacuum dried, yielding [(Phen)$Pd(OAc)_2$] (336 mg, 0.83 mmol, 57%) as a canary yellow solid, as described in the literature [60]. A stirred solution of **7a** (104 mg, 0.31 mmol), 4-methoxybenzonitrile (119 mg, 0.89 mmol) and [(Phen)$Pd(OAc)_2$] (13 mg, 31.0 μmol) dissolved in H_2O (0.12 mL), glacial AcOH (0.18 mL)

and 1,4-dioxane (0.6 mL) was heated to 140°C in a sealed pressure tube for 42 h. The reaction mixture was cooled to rt, diluted with DCM (18 mL), filtered through a celite pad and the celite washed with DCM (6 mL). The filtrate was evaporated under reduced pressure. The crude residue was purified by flash silica column chromatography (99:1 DCM:MeOH with 0.3% Et_3N to load silica), and recrystallized using MeOH to yield **8a** (74 mg, 0.16 mmol, 51%) as dark brown crystals (R_f 0.53, 95:5 DCM:MeOH). ^{1}H NMR (400 MHz, $CDCl_3$) δ 8.06 (d, *J* = 2.4 Hz, 1H, ArH indole), 7.90 – 7.81 (m, 2H, ArH MeOPh), 7.65 (s, 1H, ArH indole), 7.53 – 7.47 (m, 2H, ArH Bn), 7.43 – 7.36 (m, 2H, ArH Bn), 7.35 – 7.31 (m, 1H, ArH Bn), 7.29 (dd, *J* = 8.9, 0.5 Hz, 1H, ArH, indole), 7.05 (dd, *J* = 8.9, 2.5 Hz, 1H, ArH indole), 7.02 – 6.96 (m, 2H, ArH MeOPh), 5.17 (s, 2H, CH_2 Bn), 4.22 (t, *J* = 6.3 Hz, 2H, N1-CH_2), 3.90 (s, 3H, O-CH_3), 3.70 (t, *J* = 4.6 Hz, 4H, O-CH_2 morpholino), 2.77 (t, *J* = 6.4 Hz, 2H, N1-$CH_2C\underline{H_2}$), 2.48 (t, *J* = 4.7 Hz, 4H, N-CH_2 morpholino). ^{13}C NMR (101 MHz, $CDCl_3$) δ 189.85, 162.30, 155.70, 137.49, 137.18, 133.59, 131.90, 130.98, 128.64, 128.31, 127.95, 127.81, 115.46, 114.71, 113.63, 110.48, 105.36, 70.69, 67.02, 57.84, 55.58, 53.82, 44.45. HRMS-ESI calculated for $C_{29}H_{31}N_2O_4$ $[M+H]^+$ 471.2278, found *m/z* 471.2239.

6-(Benzyloxy)-3-(4-methoxybenzoyl)-1-[2-(morpholin-4-yl)ethyl]-1*H*-indole (8b)

A solution of **7b** (123 mg, 0.37 mmol), 4-methoxybenzonitrile (144 mg, 1.1 mmol) and [(Phen)$Pd(OAc)_2$] (14 mg, 37.0 μmol) in H_2O (0.14 mL), glacial AcOH (0.21 mL) and 1,4-dioxane (0.7 mL) was reacted as described in the procedure for **8a**. The crude residue was purified by flash silica column chromatography (99:1 DCM:MeOH, with 0.3% ammonia to load silica) to yield **8b** (129 mg, 0.27 mmol, 75%) as a brown solid (R_f 0.47, 95:5 DCM:MeOH). ^{1}H NMR (500 MHz, $CDCl_3$) δ 8.29 (d, *J* = 8.7 Hz, 1H, ArH indole), 7.87 – 7.80 (m, 2H, ArH MeOPh), 7.56 (s, 1H, ArH indole), 7.50 – 7.44 (m, 2H, ArH Bn), 7.42 – 7.36 (m, 2H, ArH Bn), 7.36 – 7.30 (m, 1H, ArH Bn), 7.05 (dd, *J* = 8.7, 2.2 Hz, 1H, ArH indole), 7.00 – 6.93 (m, 2H, ArH MeOPh), 6.90 (d, *J* = 2.2 Hz, 1H, ArH indole), 5.14 (s, 2H, CH_2 Bn), 4.15 (t, *J* = 6.4 Hz, 2H, N1-CH_2), 3.87 (s, 3H, O-CH_3), 3.68 (t, *J* = 4.6 Hz, 4H, O-CH_2 morpholino), 2.72 (t, *J* = 6.4 Hz, 2H, N1-$CH_2C\underline{H_2}$), 2.46 (t, *J* = 4.7 Hz, 4H, N-CH_2 morpholino). ^{13}C NMR (126 MHz, $CDCl_3$) δ 189.64, 162.25, 156.39, 137.55, 137.15, 136.38, 133.43, 130.93, 128.65, 128.02, 127.57, 123.54, 121.79, 115.74, 113.53, 112.23, 95.19, 70.75, 66.94, 57.51, 55.50, 53.74, 44.12. HRMS-ESI calculated for $C_{29}H_{31}N_2O_4$ $[M+H]^+$ 471.2276, found *m/z* 471.2278.

5-(Benzyloxy)-1-[2-(morpholin-4-yl)ethyl]-3-(naphthalene-1-carbonyl)-1*H*-indole (8c)

A solution of **7a** (525 mg, 1.6 mmol), 1-naphthonitrile (717 mg, 4.7 mmol) and [(Phen)Pd(OAc)$_2$] (76 mg, 0.19 mmol) in H_2O (0.63 mL), glacial AcOH (0.93 mL) and 1,4-dioxane (3.1 mL) was reacted as described in the procedure for **8a**. The crude residue was purified by flash silica column chromatography twice (1st 99:1 DCM:MeOH, with 0.3% Et_3N to load silica, 2nd 10:1 EA:hexane with 0.5% ammonia to load silica) to yield **8c** (138 mg, 0.28 mmol, 18%) as a brown solid (R_f 0.34, 4:1 EA:hexane). ^{1}H NMR (400 MHz, $CDCl_3$) δ 8.22 – 8.15 (m, 2H, ArH indole & naphthalene), 8.00 – 7.89 (m, 2H, ArH naphthalene), 7.65 (dd, *J* = 7.0, 1.2 Hz, 1H, ArH naphthalene), 7.57 – 7.45 (m, 5H, ArH Bn & naphthalene), 7.45 – 7.37 (m, 3H, ArH Bn & indole), 7.37 – 7.27 (m, 2H, ArH Bn & indole), 7.08 (dd, *J* = 8.9, 2.5 Hz, 1H, ArH indole), 5.20 (s, 2H, CH_2 Bn), 4.29 – 3.97 (br m, 2H, N1-CH_2), 3.76 – 3.36 (br m, 4H, O-CH_2 morpholino), 2.85 – 2.58 (br m, 2H, N1-CH_2CH_2), 2.57 – 2.19 (br m, 4H, N-CH_2 morpholino). ^{13}C NMR (101 MHz, $CDCl_3$) δ 192.18, 156.04, 139.21, 138.98, 137.42, 133.83, 132.12, 130.87, 130.04, 128.66, 128.32, 128.00, 127.86, 127.76, 126.89, 126.43, 126.05, 125.80, 124.60, 117.54, 114.86, 110.71, 105.55, 70.72, 66.87, 57.57, 53.65, 44.40. HRMS-ESI calculated for $C_{32}H_{31}N_2O_3$ $[M+H]^+$ 491.2329, found *m/z* 491.2303.

5-(Benzyloxy)-3-cyclohexanecarbonyl-1-[2-(morpholin-4-yl)ethyl]-1*H*-indol (8d)

A solution of **7a** (100 mg, 0.3 mmol), cyclohexanecarbonitrile (106 µL, 0.89 mmol) and [(Phen)Pd(OAc)$_2$] (12 mg, 30.0 µmol) in H_2O (0.12 mL), glacial AcOH (0.18 mL) and 1,4-dioxane (0.6 mL) was reacted as described in the procedure for **8a**. The crude residue was purified by flash silica column chromatography (99:1 DCM:MeOH, with 0.3% Et_3N to load silica) to yield a red oil as a 4:1 mixture of **8d** and **7a** (100 mg) (R_f **8d** 0.17, 99:1 DCM:MeOH). This mixture could not be separated further and was therefore used without further purification in subsequent reactions. HRMS-ESI calculated for **8d** $C_{28}H_{35}N_2O_3$ $[M+H]^+$ 447.2642, found *m/z* 447.2605 (from HRMS-ESI of the 4:1 mixture).

5-(Benzyloxy)-3-(4-methoxybenzoyl)-1-[(oxan-4-yl)methyl]-1*H*-indole (8e)

A solution of **7c** (103 mg, 0.32 mmol), 4-methoxybenzonitrile (127 mg, 0.95 mmol) and [(Phen)Pd(OAc)$_2$] (14 mg, 32.0 µmol) in H_2O (0.12 mL), glacial AcOH (0.18 mL) and 1,4-dioxane (0.6 mL) was reacted as described in the procedure for **8a**. The crude residue was purified by flash silica column chromatography (2:1 PE:EA) to yield **8e** (118 mg, 0.26 mmol, 81%) as a brown oil (R_f 0.32, 1:1 PE:EA). ^{1}H NMR (400 MHz, $CDCl_3$) δ 8.04 (d, *J* = 2.5 Hz, 1H, ArH indole), 7.87 – 7.80 (m, 2H, ArH MeOPh), 7.53 – 7.47 (m, 3H, ArH Bn & ArH indole), 7.43 – 7.36 (m, 2H, ArH Bn), 7.36 – 7.30 (m, 1H, ArH Bn), 7.28 (dd, *J* = 8.9, 0.5 Hz,

1H, ArH indole), 7.06 (dd, *J* = 8.9, 2.5 Hz, 1H, ArH indole), 7.03 – 6.97 (m, 2H, ArH MeOPh), 5.17 (s, 2H, CH_2 Bn), 4.01 (d, *J* = 7.3 Hz, 2H, N-CH_2), 3.99 – 3.93 (m, 2H, O-CH_2 THP), 3.90 (s, 3H, O-CH_3), 3.31 (td, *J* = 11.8, 2.2 Hz, 2H, O-CH_2 THP), 2.21 – 2.05 (m, 1H, CH THP), 1.56 – 1.28 (m, 4H, O-$CH_2C\underline{H_2}$ THP). ^{13}C NMR (101 MHz, $CDCl_3$) δ 189.89, 162.34, 155.71, 137.47, 136.76, 133.54, 132.11, 130.96, 128.65, 128.39, 127.97, 127.82, 115.43, 114.88, 113.71, 110.83, 105.31, 70.69, 67.42, 55.58, 53.33, 36.06, 30.86. HRMS-ESI calculated for $C_{29}H_{30}NO_4$ $[M+H]^+$ 456.2169, found *m/z* 456.2128.

7-(Benzyloxy)-3-(4-methoxybenzoyl)-1-[(oxan-4-yl)methyl]-1*H*-indole (8f)

A solution of **7d** (104 mg, 0.32 mmol), 4-methoxybenzonitrile (129 mg, 0.97 mmol) and [(Phen)Pd(OAc)$_2$] (13 mg, 32.0 μmol) in H_2O (0.12 mL), glacial AcOH (0.18 mL) and 1,4-dioxane (0.6 mL) was reacted as described in the procedure for **8a**. The crude residue was purified by flash silica column chromatography (2:1 hexane:EA) to yield **8f** (85 mg, 0.19 mmol, 58%) as a pale pinkish-white solid (R_f 0.44, 1:1 hexane:EA). ^{1}H NMR (400 MHz, $CDCl_3$) δ 8.01 (dd, *J* = 8.1, 0.9 Hz, 1H, ArH indole), 7.85 – 7.78 (m, 2H, ArH MeOPh), 7.51 – 7.46 (m, 2H, ArH Bn), 7.45 – 7.37 (m, 3H, ArH Bn), 7.37 (s, 1H, ArH indole), 7.23 (t, *J* = 8.0 Hz, 1H, ArH indole), 7.02 – 6.95 (m, 2H, ArH MeOPh), 6.87 (dd, *J* = 7.9, 0.9 Hz, 1H, ArH indole), 5.15 (s, 2H, CH_2 Bn), 4.10 (d, *J* = 7.2 Hz, 2H, N-CH_2), 3.89 (s, 3H, O-CH_3), 3.86 – 3.77 (m, 2H, O-CH_2 THP), 3.12 (td, *J* = 11.6, 2.4 Hz, 2H, O-CH_2 THP), 2.14 – 1.93 (m, 1H, CH THP), 1.22 – 0.99 (m, 4H, O-$CH_2C\underline{H_2}$ THP). ^{13}C NMR (101 MHz, $CDCl_3$) δ 189.81, 162.33, 146.60, 137.85, 136.49, 133.54, 131.04, 130.25, 128.82, 128.74, 128.66, 126.27, 123.20, 115.56, 115.32, 113.64, 105.14, 70.84, 67.54, 56.29, 55.55, 37.10, 30.22. HRMS-ESI calculated for $C_{29}H_{30}NO_4$ $[M+H]^+$ 456.2169, found *m/z* 456.2129.

5-(Benzyloxy)-3-(naphthalene-1-carbonyl)-1-[(oxan-4-yl)methyl]-1*H*-indole (8g)

A solution of **7c** (103 mg, 0.32 mmol), 1-naphthonitrile (147 mg, 0.96 mmol) and [(Phen)Pd(OAc)$_2$] (14 mg, 32.0 μmol) in H_2O (0.12 mL), glacial AcOH (0.18 mL) and 1,4-dioxane (0.6 mL) was reacted as described in the procedure for **8a**. The crude residue was purified by flash silica column chromatography (2:1 PE:EA) to yield **8g** (87 mg, 0.18 mmol, 59%) as a brown oil (R_f 0.5, 1:1 PE:EA). ^{1}H NMR (400 MHz, $CDCl_3$) δ 8.19 (dd, *J* = 8.5, 1.2 Hz, 1H, ArH naphthalene), 8.13 (d, *J* = 2.5 Hz, 1H, ArH indole), 7.98 (dd, *J* = 8.3, 1.1 Hz, 1H, ArH naphthalene), 7.95 – 7.89 (m, 1H, ArH naphthalene), 7.66 (dd, *J* = 7.0, 1.3 Hz, 1H, ArH naphthalene), 7.60 – 7.44 (m, 5H, ArH Bn & naphthalene), 7.44 – 7.37 (m, 2H, ArH Bn), 7.37 – 7.31 (m, 1H, ArH indole), 7.28 (d, *J* = 8.9 Hz, 1H, ArH Bn), 7.27 (s, 1H, ArH

indole), 7.08 (dd, *J* = 8.9, 2.5 Hz, 1H, ArH indole), 5.18 (s, 2H, CH_2 Bn), 4.00 – 3.85 (m, 4H, N-CH_2 & O-CH_2 THP), 3.28 (td, *J* = 11.8, 2.1 Hz, 2H, O-CH_2 THP), 2.13 – 1.96 (m, 1H, CH THP), 1.48 – 1.24 (m, 4H, O-$CH_2C\underline{H_2}$ THP). ^{13}C NMR (101 MHz, $CDCl_3$) δ 192.14, 156.02, 139.12, 138.36, 137.40, 133.88, 132.31, 130.90, 130.16, 128.67, 128.33, 128.01, 127.88, 126.86, 126.45, 126.11, 125.97, 124.71,117.40, 114.99, 111.03, 105.44, 70.70, 67.36, 53.28, 35.93, 30.75. HRMS-ESI calculated for $C_{32}H_{29}NNaO_3$ $[M+Na]^+$ 498.2040, found *m/z* 498.1996.

5-(Benzyloxy)-3-(4-methoxybenzoyl)-1-[(oxolan-3-yl)methyl]-1*H*-indole (8h)

A solution of **7e** (87 mg, 0.28 mmol), 4-methoxybenzonitrile (130 mg, 0.98 mmol) and [(Phen)$Pd(OAc)_2$] (13 mg, 28.0 μmol) in H_2O (0.12 mL), glacial AcOH (0.18 mL) and 1,4-dioxane (0.6 mL) was reacted as described in the procedure for **8a**. The crude residue was purified by flash silica column chromatography (2:1 PE:EA) to yield **8h** (84 mg, 0.19 mmol, 67%) as a light brown oil (R_f 0.12, 2:1 PE:EA). ^{1}H NMR (400 MHz, $CDCl_3$) δ 8.05 (d, *J* = 2.5 Hz, 1H, ArH indole), 7.83 (dt, *J* = 8.7, 2.8, 2.6 Hz, 2H, ArH MeOPh), 7.54 (s, 1H, ArH indole), 7.50 (d, *J* = 6.9 Hz, 2H, ArH Bn), 7.40 (t, *J* = 7.2 Hz, 2H, ArH Bn), 7.32 (dd, *J* = 9.4, 8.1 Hz, 2H, ArH Bn, ArH indole), 7.07 (dd, *J* = 8.9, 2.5 Hz, 1H, ArH indole), 7.00 (dt, *J* = 8.7, 2.8, 2.6 Hz, 2H, ArH MeOPh), 5.17 (s, 2H, CH_2 Bn), 4.11 (d, *J* = 7.8 Hz, 2H, N-CH_2), 3.97 (td, *J* = 8.3, 5.4 Hz, 1H, O-CH_2 THF), 3.90 (s, 3H, O-CH_3), 3.77 (t, *J* = 8.3, 6.9 Hz, 1H, O-CH_2 THF), 3.71 (dd, *J* = 9.1, 6.4 Hz, 1H, O-CH_2 THF), 3.61 (dd, *J* = 9.1, 4.4 Hz, 1H, O-CH_2 THF), 2.92 – 2.79 (m, 1H, CH THF), 2.12 – 1.99 (m, 1H, CH_2 THF), 1.73 – 1.60 (m, 1H, CH_2 THF). ^{13}C NMR (101 MHz, $CDCl_3$) δ 189.91, 162.36, 155.77, 137.45, 136.23, 133.48, 132.00, 130.96, 128.65, 128.41, 127.97, 127.82, 115.71, 114.99, 113.73, 110.68, 105.34, 70.85, 70.69, 67.62, 55.58, 49.90, 39.74, 29.86. HRMS-ESI calculated for $C_{28}H_{28}NO_4$ $[M+H]^+$ 442.2013, found *m/z* 442.1985.

3-(4-Methoxybenzoyl)-1-[2-(morpholin-4-yl)ethyl]-1*H*-indol-5-ol (9a)

A flask containing a stirred solution of **8a** (497 mg, 1.1 mmol), EtOH (12 mL), MeOH (12 mL) and AcOH (1 mL) was evacuated and purged with N_2, followed by addition of Pd/C (10% by weight loading (dry basis), matrix carbon powder, wet support) (50 mg). The solution was placed under an atmosphere of hydrogen (balloon) (evacuated and purged with H_2 three times) and stirred for 20 h at rt. The solution was then filtered through celite, the celite washed with 1:1 EtOH:MeOH and then MeOH, and the filtrate evaporated under reduced pressure. The crude residue was purified by precipitation in EA to yield the desired

product **9a** (54 mg, 0.14 mmol, 13%) as a pale fawn solid (R_f 0.29, 95:5 DCM:MeOH). ^{1}H NMR (400 MHz, DMSO-d_6) δ 9.08 (s, 1H, OH), 7.93 (s, 1H, ArH indole), 7.77 (d, *J* = 8.3 Hz, 2H, ArH MeOPh), 7.66 (s, 1H, ArH indole), 7.41 (d, *J* = 8.8 Hz, 1H, ArH indole), 7.06 (d, *J* = 8.3 Hz, 2H, ArH MeOPh), 6.76 (d, *J* = 8.7 Hz, 1H, ArH indole), 4.30 (t, *J* = 6.2 Hz, 2H, N1-CH_2), 3.85 (s, 3H, O-CH_3), 3.54 (t, *J* = 4.6 Hz, 4H, O-CH_2 morpholino), 2.67 (t, *J* = 6.3 Hz, 2H, N1-$CH_2C\underline{H_2}$), 2.47 – 2.35 (br m, 4H, N-CH_2 morpholino). ^{13}C NMR (101 MHz, DMSO-d_6) δ 188.12, 161.52, 153.35, 138.50, 133.22, 130.81, 130.44, 127.90, 113.54, 113.22, 112.71, 111.12, 106.06, 66.26, 57.30, 55.40, 53.17, 43.09. HRMS-ESI calculated for $C_{22}H_{25}N_2O_4$ $[M+H]^+$ 381.1809, found *m/z* 381.1779. Analytical RP-HPLC R_t = 12.89 min.

3-(4-Methoxybenzoyl)-1-[2-(mopholin-4-yl)ethyl]-1*H*-indol-6-ol (9b)

A mixture of **8b** (75 mg, 0.16 mmol), EtOH (2.6 mL), EA (1.3 mL) and Pd/C (7.5 mg) was reacted as described in the procedure for **9a**. The reaction mixture was filtered through celite, the celite washed with 2:1 EtOH:EA and then MeOH, and the filtrate evaporated under reduced pressure. The crude residue was purified by precipitation in EA and semi-preparative RP-HPLC to yield the desired product **9b** (4.8 mg, 12.6 µmol, 8%) as a brown solid (R_f 0.21, 95:5 DCM:MeOH). ^{1}H NMR (400 MHz, DMSO-d_6) δ 9.38 (s, 1H, ArOH), 8.00 (d, *J* = 8.6 Hz, 1H, ArH indole), 7.84 (s, 1H, ArH indole), 7.81 – 7.75 (m, 2H, ArH MeOPh), 7.09 – 7.03 (m, 2H, ArH MeOPh), 6.88 (d, *J* = 2.1 Hz, 1H, ArH indole), 6.76 (dd, *J* = 8.5, 2.1 Hz, 1H, ArH indole), 4.25 (t, *J* = 6.3 Hz, 2H, N1-CH_2), 3.85 (s, 3H, O-CH_3), 3.55 (t, *J* = 4.6 Hz, 4H, O-CH_2 morpholino), 2.66 (t, *J* = 6.3 Hz, 2H, N1-$CH_2C\underline{H_2}$), 2.44 (t, *J* = 4.6 Hz, 4H, N-CH_2 morpholino). ^{13}C NMR (126 MHz, DMSO-d_6) δ 188.10, 161.59, 154.39, 137.76, 137.37, 133.07, 130.45, 122.27, 119.71, 114.01, 113.54, 112.04, 95.81, 66.25, 57.07, 55.41, 53.18, 42.91. HRMS-ESI calculated for $C_{22}H_{25}N_2O_4$ $[M+H]^+$ 381.1809, found *m/z* 381.1804. Analytical RP-HPLC R_t = 13.78 min.

1-[2-(Morpholin-4-yl)ethyl]-3-(naphthalene-1-carbonyl)-1*H*-indol-5-ol (9c)

A mixture of **8c** (299 mg, 0.61 mmol), EtOH (11 mL), EA (5.5 mL) and Pd/C (30 mg) was reacted as described in the procedure for **9a**. The reaction mixture was filtered through celite, the celite washed with 2:1 EtOH:EA and then MeOH, and the filtrate evaporated under reduced pressure. The crude residue was purified by precipitation in EA to yield the desired product **9c** (95 mg, 0.24 mmol, 39%) as a white solid (R_f 0.35, 95:5 DCM:MeOH). ^{1}H NMR (400 MHz, MeOD-d_4) δ 8.03 (dd, *J* = 8.2, 4.6 Hz, 2H, ArH naphthalene), 7.99 – 7.94 (m, 1H, ArH naphthalene), 7.82 (d, *J* = 2.4 Hz, 1H, ArH indole), 7.65 (dd, *J* = 7.0, 1.4 Hz, 1H, ArH

naphthalene), 7.62 – 7.57 (m, 1H, ArH naphthalene), 7.55 (s, 1H, ArH indole), 7.55 – 7.46 (m, 2H, ArH naphthalene), 7.39 (d, *J* = 8.8 Hz, 1H, ArH indole), 6.88 (dd, *J* = 8.8, 2.5 Hz, 1H, ArH indole), 4.21 (t, *J* = 6.1 Hz, 2H, N1-CH_2), 3.53 – 3.40 (m, 4H, O-CH_2 morpholino), 2.67 (t, *J* = 6.1 Hz, 2H, N1-$CH_2C\underline{H_2}$), 2.37 (t, *J* = 4.6 Hz, 4H, N-CH_2 morpholino). ^{13}C NMR (126 MHz, $CDCl_3$) δ 194.66, 155.60, 141.78, 141.08, 135.85, 134.00, 132.88, 132.13, 130.36, 129.98, 128.93, 128.49, 128.07, 127.79, 126.68, 119.17, 115.54, 112.71, 109.78, 68.95, 59.58, 55.73, 46.54. HRMS-ESI calculated for $C_{25}H_{25}N_2O_3$ $[M+H]^+$ 401.1860, found *m/z* 401.1850. Analytical RP-HPLC R_t = 14.70 min.

3-Cyclohexanecarbonyl-1-[2-(morpholin-4-yl)ethyl]-1*H*-indol-5-ol (9d)

A mixture of **8d** (85 mg, 0.19 mmol), EtOH (3 mL), EA (1.5 mL) and Pd/C (8.5 mg) was reacted as described in the procedure for **9a**. The reaction mixture was filtered through celite, the celite washed with 2:1 EtOH:EA and then MeOH, and the filtrate evaporated under reduced pressure. The crude residue was purified by flash silica gel column chromatography (1:1 PE:EA) and precipitation in EA to yield the desired product **9d** (11 mg, 30.9 µmol, 16%) as a pale pink solid (R_f 0.54, 95:5 DCM:MeOH). ^{1}H NMR (400 MHz, DMSO-d_6) δ 9.01 (s, 1H, ArOH), 8.26 (s, 1H, ArH indole), 7.60 (d, *J* = 2.4 Hz, 1H, ArH indole), 7.35 (d, *J* = 8.8 Hz, 1H, ArH indole), 6.71 (dd, *J* = 8.8, 2.4 Hz, 1H, ArH indole), 4.27 (t, *J* = 6.4 Hz, 2H, N1-CH_2), 3.53 (t, *J* = 4.6 Hz, 4H, O-CH_2 morpholino), 3.12 – 2.99 (m, 1H, CH cyclohexane), 2.66 (t, *J* = 6.4 Hz, 2H, N1-$CH_2C\underline{H_2}$), 2.43 (t, *J* = 4.7 Hz, 4H, N-CH_2 morpholino), 1.84 – 1.65 (m, 5H, CH_2 cyclohexane), 1.49 – 1.31 (m, 4H, CH_2 cyclohexane), 1.27 – 1.13 (m, 1H, CH_2 cyclohexane). ^{13}C NMR (126 MHz, DMSO-d_6) δ 197.90, 153.24, 136.82, 130.92, 127.23, 113.26, 112.37, 110.97, 106.11, 66.23, 57.20, 53.14, 46.27, 43.26, 29.73, 25.67, 25.49. HRMS-ESI calculated for $C_{21}H_{29}N_2O_3$ $[M+H]^+$ 357.2173, found *m/z* 357.2154. Analytical RP-HPLC R_t = 13.77 min.

3-(4-Methoxybenzoyl)-1-[(oxan-4-yl)methyl]-1*H*-indol-5-ol (9e)

A mixture of **8e** (1.10 g, 2.4 mmol), EtOH (15 mL), $CHCl_3$ (40 mL), AcOH (1 mL) and Pd/C (110 mg) was reacted as described in the procedure for **9a**. The reaction mixture was filtered through celite, the celite washed with 3:1 $CHCl_3$:EtOH and then MeOH, and the filtrate evaporated under reduced pressure. The crude residue was purified by precipitation in 1:1 EtOH:MeOH to yield the desired product **9e** (588 mg, 1.6 mmol, 67%) as a creamy pearl solid (R_f 0.37, 95:5 DCM:MeOH). ^{1}H NMR (400 MHz, DMSO-d_6) δ 9.11 (s, 1H, OH), 7.89 (s, 1H, ArH indole), 7.82 – 7.73 (m, 2H, ArH MeOPh), 7.68 (d, *J* = 2.4 Hz, 1H, ArH indole),

7.45 (d, *J* = 8.8 Hz, 1H, ArH indole), 7.12 – 7.03 (m, 2H, ArH MeOPh), 6.78 (dd, *J* = 8.8, 2.4 Hz, 1H, ArH indole), 4.11 (d, *J* = 7.2 Hz, 2H, N-CH_2), 3.85 (s, 3H, O-CH_3), 3.84 – 3.76 (m, 2H, O-CH_2 THP), 3.19 (td, *J* = 11.5, 2.3 Hz, 2H, O-CH_2 THP), 2.15 – 1.98 (m, 1H, CH THP), 1.41 – 1.19 (m, 4H O-$CH_2C\underline{H_2}$ THP). ^{13}C NMR (101 MHz, DMSO-d_6) δ 188.18, 161.54, 153.40, 138.08, 133.15, 131.11, 130.46, 128.00, 113.62, 113.26, 112.86, 111.46, 106.07, 66.48, 55.38, 51.59, 35.29, 30.00. HRMS-ESI calculated for $C_{22}H_{23}NNaO_4$ $[M+Na]^+$ 388.1519, found *m/z* 388.1489. Analytical RP-HPLC R_t = 18.02 min.

3-(4-Methoxybenzoyl)-1-[(oxan-4-yl)methyl]-1*H*-indol-7-ol (9f)

A mixture of **8f** (723 mg, 1.6 mmol), EtOH (12 mL), $CHCl_3$ (32 mL) and Pd/C (72 mg) was reacted as described in the procedure for **9a**. The crude residue was purified by flash silica gel column chromatography (2:1 hexane:EA) to yield the desired product **9f** (322 mg, 0.88 mmol, 55%) as a brown oil, (R_f 0.47, 1:1 PE:EA). ^{1}H NMR (400 MHz, $CDCl_3$) δ 7.96 – 7.89 (m, 1H, ArH indole), 7.87 – 7.79 (m, 2H, ArH MeOPh), 7.44 (s, 1H, ArH indole), 7.07 (t, *J* = 7.9 Hz, 1H, ArH indole), 7.02 – 6.95 (m, 2H, ArH MeOPh), 6.69 (dt, *J* = 7.6, 1.1 Hz, 1H, ArH indole), 4.31 (d, *J* = 7.2 Hz, 2H, N-CH_2), 4.02 – 3.91 (m, 2H, O-CH_2 THP), 3.89 (s, 3H, O-CH_3), 3.31 (td, *J* = 11.7, 2.3 Hz, 2H, O-CH_2 THP), 2.31 – 2.07 (m, 1H, CH THP), 1.58 – 1.27 (m, 4H, O-$CH_2C\underline{H_2}$ THP). ^{13}C NMR (101 MHz, $CDCl_3$) δ 190.53, 162.47, 143.72, 138.20, 133.38, 131.19, 130.33, 126.12, 123.47, 115.56, 114.63, 113.71, 109.48, 67.65, 55.72, 55.59, 37.41, 30.45. HRMS-ESI calculated for $C_{22}H_{23}NNaO_4$ $[M+Na]^+$ 388.1519, found *m/z* 388.1553. Analytical RP-HPLC R_t = 18.19 min.

3-(Naphthalene-1-carbonyl)-1-[(oxan-4-yl)methyl]-1*H*-indol-5-ol (9g)

A mixture of **8g** (54 mg, 0.11 mmol), EtOH (2.5 mL), EA (1.25 mL) and Pd/C (6 mg) was reacted as described in the procedure for **9a**. The reaction mixture was filtered through celite, the celite washed with 2:1 EtOH:EA and then MeOH, and the filtrate evaporated under reduced pressure. The crude residue was purified by flash silica gel column chromatography (10:1 EA:hexane), recrystallisation in MeOH and semi-preparative RP-HPLC to yield the desired product **9g** (14.7 mg, 38.1 µmol, 33%) as a brown solid (R_f 0.65, 95:5 DCM:MeOH). ^{1}H NMR (400 MHz, MeOD-d_4) δ 8.06 – 7.99 (m, 2H, ArH naphthalene), 7.98 – 7.92 (m, 1H, ArH naphthalene), 7.82 (d, *J* = 2.7 Hz, 1H, ArH indole), 7.65 – 7.60 (m, 1H, ArH naphthalene), 7.60 – 7.49 (m, 2H, ArH naphthalene), 7.48 – 7.42 (m, 2H, ArH indole & naphthalene), 7.40 – 7.36 (m, 1H, ArH indole), 6.88 (dd, *J* = 8.8, 2.5 Hz, 1H, ArH indole), 4.06 – 3.94 (m, 2H, N-CH_2), 3.92 – 3.80 (m, 2H, O-CH_2 THP), 3.26 (dd, *J* = 11.7, 2.1 Hz,

2H, O-CH_2 THP), 2.12 – 1.98 (m, 1H, CH THP), 1.41 – 1.21 (m, 4H, O-$CH_2C\underline{H_2}$ THP). HRMS-ESI calculated for $C_{25}H_{23}NNaO_3$ $[M+Na]^+$ 408.1570, found *m/z* 408.1535. Analytical RP-HPLC R_t = 19.69 min.

3-(4-Methoxybenzoyl)-1-[(oxolan-3-yl)methyl]-1*H*-indol-5-ol (9h)

A mixture of **8h** (72 mg, 0.16 mmol), EtOH (2.5 mL), EA (1.4 mL) and Pd/C (7 mg) was reacted as described in the procedure for **9a**. The reaction mixture was filtered through celite, the celite washed with 2:1 EtOH:EA and then MeOH, and the filtrate evaporated under reduced pressure. The crude residue was purified by flash silica gel column chromatography (1:1 hexane:EA) to give **9h** (6.8 mg, 19.4 μmol, 12%) as a brown oil (R_f 0.27, 1:1 hexane:EA). Significant degradation upon storage (56% purity according to analytical RP-HPLC) necessitated further purification immediately prior to biological testing, therefore a small amount of this material (4 mg) was purified using semi-preparative RP-HPLC to yield a sample of **9h** (1.58 mg) as a pale fawn solid. ^{1}H NMR (400 MHz, $CDCl_3$) δ 8.41 (d, *J* = 2.4 Hz, 1H, ArH indole), 7.83 (d, *J* = 8.5 Hz, 2H, ArH MeOPh), 7.52 (s, 1H, ArH indole), 7.28 (d, *J* = 6.1 Hz, 1H, ArH indole), 7.02 (d, *J* = 8.6 Hz, 2H, ArH MeOPh), 6.98 (dd, *J* = 8.8, 2.4 Hz, 1H, ArH indole), 4.10 (d, *J* = 7.8 Hz, 2H, N-CH_2), 3.96 (td, *J* = 8.3, 5.4 Hz, 1H, O-CH_2 THF), 3.90 (s, 3H, O-CH_3), 3.81 – 3.66 (m, 2H, O-CH_2 THF), 3.61 (dd, *J* = 9.1, 4.3 Hz, 1H, O-CH_2 THF), 2.86 (td, *J* = 12.8, 6.2 Hz, 1H, CH THF), 2.05 (m, 1H, CH_2 THF), 1.66 (m, 1H, CH_2 THF). ^{13}C NMR (101 MHz, $CDCl_3$) δ 191.02, 162.49, 154.10, 137.38, 133.26, 131.70, 131.01, 128.69, 115.23, 113.97, 113.95, 110.69, 107.61, 70.89, 67.65, 55.62, 50.05, 39.66, 29.90. HRMS-ESI calculated for $C_{21}H_{21}NNaO_4$ $[M+Na]^+$ 374.1363, found *m/z* 374.1345. Analytical RP-HPLC R_t = 17.16 min.

***tert*-Butyl 2-{[3-(4-methoxybenzoyl)-1-[2-(morpholin-4-yl)ethyl]-1*H*-indol-5-yl]oxy}acetate (10a)**

A stirred solution of **9a** (87 mg, 0.23 mmol) in anhydrous DMF (2.5 mL) was added dropwise to a mixture of NaH (60% by mass dispersion in mineral oil) (13 mg, 0.54 mmol) in anhydrous DMF (1 mL). The mixture was heated to 60°C for 1 h, then cooled to rt and a solution of *tert*-butylbromoacetate (44 μL, 0.30 mmol) in anhydrous DMF (1 mL) was added. The reaction was stirred at 60°C for 3 h, then quenched with sat. aq. NH_4CL (4 mL) and H_2O (4 mL) and extracted with EA (4 × 4 mL). The combined organics were washed with H_2O (3 × 7 mL), dried over $MgSO_4$ and evaporated under reduced pressure. The crude product was purified by flash silica gel column chromatography (99:1 DCM:MeOH with 0.3% ammonia

to load silica) to yield **10a** (51 mg, 0.10 mmol, 45%) as a pale yellow oil, (R_f 0.39, 95:5 DCM:MeOH). ^{1}H NMR (400 MHz, $CDCl_3$) δ 7.89 (d, *J* = 2.6 Hz, 1H, ArH indole), 7.87 – 7.80 (m, 2H, ArH MeOPh), 7.65 (s, 1H, ArH indole), 7.29 (d, *J* = 8.9 Hz, 1H, ArH indole), 7.07 (dd, *J* = 8.9, 2.6 Hz, 1H, ArH indole), 7.02 – 6.95 (m, 2H, ArH MeOPh), 4.62 (s, 2H, O-CH_2), 4.36 – 4.08 (br m, 2H, N1-CH_2), 3.89 (s, 3H, O-CH_3), 3.78 – 3.62 (br m, 4H, O-CH_2 morpholino), 2.91 – 2.65 (br m, 2H, N1-$CH_2C\underline{H_2}$), 2.63 – 2.36 (br m, 4H, N-CH_2 morpholino), 1.51 (s, 9H, CH_3 *t* Bu). ^{13}C NMR (126 MHz, $CDCl_3$) δ 189.67, 168.39, 162.25, 154.71, 137.26, 133.53, 132.16, 130.89, 128.10, 115.42, 114.60, 113.60, 110.59, 105.12, 82.27, 66.91, 66.33, 57.73, 55.54, 53.73, 44.28, 28.19. HRMS-ESI calculated for $C_{28}H_{35}N_2O_6$ $[M+H]^+$ 495.2490, found *m/z* 495.2457.

***tert*-Butyl 2-({1-[2-(morpholin-4-yl)ethyl]-3-(naphthalene-1-carbonyl)-1*H*-indol-5-yl}oxy)acetate (10b)**

A solution of **9c** (71 mg, 0.18 mmol), NaH (14 mg, 0.36 mmol) and *tert*-butylbromoacetate (34 µL, 0.23 mmol) in DMF (3 mL) was reacted as described in the procedure for **10a**. The crude product was purified by flash silica gel column chromatography (99:1 DCM:MeOH with 0.3% ammonia to load silica) to yield **10b** (56 mg, 0.11 mmol, 61%) as a brown oil (R_f 0.6, 95:5 DCM:MeOH). ^{1}H NMR (400 MHz, $CDCl_3$) δ 8.14 (d, *J* = 8.3 Hz, 1H, ArH naphthalene), 8.02 (d, *J* = 2.5 Hz, 1H, ArH indole), 7.96 (d, *J* = 8.2 Hz, 1H, ArH naphthalene), 7.90 (d, *J* = 8.0 Hz, 1H, ArH naphthalene), 7.63 (d, *J* = 6.9 Hz, 1H, ArH naphthalene), 7.56 – 7.42 (m, 3H, ArH naphthalene), 7.38 (s, 1H, ArH indole), 7.29 (d, *J* = 8.9 Hz, 1H, ArH indole), 7.10 (dd, *J* = 9.0, 2.6 Hz, 1H, ArH indole), 4.67 (s, 2H, O-CH_2), 4.25 – 4.00 (br m, 2H, N1-CH_2), 3.70 – 3.43 (br m, 4H, O-CH_2 morpholino), 2.80 – 2.57 (br m, 2H, N1-$CH_2C\underline{H_2}$), 2.54 – 2.24 (br m, 4H, N-CH_2 morpholino), 1.54 (s, 9H, CH_3 *t* Bu). ^{13}C NMR (101 MHz, $CDCl_3$) δ 192.09, 168.44, 155.09, 139.13, 139.05, 133.85, 132.38, 130.85, 130.04, 128.33, 127.60, 126.88, 126.43, 125.99, 125.72, 124.61, 117.58, 114.92, 110.86, 105.20, 82.45, 66.79, 66.32, 57.49, 53.59, 44.28, 28.25. HRMS-ESI calculated for $C_{31}H_{35}N_2O_5$ $[M+H]^+$ 515.2540, found *m/z* 515.2497.

***Tert*-Butyl 2-{[3-(4-methoxybenzoyl)-1-[(oxan-4-yl)methyl]-1*H*-indol-5-yl]oxy}acetate (10c)**

A solution of **9e** (50 mg, 0.14 mmol), NaH (11 mg, 0.27 mmol) and *tert*-butylbromoacetate (26 µL, 0.18 mmol) in DMF (3 mL) was reacted as described in the procedure for **10a**. The crude product was purified by flash silica gel column chromatography (1:1 hexane:EA) to

yield **10c** (50 mg, 0.10 mmol, 76%) as a colourless oil (R_f 0.41, 1:1 hexane:EA). ^{1}H NMR (400 MHz, $CDCl_3$-*d*) δ 7.87 (d, *J* = 2.5 Hz, 1H, ArH indole), 7.83 – 7.78 (m, 2H, ArH MeOPh), 7.48 (s, 1H, ArH indole), 7.27 (d, *J* = 7.8 Hz, 1H, ArH indole), 7.07 (dd, *J* = 8.9, 2.6 Hz, 1H, ArH indole), 7.02 – 6.95 (m, 2H, ArH MeOPh), 4.62 (s, 2H, O-CH_2), 4.03 – 3.91 (m, 4H, N-CH_2, O-CH_2 THP), 3.88 (s, 3H, O-CH_3), 3.30 (td, *J* = 11.8, 2.1 Hz, 2H, O-CH_2 THP), 2.16 – 2.04 (m, 1H, CH THP), 1.53 – 1.31 (m, 13H, O-$CH_2C\underline{H_2}$ THP & CH_3 *t*-Bu).^{13}C NMR (101 MHz, $CDCl_3$) δ 189.71, 168.38, 162.28, 154.73, 136.82, 133.53, 132.39, 130.87, 128.20, 115.41, 114.82, 113.69, 110.93, 105.05, 82.30, 67.39, 66.32, 55.55, 53.31, 36.00, 30.83, 28.21. HRMS -ESI calculated for $C_{28}H_{33}NNaO_6$ $[M+Na]^+$ 502.2200, found *m/z* 502.2164.

***tert*-Butyl 2-{[3-(4-methoxybenzoyl)-1-[(oxan-4-yl)methyl]-1*H*-indol-7-yl]oxy}acetate (10d)**

A solution of **9f** (11 mg, 30.1 µmol), NaH (2.4 mg, 60.2 µmol) and *tert*-butylbromoacetate (5.8 µL, 39.1 µmol) in anhydrous DMF (1.8 mL) was reacted as described in the procedure for **10a**. The crude product was purified by flash silica gel column chromatography (1:1 hexane:EA) to yield **10d** (4.7 mg, 9.8 µmol, 33%) as a yellow oil (R_f 0.6, 1:2 hexane:EA). ^{1}H NMR (400 MHz, $CDCl_3$) δ 8.02 (dd, *J* = 8.1, 0.8 Hz, 1H, ArH indole), 7.87 – 7.79 (m, 2H, ArH MeOPh), 7.43 (s, 1H, ArH indole), 7.17 (t, *J* = 8.0 Hz, 1H, ArH indole), 7.03 – 6.95 (m, 2H, ArH MeOPh), 6.64 (dd, *J* = 8.0, 0.8 Hz, 1H, ArH indole), 4.64 (s, 2H, O-CH_2), 4.39 (d, *J* = 7.2 Hz, 2H, N-CH_2), 3.94 (dd, *J* = 11.5, 4.0 Hz, 2H, O-CH_2 THP), 3.90 (s, 3H, O-CH_3), 3.30 (td, *J* = 11.8, 2.1 Hz, 2H, O-CH_2 THP), 2.28 – 2.11 (m, 1H, CH THP), 1.57 – 1.31 (m, 13H, O-$CH_2C\underline{H_2}$ THP & CH_3 *t* Bu). ^{13}C NMR (101 MHz, $CDCl_3$) δ 189.86, 167.36, 162.39, 145.50, 138.02, 133.53, 131.11, 130.38, 126.44, 123.03, 116.18, 115.46, 113.69, 105.22, 82.60, 67.68, 65.99, 56.19, 55.60, 37.29, 30.53, 28.25. HRMS -ESI calculated for $C_{28}H_{34}NO_6$ $[M+H]^+$ 480.2381, found *m/z* 480.2346.

2-{[3-(4-Methoxybenzoyl)-1-[2-(morpholin-4-yl)ethyl]-1*H*-indol-5-yl]oxy}acetic acid (11a)

To a stirred solution of **10a** (25 mg, 51.5 µmol) in anhydrous DCM (1.8 mL) at 0℃, was added TFA (0.9 mL). The reaction mixture was stirred at rt for 3h, then evaporated under N_2 stream, followed by reduced pressure. The TFA salt of the crude product **11a** (34 mg), was used in the next reaction without further purification. Some crude TFA salt **11a** (approx. 3 mg) was purified for biological testing by semi-preparative RP-HPLC, yielding **11a** (1.38

mg) as a white solid. HRMS-ESI calculated for $C_{24}H_{27}N_2O_6$ $[M+H]^+$ 439.1864, found *m/z* 439.1826. Analytical RP-HPLC R_t = 13.20 min.

HRMS-ESI calculated for $C_{24}H_{25}NNaO_6$ $[M+Na]^+$ 446.1574, found *m/z* 446.1561.

2-({1-[2-(Morpholin-4-yl)ethyl]-3-(naphthalene-1-carbonyl)-1*H*-indol-5-yl}oxy)acetic acid (11b)

10b (18 mg, 35.9 µmol) and TFA (0.75 mL) in anhydrous DCM (1.5 mL) were reacted as described in the procedure for **11a**. The TFA salt of the crude product **11b** (24 mg) was used in the next reaction without further purification. Some crude TFA salt **11b** (approx. 3 mg) was purified for biological testing by semi-preparative RP-HPLC, yielding **11b** (1.1 mg) as a white solid. HRMS-ESI calculated for $C_{27}H_{27}N_2O_5$ $[M+H]^+$ 459.1914, found *m/z* 459.1889. Analytical RP-HPLC R_t = 14.96 min.

2-{[3-(4-Methoxybenzoyl)-1-[(oxan-4-yl)methyl]-1*H*-indol-5-yl]oxy}acetic acid (11c)

10c (17 mg, 0.04 mmol) and TFA (0.75 mL) in anhydrous DCM (1.5 mL) were reacted as described in the procedure for **11a**. The TFA salt of the crude product **11c** (21 mg) was used in the next reaction without further purification. Some crude TFA salt **11c** (approx. 3 mg) was purified for biological testing by semi-preparative RP-HPLC, yielding **11c** (1.0 mg) as a white solid. HRMS-ESI calculated for $C_{24}H_{25}NNaO_6$ $[M+Na]^+$ 446.1574, found *m/z* 446.1561. Analytical RP-HPLC R_t = 18.10.

2-{[3-(4-Methoxybenzoyl)-1-[(oxan-4-yl)methyl]-1*H*-indol-7-yl]oxy}acetic acid (11d)

10d (3.1 mg, 6.46 µmol) and TFA (0.4 mL) in anhydrous DCM (0.8 mL) were reacted as described in the procedure for **11a**. The crude was purified by semi-preparative RP-HPLC and passed through an Amberlyst A21 ion exchange resin to remove TFA, yielding **11d** (1.45 mg, 3.4 µmol, 53%), a white solid. HRMS -ESI calculated for $C_{24}H_{24}NO_6$ $[M-H]^-$ 422.1609, found *m/z* 422.1598. Analytical RP-HPLC R_t = 17.17 min.

***tert*-Butyl *N*-[8-(2-{[3-(4-methoxybenzoyl)-1-[2-(morpholin-4-yl)ethyl]-1*H*-indol-5-yl]oxy}acetamido)octyl]carbamate (12a)**

To a solution of the TFA salt of **11a** (27 mg, 41.2 µmol) in anhydrous DMF (2 mL) were added DIPEA (21.5 µL, 0.12 mmol) and HATU (16 mg, 41.2 µmol). After stirring for 5 min, a solution of *tert*-butyl *N*-(8-aminooctyl)carbamate (prepared according to a literature procedure [61]) (33 mg, 0.14 mmol) and DIPEA (21.5 µL, 0.12 mmol) in DMF (1.5 mL) was added. The reaction mixture was stirred for 14 h and then the solvent evaporated under

reduced pressure. The crude product was purified by flash silica gel column chromatography (99:1 DCM:MeOH with 0.3% ammonia to load silica) to yield **12a** (19 mg, 28.6 mmol, 69%) as a brown oil (R_f 0.28, 9:1 DCM:MeOH). ^{1}H NMR (500 MHz, $CDCl_3$) δ 7.98 (d, *J* = 2.5 Hz, 1H, ArH indole), 7.88 – 7.81 (m, 2H, ArH MeOPh), 7.70 (br s, 1H, ArH indole), 7.33 (br s, 1H, ArH indole), 7.02 – 6.97 (m, 2H, ArH MeOPh), 6.70 (t, *J* = 5.8 Hz, 1H, ArH indole), 4.56 (s, 2H, O-CH_2), 4.52 (br s, 1H, NH), 4.31 - 4.15 (br m, 2H, N1-CH_2), 3.90 (s, 3H, O-CH_3), 3.79 – 3.56 (br m, 4H, O-CH_2 morpholino), 3.41 – 3.31 (m, 2H, CH_2 octyl), 3.14 – 3.01 (m, 2H, CH_2 octyl), 2.86 – 2.69 (br m, 2H, N1-$CH_2C\underline{H_2}$), 2.63 – 2.31 (br m, 4H, N-CH_2 morpholino), 1.60 – 1.51 (m, 2H, CH_2 octyl), 1.50 – 1.39 (m, 11H, CH_2 octyl & CH_3 *t* Bu), 1.37 – 1.23 (m, 8H, CH_2 octyl). HRMS-ESI calculated for $C_{37}H_{52}N_4NaO_7$ $[M+Na]^+$ 687.3728, found *m/z* 687.3717.

***tert*-Butyl *N*-(2-{2-[2-(2-{[3-(4-methoxybenzoyl)-1-[2-(morpholin-4-yl)ethyl]-1*H*-indol-5-yl]oxy}acetamido)ethoxy]ethoxy}ethyl)carbamate (12b)**

The TFA salt of **11a** (23 mg, 34.4 μmol), *tert*□butyl *N*-{2-[2-(2-aminoethoxy)ethoxy]-ethyl}carbamate (prepared according to a literature procedure [62]) (26 mg, 0.11 mmol) DIPEA (36 μL, 0.21 mmol) and HATU (13 mg, 34.4 μmol) in DMF (3 mL) were reacted as described in the procedure for **12a**. The crude product was purified by flash silica gel column chromatography (99:1 DCM:MeOH with 0.3% ammonia to load silica) to yield **12b** (22 mg, 32.9 μmol, 94%) as a brown oil (R_f 0.38, 9:1 DCM:MeOH). ^{1}H NMR (500 MHz, $CDCl_3$-*d*) δ 7.97 (d, *J* = 2.5 Hz, 1H, ArH indole), 7.88 – 7.82 (m, 2H, ArH MeOPh), 7.69 (br s, 1H, ArH indole), 7.33 (br s, 1H, ArH indole), 7.18 – 7.10 (br m, 1H, ArH indole), 7.06 – 6.97 (m, 3H, ArH MeOPh & NH), 5.08 (br s, 1H, NH), 4.59 (s, 2H, indole-O-CH_2), 4.31 – 4.15 (br m, 2H, N1-CH_2), 3.90 (s, 3H, O-CH_3), 3.75 – 3.51 (m, 14H, $([CH_2]_2O)_2(CH_2)_2$ & O-CH_2 morpholino), 3.32 – 3.25 (br m, 2H, $([CH_2]_2O)_2(CH_2)_2$), 2.82 – 2.71 (br m, 2H, N1-$CH_2C\underline{H_2}$), 2.61 – 2.38 (br m, 4H, N-CH_2 morpholino), 1.42 (s, 9H, CH_3 *t* Bu). ^{13}C NMR (126 MHz, $CDCl_3$) δ 162.37, 156.57, 137.17, 136.76, 133.55, 131.98, 131.04, 131.00, 128.45, 114.67, 114.38, 113.80, 113.73, 110.81, 105.54, 103.99, 74.21, 67.44, 67.42, 65.72, 55.97, 55.62, 55.60, 53.37, 43.78, 36.08, 30.87, 30.85. HRMS-ESI calculated for $C_{35}H_{48}N_4NaO_9$ $[M+Na]^+$ 691.3313, found *m/z* 691.3320.

***tert*-Butyl *N*-{8-[2-({1-[2-(morpholin-4-yl)ethyl]-3-(naphthalene-1-carbonyl)-1*H*-indol-5-yl}oxy)acetamido]octyl}carbamate (12c)**

The TFA salt of **11b** (12 mg, 18.1 μmol), *tert*-butyl *N*-(8-aminooctyl)carbamate (16 mg, 67.1 μmol), DIPEA (19 μL, 0.11 mmol) and HATU (6.8 mg, 18.1 μmol) in DMF (1.8 mL) were reacted as described in the procedure for **12a**. The crude product was purified by flash silica gel column chromatography (97:3 DCM:MeOH with 0.3% ammonia to load silica) to yield **12c** (8.3 mg, 12.1 μmol, 67%) as a brown oil (R_f 0.48, 9:1 DCM:MeOH). ^{1}H NMR (500 MHz, $CDCl_3$) δ 8.14 (d, *J* = 8.4 Hz, 1H, ArH naphthalene), 8.08 (br s, 1H, ArH indole), 7.97 (dt, *J* = 8.3, 1.0 Hz, 1H, ArH naphthalene), 7.94 – 7.87 (m, 1H, ArH naphthalene), 7.63 (dd, *J* = 7.0, 1.2 Hz, 1H, ArH naphthalene), 7.57 – 7.50 (m, 2H, ArH naphthalene), 7.47 (ddd, *J* = 8.3, 6.8, 1.5 Hz, 1H, ArH naphthalene), 7.44 (s, 1H, ArH indole), 7.32 (d, *J* = 13.2 Hz, 1H, ArH indole), 7.03 (d, *J* = 8.8 Hz, 1H, ArH indole), 6.79 – 6.67 (m, 1H, NH), 4.58 (s, 2H, indole-O-CH_2), 4.51 (s, 1H, NH), 4.21-4.05 (br m, 2H, N1-CH_2), 3.71 – 3.42 (br m, 4H, O-CH_2 morpholino), 3.41 – 3.32 (m, 2H, CH_2 octyl), 3.08 (q, *J* = 6.8 Hz, 2H, CH_2 octyl), 2.78 – 2.60 (br m, 2H, N1-$CH_2C\underline{H_2}$), 2.56 – 2.22 (br m, 4H, N-CH_2 morpholino), 1.78 – 1.52 (m, 4H, CH_2 octyl), 1.43 (s, 9H, CH_3 *t* Bu), 1.38 – 1.16 (m, 8H, CH_2 octyl). ^{13}C NMR (126 MHz, $CDCl_3$) δ 192.05, 168.33, 156.12, 154.48, 139.48, 133.89, 130.80, 130.29, 128.43, 127.95, 127.01, 126.53, 125.89, 124.63, 113.09, 110.90, 107.55, 79.12, 68.48, 66.92, 57.63, 53.66, 44.53, 40.74, 39.19, 30.17, 29.71, 29.32, 29.30, 28.58, 26.96, 26.86 (four quaternary carbons were not observed). HRMS-ESI calculated for $C_{40}H_{53}N_4O_6$ $[M+H]^+$ 685.3960, found *m/z* 685.3955.

***tert*-Butyl *N*-[2-(2-{2-[2-({1-[2-(morpholin-4-yl)ethyl]-3-(naphthalene-1-carbonyl)-1*H*-indol-5-yl}oxy)acetamido]ethoxy}ethoxy)ethyl]carbamate (12d)**

The TFA salt of **11b** (27 mg, 39.1 μmol), *tert*-butyl *N*-{2-[2-(2-aminoethoxy)ethoxy]-ethyl}carbamate (33 mg, 0.13 mmol), DIPEA (41 μL, 0.23 mmol) and HATU (15 mg, 39.1 μmol) in DMF (3.5 mL) were reacted as described in the procedure for **12a**. The crude product was purified by flash silica gel column chromatography (98:2 DCM:MeOH with 0.3% ammonia to load silica) to yield **12d** (13 mg, 18.9 μmol, 50%) as a brown oil (R_f 0.36, 9:1 DCM:MeOH). ^{1}H NMR (400 MHz, $CDCl_3$) δ 8.19 – 8.12 (m, 1H, ArH naphthalene), 8.09 (d, *J* = 2.6 Hz, 1H, ArH indole), 7.96 (d, *J* = 8.0 Hz, 1H, ArH naphthalene), 7.91 (dd, *J* = 7.8, 1.5 Hz, 1H, ArH naphthalene), 7.64 (dd, *J* = 7.0, 1.3 Hz, 1H, ArH naphthalene), 7.57 – 7.44 (m, 3H, ArH naphthalene), 7.42 (s, 1H, ArH indole), 7.33 (d, *J* = 9.1 Hz, 1H, ArH indole), 7.17 (br s, 1H, NH), 7.03 (dd, *J* = 8.9, 2.6 Hz, 1H, ArH indole), 5.08 (br s, 1H, NH), 4.62 (s, 2H, indole-O-CH_2), 4.29 – 4.03 (br m, 2H, N1-CH_2), 3.68 – 3.50 (m, 14H,

($[CH_2]_2O)_2(CH_2)_2$ & O-CH_2 morpholino), 3.36 – 3.24 (m, 2H, ($[CH_2]_2O)_2(CH_2)_2$), 2.75 – 2.61 (br m, 2H, N1-$CH_2C\underline{H_2}$), 2.52 – 2.25 (br m, 4H, N-CH_2 morpholino), 1.41 (s, 9H, CH_3 *t* Bu). ^{13}C NMR (126 MHz, $CDCl_3$) δ 192.04, 168.56, 156.11, 154.50, 139.38, 138.88, 133.86, 132.70, 130.78, 130.24, 128.39, 127.86, 126.97, 126.49, 125.87, 125.83, 124.61, 117.72, 113.69, 110.96, 107.14, 79.33, 70.44, 70.36, 70.34, 69.93, 68.47, 66.84, 57.47, 53.52, 44.44, 40.48, 38.94, 28.53. HRMS-ESI calculated for $C_{38}H_{49}N_4O_8$ $[M+H]^+$ 689.3545, found *m/z* 689.3546.

***N*-(8-Aminooctyl)-2-{[3-(4-methoxybenzoyl)-1-[2-(morpholin-4-yl)ethyl]-1*H*-indol-5-yl]oxy}acetamide (13a)**

12a (7.3 mg, 10.9 µmol) was dissolved in DCM (1.6 mL) and TFA (1.6 mL) was added. After 1 h stirring, the reaction mixture was evaporated under N_2 stream, followed by reduced pressure. The crude was purified by semi-preparative RP-HPLC to yield the TFA salt of **13a** (5.2 mg, 5.7 µmol, 52%) as a white solid. HRMS-ESI calculated for $C_{32}H_{45}N_4O_5$ $[M+H]^+$ 565.3384, found *m/z* 565.3338. Analytical RP-HPLC R_t = 13.43 min.

***N*-{2-[2-(2-Aminoethoxy)ethoxy]ethyl}2-{[3-(4-methoxybenzoyl)-1-[2-(morpholin-4-yl)ethyl]-1*H*-indol-5-yl]oxy}acetamide (13b)**

12b (8.4 mg, 12.6 µmol) and TFA (1.6 mL) in DCM (1.6 mL) were reacted as described in the procedure for **13a**. The crude was purified by semi-preparative RP-HPLC to yield the TFA salt of **13b** (8.8 mg, 9.7 µmol, 77%) as a white solid. HRMS-ESI calculated for $C_{30}H_{41}N_4O_7$ $[M+H]^+$ 569.2970, found *m/z* 569.2926. Analytical RP-HPLC R_t = 11.92 min.

***N*-(8-Aminooctyl)-2-({1-[2-(morpholin-4-yl)ethyl]-3-(naphthalene-1-carbonyl)-1*H*-indol-5-yl}oxy)acetamide (13c)**

12c (7 mg, 10.2 µmol) and TFA (1 mL) in DCM (1 mL) were reacted as described in the procedure for **13a**. The crude was purified by semi-preparative RP-HPLC to yield the TFA salt of **13c** (5.3 mg, 5.7 µmol, 56%) as a white solid. HRMS-ESI calculated for $C_{35}H_{45}N_4O_4$ $[M+H]^+$ 585.3435, found *m/z* 585.3384. Analytical RP-HPLC R_t = 14.32 min.

***N*-{2-[2-(2-Aminoethoxy)ethoxy]ethyl}-2-({1-[2-(morpholin-4-yl)ethyl]-3-(naphthalene-1-carbonyl)-1*H*-indol-5-yl}oxy)acetamide (13d)**

12d (12 mg, 17.4 µmol) and TFA (1 mL) in DCM (1 mL) were reacted as described in the procedure for **13a**. The crude was purified by semi-preparative RP-HPLC to yield the TFA salt of **13d** (4.3 mg, 4.6 µmol, 27%) as a white solid. HRMS-ESI calculated for $C_{33}H_{41}N_4O_6$ $[M+H]^+$ 589.3021, found *m/z* 589.2984. Analytical RP-HPLC R_t = 12.95 min.

Fmoc-Ala-Ala-trityl resin (for preparation of 13e-g)

This was assembled according to standard Fmoc solid-phase peptide synthesis. In brief, 1,2-diaminoethane trityl resin (300 mg, 1.8 mmol/g) was loaded by double coupling with Fmoc-Ala-OH (504 mg, 1.6 mmol), HBTU (614 mg, 1.6 mmol) and DIPEA (0.56 mL, 3.2 mmol) in DMF (3.2 mL). The resin was capped by double treatment with acetic anhydride (500 µL) and DIPEA (500 µL) in DMF (1 mL), and the loading determined by Fmoc measurement to be 0.68 mmol/g. The Fmoc was cleaved using 20% *v*/*v* piperidine/DMF then reacted with a solution of Fmoc-Ala-OH (224 mg, 0.72 mmol), HBTU (273 mg, 0.72 mmol) and DIPEA (0.25 mL, 1.4 mmol) in DMF (1.4 mL). The resin was washed and dried under vacuum.

(2*S*)-*N*-[(1*S*)-1-[(2□aminoethyl)carbamoyl]ethyl]-2-(2-{[3-(4-methoxybenzoyl)-1-[2-(morpholin-4-yl)ethyl]-1*H*-indol-5-yl]oxy}acetamido)propanamide (13e)

Fmoc-Ala-Ala-trityl resin (58 mg, 41.4 µmol) was swelled in DMF, Fmoc-deprotected using 20% *v*/*v* piperidine/DMF and then washed thoroughly with DMF. A solution of the TFA salt of **11a** (23 mg, 34.3 µmol), HATU (16 mg, 41.4 µmol) and DIPEA (29 µL, 0.17 mmol) in DMF (83 µL) was swirled for 1 min and then added to the drained resin and left for 2 h. The resin was drained, washed with DMF and DCM and dried under vacuum. The resin was transferred to a round bottom flask and cleaved using a solution of TFA in DCM (5 mL, 5% *v*/*v*), stirring for 1 h. The mixture was filtered, washed with DCM and the filtrate dried under reduced pressure. The crude was purified using semi-preparative RP-HPLC, to yield the TFA salt of **13e** (9.9 mg, 10.2 µmol, 30%) as a white solid. HRMS-ESI calculated for $C_{32}H_{43}N_6O_7$ $[M+H]^+$ 623.3188, found *m/z* 623.3133. Analytical RP-HPLC R_t = 11.83 min.

(2*S*)-*N*-[(1*S*)-1-[(2-aminoethyl)carbamoyl]ethyl]-2-[2-({1-[2-(morpholin-4-yl)ethyl]-3-(naphthalene-1-carbonyl)-1*H*-indol-5-yl}oxy)acetamido]propanamide (13f)

Fmoc-Ala-Ala-trityl resin (38 mg, 27.3 µmol), piperidine in DMF (20% *v*/*v*), **11b** (16 mg, 22.7 µmol), HATU (10 mg, 27.3 µmol), DIPEA (19 µL, 0.11 mmol), TFA in DCM (5 mL 5% *v*/*v*) were used as in the procedure for **13e.** The crude was purified using semi-preparative RP-HPLC, to yield the TFA salt of **13f** (5.14 mg, 6.2 µmol, 27%) as a white solid. HRMS-ESI calculated for $C_{35}H_{43}N_6O_6$ $[M+H]^+$ 643.3239, found *m/z* 643.3194. Analytical RP-HPLC R_t = 13.21 min.

(2*S*)-*N*-[(1*S*)-1-[(2-aminoethyl)carbamoyl]ethyl]-2-(2-{[3-(4-methoxybenzoyl)-1-[(oxan□4-yl)methyl]-1*H*-indol-5-yl]oxy}acetamido)propanamide (13g)

Fmoc-Ala-Ala-trityl resin (44 mg, 31.7 μmol), piperidine in DMF (20% *v*/*v*), the TFA salt of **11c** (17 mg, 31.7 μmol), HATU (12 mg, 31.7 μmol), DIPEA (22 μL, 0.13 mmol), TFA in DCM (5 mL 5% *v*/*v*) were used as in the procedure for **13e.** The crude was purified using semi-preparative RP-HPLC, to yield the TFA salt of **13g** (7.45 mg, 8.9 μmol, 28%) as a white solid. HRMS-ESI calculated for $C_{32}H_{42}N_5O_7$ $[M+H]^+$ 608.3079, found *m/z* 608.3031. Analytical RP-HPLC R_t = 15.63 min.

***N*-{2-[2-(2-Acetamidoethoxy)ethoxy]ethyl}-2-{[3-(4-methoxybenzoyl)-1-[2-(morpholin-4-yl)ethyl]-1*H*-indol-5-yl]oxy}acetamide (14)**

To a solution of the TFA salt of **13b** (2.6 mg, 2.9 μmol) and DIPEA (1.71 μL, 9.8 μmol, added as a 1:10 solution in DCM) was added acetic anhydride (0.34 μL 3.6 μmol, added as a 1:10 solution in DCM) and the mixture was stirred at rt for 1 h. The reaction solvent was evaporated under N_2 stream. The product was purified by semi-preparative RP-HPLC and passed through an Amberlyst A21 ion exchange resin to remove TFA, yielding **14** (1.69 mg, 2.8 μmol, 97%) as a white solid. HRMS-ESI calculated for $C_{32}H_{43}N_4O_8$ $[M+H]^+$ 611.3075, found *m/z* 611.3068. Analytical RP-HPLC R_t = 13.49 min.

6-(2-{4-[(*E*)-2-[2,2-Difluoro-4-(thiophen-2-yl)-1λ4,3-diaza-2λ4-boratricyclo[7.3.0.0^{3,7}]dodeca-1(12),4,6,8,10-pentaen-12-yl]ethenyl]phenoxy}acetamido)-*N*-[8-(2-{[3-(4-methoxybenzoyl)-1-[2-(morpholin-4-yl)ethyl]-1*H*-indol-5-yl]oxy}acetamido)octyl]hexanamide (15a)

To a solution of the TFA salt of **13a** (2.82 mg, 3.11 μmol) in anhydrous DMF (500 μL), was added a solution of DIPEA (1.91 μL, 11.0 μmol) in anhydrous DMF (30.59 μL), followed by a solution of BODIPY 630/650-X-OSu (1.25 mg, 1.89 μmol) in anhydrous DMF (300 μL). The mixture was swirled, left standing for 12 h, then evaporated under reduced pressure. The crude product was purified by semi-preparative RP-HPLC and passed through an Amberlyst A21 ion exchange resin to remove TFA, yielding **15a** (1.56 mg, 1.41 μmol, 74%) as a bright blue solid. HRMS-ESI calculated for $C_{61}H_{70}BF_2N_7NaO_8S$ $[M+Na]^+$ 1132.4970, found *m/z* 1132.5064. Analytical RP-HPLC R_t = 22.33 min.

6-(2-{4-[(*E*)-2-[2,2-Difluoro-4-(thiophen-2-yl)-1λ4,3-diaza-2λ4-boratricyclo[7.3.0.0^{3,7}]dodeca-1(12),4,6,8,10-pentaen-12-yl]ethenyl]phenoxy}acetamido)-*N*-(2-{2-[2-(2-{[3-(4-methoxybenzoyl)-1-[2-(morpholin-4-yl)ethyl]-1*H*-indol-5-yl]oxy}acetamido)ethoxy]ethoxy}ethyl)hexanamide (15b)

The TFA salt of **13b** (3.59 mg, 3.94 µmol), DIPEA (2.24 µL, 12.9 µmol),BODIPY 630/650-X-OSu (1.25 mg, 1.89 µmol) and DMF (836 µL) were reacted as described in the procedure for **15a**. The crude product was purified by semi-preparative RP-HPLC and passed through an Amberlyst A21 ion exchange resin to remove TFA, yielding **15b** (1.26 mg,1.13 µmol, 60%) as a bright blue solid. HRMS-ESI calculated for $C_{59}H_{66}BF_2N_7NaO_{10}S$ $[M+Na]^+$ 1136.4555, found *m/z* 1136.4618. Analytical RP-HPLC R_t = 21.36 min.

6-(2-{4-[(*E*)-2-[2,2-Difluoro-4-(thiophen-2-yl)-1λ4,3-diaza-2λ4-boratricyclo[7.3.0.0^{3,7}]dodeca-1(12),4,6,8,10-pentaen-12-yl]ethenyl]phenoxy}acetamido)-*N*-{8-[2-({1-[2-(morpholin-4-yl)ethyl]-3-(naphthalene-1-carbonyl)-1*H*-indol-5-yl}oxy)acetamido]octyl}hexanamide (15c)

The TFA salt of **13c** (3.22 mg, 3.47 µmol), DIPEA (2.04 µL, 11.7 µmol),BODIPY 630/650-X-OSu (1.25 mg, 1.89 µmol) and DMF (832 µL) were reacted as described in the procedure for **15a**. The crude product was purified by semi-preparative RP-HPLC and passed through an Amberlyst A21 ion exchange resin to remove TFA, yielding **15c** (1.88 mg, 1.66 µmol, 88%) as a bright blue solid. HRMS-ESI calculated for $C_{64}H_{70}BF_2N_7NaO_7S$ $[M+Na]^+$ 1152.5021, found *m/z* 1152.5090. Analytical RP-HPLC R_t = 23.05 min.

6-(2-{4-[(*E*)-2-[2,2-Difluoro-(thiophen-2-yl)-1λ4,3-diaza-2λ4-boratricyclo[7.3.0.0^{3,7}]dodeca-1(12),4,6,8,10-pentaen-12-yl]ethenyl]phenoxy}acetamido)-*N*-[2-(2-{2-[2-({1-[2-(morpholin-4-yl)ethyl]-3-(naphthalene-1-carbonyl)-1*H*-indol-5-yl}oxy)acetamido]ethoxy}ethoxy)ethyl]hexanamide (15d)

The TFA salt of **13d** (2.41 mg, 2.59 µmol), DIPEA (1.71 µL, 9.8 µmol), BODIPY 630/650-X-OSu (1.25 mg, 1.89 µmol) and DMF (827 µL) were reacted as described in the procedure for **15a**. The crude product was purified by semi-preparative RP-HPLC and passed through an Amberlyst A21 ion exchange resin to remove TFA, yielding **15d** (1.75 mg, 1.54 µmol, 82%) as a bright blue solid. HRMS-ESI calculated for $C_{62}H_{66}BF_2N_7NaO_9S$ $[M+Na]^+$ 1156.4606, found *m/z* 1156.4661. Analytical RP-HPLC R_t = 22.02 min.

6-(2-{4-[(*E*)-2-[2,2-Difluoro-4-(thiophen-2-yl)-1λ4,3-diaza-2λ4-boratricyclo[7.3.0.0^{3,7}]dodeca-1(12),4,6,8,10-pentaen-12-yl]ethenyl]phenoxy}acetamido)-*N*-(2-{2-[2-(2-{[3-(4-methoxybenzoyl)-1-[2-(morpholin-4-yl)ethyl]-1*H*-indol-5-yl]oxy}acetamido)propanamido]propanamido}ethyl)hexanamide 15e)

The TFA salt of **13e** (3.67 mg, 3.80 µmol), DIPEA (2.37 µL, 13.6 µmol),BODIPY 630/650-X-OSu (1.67 mg, 2.52 µmol) and DMF (840 µL) were reacted as described in the procedure

for **15a**. The crude product was purified by semi-preparative RP-HPLC and passed through an Amberlyst A21 ion exchange resin to remove TFA, yielding **15e** (1.56 mg, 1.34 µmol, 53%) as a bright blue solid. HRMS-ESI calculated for $C_{61}H_{68}BF_2N_9NaO_{10}S$ $[M+Na]^+$ 1190.4773, found *m/z* 1190.4840. Analytical RP-HPLC R_t = 21.18 min.

6-(2-{4-[(*E*)-2-[2,2-Difluoro-4-(thiophen-2-yl)-1λ4,3-diaza-2λ4-boratricyclo[7.3.0.0^{3,7}]dodeca-1(12),4,6,8,10-pentaen-12-yl]ethenyl]phenoxy}acetamido)-*N*-[2-(2-{2-[2-({1-[2-(morpholin-4-yl)ethyl]-3-(naphthalene-1-carbonyl)-1*H*-indol-5-yl}oxy)acetamido]propanamido}propanamido)ethyl]hexanamide (15f)

The TFA salt of **13f** (3.32 mg, 3.37 µmol), DIPEA (2.19 µL, 12.6 µmol),BODIPY 630/650-X-OSu (1.67 mg, 2.52 µmol) and DMF (837 µL) were reacted as described in the procedure for **15a**. The crude product was purified by semi-preparative RP-HPLC and passed through an Amberlyst A21 ion exchange resin to remove TFA, yielding **15f** (2.08 mg, 1.75 µmol, 70%) as a bright blue solid. HRMS-ESI calculated for $C_{64}H_{69}BF_2N_9O_9S$ $[M+H]^+$ 1188.5005, found *m/z* 1188.5012. Analytical RP-HPLC R_t = 21.76 min.

6-(2-{4-[(*E*)-2-[2,2-Difluoro-4-(thiophen-2-yl)-1λ4,3-diaza-2λ4-boratricyclo[7.3.0.0^{3,7}]dodeca-1(12),4,6,8,10-pentaen-12-yl]ethenyl]phenoxy}acetamido)-*N*-(2-{2-[2-(2-{[3-(4-methoxybenzoyl)-1-[(oxan-4-yl)methyl]-1*H*-indol-5-yl]oxy}acetamido)propanamido]propanamido}ethyl)hexanamide (15g)

The TFA salt of **13g** (3.89 mg, 4.65 µmol), DIPEA (2.46 µL, 14.1 µmol),BODIPY 630/650-X-OSu (1.67 mg, 2.52 µmol) and DMF (842 µL) were reacted as described in the procedure for **15a**. The crude product was purified by semi-preparative RP-HPLC and passed through an Amberlyst A21 ion exchange resin to remove TFA, yielding **15g** (1.06 mg, 0.92 µmol, 36%) as a bright blue solid. HRMS-ESI calculated for $C_{61}H_{67}BF_2N_8NaO_{10}S$ $[M+Na]^+$ 1175.4664, found *m/z* 1175.4655. Analytical RP-HPLC R_t = 23.14 min.

3-(4-Methoxybenzoyl)-1-[(oxan-4-yl)methyl]-5-propoxy-1*H*-indole (16a)

To a solution of **9e** (50 mg, 0.14 mmol) in anhydrous DMF (3 mL) was added NaH (60% by mass dispersion in mineral oil) (20 mg, 0.50 mmol), followed by dropwise addition of 1-bromopropane (18.6 µL, 0.21 mmol) in anhydrous DMF (2 mL). After stirring for 20 h, the reaction was quenched with sat. aq. NH_4Cl (2 mL) and H_2O (3 mL) and extracted with EA (4 × 5 mL). The combined organics were washed with H_2O (4 × 20 mL), dried over $MgSO_4$, filtered and evaporated under reduced pressure. The crude product was purified using flash silica column chromatography (99:1 DCM:MeOH) to yield the desired **16a** (46 mg, 0.11

mmol, 83%), as a white-opaque solid (R_f 0.57, 99:1 DCM:MeOH). ^{1}H NMR (400 MHz, $CDCl_3$) δ 7.93 (d, *J* = 2.5 Hz, 1H, ArH indole), 7.86 – 7.79 (m, 2H, ArH MeOPh), 7.48 (s, 1H, ArH indole), 7.25 (dd, *J* = 8.9, 0.5 Hz, 1H, ArH indole), 7.03 – 6.95 (m, 3H, ArH indole & ArH MeOPh), 4.07 – 3.92 (m, 6H, O-CH_2 propyl, N-CH_2 & O-CH_2 THP), 3.89 (s, 3H, O-CH_3), 3.31 (td, *J* = 11.8, 2.2 Hz, 2H, O-CH_2 THP), 2.19 – 2.03 (m, 1H, CH THP), 1.93 – 1.76 (m, 2H, O-CH_2-$\underline{CH_2}$ propyl), 1.55 – 1.30 (m, 4H, O-$CH_2C\underline{H_2}$ THP), 1.05 (t, *J* = 7.4 Hz, 3H, CH_3 propyl). ^{13}C NMR (101 MHz, $CDCl_3$) δ 189.83, 162.29, 156.02, 136.66, 133.58, 131.88, 130.93, 128.43, 115.32, 114.72, 113.67, 110.71, 104.90, 70.25, 67.41, 55.55, 53.29, 36.03, 30.84, 22.80, 10.71. HRMS-ESI calculated for $C_{25}H_{29}NNaO_4$ $[M+Na]^+$ 430.1989, found *m/z* 430.1954. Analytical RP-HPLC R_t = 22.17 min.

3-(4-Methoxybenzoyl)-1-[(oxan-4-yl)methyl]-7-propoxy-1*H*-indole (16b)

A solution of **9f** (9.5 mg, 25.9 μmol), NaH (3.1 mg, 77.7 μmol), and 1-bromopropane (3.5 μL, 38.9 μmol) in DMF (0.95 mL) was reacted as described in the procedure for **16a**. The crude product was purified using flash silica column chromatography (2:1 hexane:EA) to yield the desired **16b** (6.1 mg, 15.0 μmol, 57%), as a colourless oil (R_f 0.56, 1:1 hexane:EA). ^{1}H NMR (400 MHz, $CDCl_3$) δ 7.96 (dd, *J* = 8.1, 0.9 Hz, 1H, ArH indole), 7.86 – 7.77 (m, 2H, ArH MeOPh), 7.40 (s, 1H, ArH indole), 7.18 (t, *J* = 7.9 Hz, 1H, ArH indole), 7.03 – 6.95 (m, 2H, ArH MeOPh), 6.74 (dd, *J* = 7.9, 0.9 Hz, 1H, ArH indole), 4.29 (d, *J* = 7.3 Hz, 2H, N-CH_2), 4.10 (t, *J* = 6.5 Hz, 2H, O-CH_2 propyl), 4.01 – 3.92 (m, 2H, O-CH_2 THP), 3.89 (s, 3H, O-CH_3), 3.30 (td, *J* = 11.7, 2.3 Hz, 2H, O-CH_2 THP), 2.26 – 2.11 (m, 1H, CH THP), 1.99 – 1.82 (m, 2H, O-CH_2-$\underline{CH_2}$ propyl), 1.52 – 1.28 (m, 4H, O-$CH_2C\underline{H_2}$ THP), 1.12 (t, *J* = 7.4 Hz, 3H, CH_3 propyl). ^{13}C NMR (101 MHz, $CDCl_3$) δ 189.88, 162.34, 146.87, 137.66, 133.65, 131.09, 130.10, 126.36, 123.25, 115.50, 115.13, 113.67, 105.03, 69.83, 67.63, 56.21, 55.59, 37.29, 30.58, 22.97, 11.04. HRMS-ESI calculated for $C_{25}H_{29}NNaO_4$ $[M+Na]^+$ 430.1989, found *m/z* 430.1994. Analytical RP-HPLC R_t = 22.55 min.

***tert*-Butyl *N*-(2-{2-[2-(2-{[3-(4-methoxybenzoyl)-1-[(oxan-4-yl)methyl]-1*H*-indol-5-yl]oxy}ethoxy)ethoxy]ethoxy}ethyl)carbamate (17)**

To a stirred solution of 2-(2-(2-(2-aminoethoxy)ethoxy)ethoxy)ethanol (100 μL, 0.55 mmol) in dioxane (1 mL) was added Boc_2O (152 μL, 0.66 mmol). The mixture was stirred for 18 h at rt and then evaporated under reduced pressure. The crude was taken up in DCM (6 mL), washed with H_2O (2 × 6 mL) and brine (1 × 5 mL), dried over $MgSO_4$, filtered and evaporated under reduced pressure. The crude product was purified using flash silica column

chromatography (99:1 DCM:MeOH) to yield the desired *tert*-butyl *N*-(2-{2-[2-(2-hydroxyethoxy)ethoxy]ethoxy}ethyl)carbamate (24 mg, 81.8 µmol, 15%), as a pale yellow oil (R_f 0.52, 9:1 DCM:MeOH). ^{1}H NMR (400 MHz, $CDCl_3$) δ 3.75 – 3.67 (m, 4H, O-CH_2), 3.66 – 3.57 (m, 8H, O-CH_2CH_2-O), 3.52 (t, *J* = 5.2 Hz, 2H, O-CH_2), 3.29 (t, *J* = 5.2 Hz, 2H, NH-C$\underline{H_2}$), 1.43 (s, 9H, CH_3 *t* Bu). ^{13}C NMR (101 MHz, $CDCl_3$) δ 156.31, 79.19, 72.77, 70.72, 70.67, 70.55, 70.36, 70.20, 61.76, 40.67, 28.56. HRMS-ESI calculated for $C_{13}H_{27}NNaO_6$ $[M+Na]^+$ 316.1731, found *m/z* 316.1738. A solution of bromine (7.3 µL, 0.14 mmol) in DCM (0.2 mL) at 0°C was added to a solution of triphenylphosphine (37 mg, 0.14 mmol) and Et_3N (20 µL, 0.14 mmol) in anhydrous DCM (0.2 mL) at 0°C. Following stirring at 0°C for 30 min, a solution of *tert*-butyl *N*-(2-{2-[2-(2-hydroxyethoxy)ethoxy]ethoxy}ethyl)carbamate (42 mg, 0.14 mmol) in DCM (0.2 mL) was added dropwise. After stirring at 0°C for 2 h, the mixture was evaporated under reduced pressure. The crude product was purified using flash silica column chromatography (5:1 hexane:EA) to yield the desired *tert*-butyl *N*-(2-{2-[2-(2-bromoethoxy)ethoxy]ethoxy}ethyl)carbamate (13 mg, 36.5 µmol, 26%) as a colourless oil. ^{1}H NMR (400 MHz, $CDCl_3$) δ 5.03 (br s, 1H, NH), 3.81 (t, *J* = 6.3 Hz, 2H, O-CH_2), 3.73 – 3.58 (m, 8H, O-CH_2CH_2-O), 3.54 (t, *J* = 5.1 Hz, 2H, O-CH_2), 3.47 (t *J* = 6.3, 1.2 Hz, 2H, CH_2Br), 3.31 (q, *J* = 5.6 Hz, 2H, NH-C$\underline{H_2}$), 1.44 (s, 9H, CH_3 *t* Bu). HRMS-ESI calculated for $C_{13}H_{26}BrNNaO_5$ $[M+Na]^+$ 378.0887, found *m/z* 378.0894. To a solution of **9e** (13 mg, 35.1 µmol) in anhydrous DMF (0.7 mL) was added NaH (60% by mass dispersion in mineral oil) (5.5 mg, 0.14 mmol). After stirring for 30 min, a solution of *tert*-butyl *N*-(2-{2-[2-(2-bromoethoxy)ethoxy]ethoxy}ethyl)carbamate (12.5 mg, 35.1 µmol) in anhydrous DMF (0.6 mL) was added. The reaction mixture was stirred for 18 h, then quenched with H_2O (1.5 mL), extracted with EA (4 × 2 mL), washed with H_2O (2 × 7 mL), dried over $MgSO_4$, filtered and evaporated under reduced pressure. The crude product was purified using flash silica column chromatography (99:1 DCM:MeOH) and semi-preparative RP-HPLC to yield the desired **17** (6.88 mg, 10.7 µmol, 31%), as a white solid. ^{1}H NMR (400 MHz, DMSO-d_6) δ 7.97 (s, 1H, ArH indole), 7.81 – 7.75 (m, 3H, ArH indole and MeOPh), 7.58 (d, *J* = 9.0 Hz, 1H, ArH indole), 7.12 – 7.05 (m, 2H, ArH MeOPh), 6.95 (dd, *J* = 8.9, 2.5 Hz, 1H, ArH indole), 6.74 (br s, 1H, NH), 4.21 – 4.07 (m, 4H, N1-CH_2 & indole-O-CH_2), 3.86 (s, 3H, O-CH_3), 3.85 – 3.75 (m, 4H, O-CH_2 & O-CH_2 THP), 3.65 – 3.45 (m, 8H, O-CH_2CH_2-O), 3.37 (t, *J* = 6.1 Hz, 2H, O-CH_2), 3.19 (td, *J* = 11.7, 2.0 Hz, 2H, O-CH_2 THP), 3.05 (q, *J* = 6.0 Hz, 2H, NH-C$\underline{H_2}$),

2.13 – 2.02 (m, 1H, CH THP), 1.41 – 1.21 (m, 13H, O-$CH_2C\underline{H_2}$ THP, CH_3 *t* Bu). HRMS-ESI calculated for $C_{35}H_{48}N_2NaO_9$ $[M+Na]^+$ 663.3252, found *m/z* 663.3247. Analytical RP-HPLC R_t = 21.00 min.

_N_-(2-{2-[2-(2-{[3-(4-Methoxybenzoyl)-1-[(oxan-4-yl)methyl]-1*H*-indol-5-yl]oxy}ethoxy)ethoxy]ethoxy}ethyl)acetamide (18)

To a solution of **17** (1.81 mg, 2.8 µmol) in DCM (0.45 mL) was added TFA (0.45 mL). The reaction mixture was swirled, left to stand for 1 h and then evaporated under reduced pressure. The residue was then dissolved in a solution of DCM (0.4 mL) and a solution of DIPEA (1.48 µL, 8.5 µmol, added as a 1:50 solution in DCM) added, followed by a solution of acetic anhydride (0.29 µL, 3.1 µmol, added as a 1:50 solution in DCM). The reaction mixture was swirled and then left to stand for 1.5 h, after which the reaction solvent was evaporated under air. The product was purified by semi-preparative RP-HPLC and passed through an Amberlyst A21 ion exchange resin to remove TFA, yielding **18** (1.17 mg, 2.0 µmol, 71%), as a white solid. HRMS-ESI calculated for $C_{32}H_{42}N_2NaO_8$ $[M+Na]^+$ 605.2833, found *m/z* 605.2828. Analytical RP-HPLC R_t = 18.12 min.

Methyl 5-{[3-(4-methoxybenzoyl)-1-[(oxan-4-yl)methyl]-1*H*-indol-7-yl]oxy}pentanoate (19)

A solution of **9f** (261 mg, 0.71 mmol), NaH (86 mg, 2.1 mmol) and methyl 5-bromovalerate (153 µL, 1.1 mmol) in DMF (20 mL) was reacted as described in the procedure for **16a**. The crude product was purified using flash silica column chromatography (4:1 hexane:EA) to yield the desired **19** (103 mg, 0.28 mmol, 30%), as a white solid (R_f 0.32, 1:1 hexane:EA). ^{1}H NMR (400 MHz, $CDCl_3$) δ 7.97 (dd, *J* = 8.1, 0.8 Hz, 1H, ArH indole), 7.84 – 7.80 (m, 2H, ArH MeOPh), 7.40 (s, 1H, ArH indole), 7.18 (t, *J* = 8.0 Hz, 1H, ArH indole), 7.01 – 6.96 (m, 2H, ArH MeOPh), 6.73 (dd, *J* = 7.9, 0.9 Hz, 1H, ArH indole), 4.28 (d, *J* = 7.3 Hz, 2H, N-CH_2), 4.15 (t, *J* = 5.8 Hz, 2H, O-CH_2 butyl), 3.98 – 3.92 (m, 2H, O-CH_2 THP), 3.89 (s, 3H, Ph-O-CH_3), 3.69 (s, 3H, $COOCH_3$), 3.29 (td, *J* = 11.6, 2.4 Hz, 2H, O-CH_2 THP), 2.43 (t, *J* = 6.9 Hz, 2H, CH_2COO), 2.22 – 2.08 (m, 1H, CH THP), 1.96 – 1.83 (m, 4H, CH_2CH_2), 1.48 – 1.30 (m, 4H, O-$CH_2C\underline{H_2}$ THP). ^{13}C NMR (101 MHz, $CDCl_3$) δ 189.89, 173.66, 162.36, 146.64, 137.77, 133.52, 131.10, 130.14, 126.27, 123.24, 115.45, 115.30, 113.66, 105.06, 67.63, 67.57, 56.20, 55.58, 51.79, 37.28, 33.71, 30.56, 29.06, 21.94. HRMS-ESI calculated for $C_{28}H_{34}NO_6$ $[M+H]^+$ 480.2381, found *m/z* 480.2366. Analytical RP-HPLC R_t = 20.92 min.

5-{[3-(4-Methoxybenzoyl)-1-[(oxan-4-yl)methyl]-1*H*-indol-7-yl]oxy}pentanoic acid (20)

To a stirred solution of **19** (91 mg, 0.19 mmol) in THF (1.6 mL) at 0°C was added dropwise 0.2 M aq. lithium hydroxide monohydrate solution (2.4 mL). The mixture was stirred at 0°C for 18 h, then quenched with biphase of 0.2 M aq. HCl/EA (1:1 *v/v)* until pH 4. The aqueous layer was extracted with EA (4 × 4 mL), dried over $MgSO_4$, filtered and evaporated under reduced pressure to yield the hydrochloride salt of **20** (84 mg, 0.17 mmol, 88%) as a brown solid. ^{1}H NMR (400 MHz, $CDCl_3$) δ 7.97 (dd, *J* = 8.1, 0.8 Hz, 1H, ArH indole), 7.85 – 7.79 (m, 2H, ArH MeOPh), 7.40 (s, 1H, Ar indole), 7.18 (t, *J* = 8.0 Hz, 1H, ArH indole), 7.02 – 6.95 (m, 2H, ArH MeOPh), 6.74 (dd, *J* = 8.2, 0.7 Hz, 1H, ArH indole), 4.29 (d, *J* = 7.3 Hz, 2H, N-CH_2), 4.16 (t, *J* = 5.6 Hz, 2H, O-CH_2 butyl), 3.99 – 3.92 (m, 2H, O-CH_2 THP), 3.89 (s, 3H, O-CH_3), 3.30 (td, *J* = 11.6, 2.5 Hz, 2H, O-CH_2 THP), 2.48 (t, *J* = 6.9 Hz, 2H, $C\underline{H_2}COOH$), 2.21 – 2.11 (m, 1H, CH THP), 2.00 – 1.84 (m, 4H, CH_2CH_2), 1.48 – 1.31 (m, 4H, O-$CH_2C\underline{H_2}$ THP). HRMS-ESI calculated for $C_{27}H_{31}NNaO_6$ $[M+Na]^+$ 488.2044, found *m/z* 488.2007. Analytical RP-HPLC R_t = 18.68 min.

***Tert*-Butyl *N*-(2-{2-[2-(5-{[3-(4-methoxybenzoyl)-1-[(oxan-4-yl)methyl]-1*H*-indol-7-yl]oxy}pentanamido)ethoxy]ethoxy}ethyl)carbamate (21)**

The hydrochloride salt of **20** (38 mg, 74.9 μmol), DIPEA (85 μL, 0.49 mmol), HATU (31 mg, 80.8 μmol) and *tert*butyl *N*{2[2-(2-aminoethoxy)ethoxy]ethyl}carbamate (60 mg, 0.24 mmol) in DMF (5.8 mL) were reacted as described in the procedure for **12a**. The crude product was purified by flash silica gel column chromatography (99:1 DCM:MeOH) to yield **21** (46 mg, 66.1 μmol, 88%) as a brown solid (R_f 0.56, 9:1 DCM:MeOH). ^{1}H NMR (400 MHz, $CDCl_3$) δ 7.97 (dd, *J* = 8.1, 0.8 Hz, 1H, ArH indole), 7.86 – 7.78 (m, 2H, ArH MeOPh), 7.39 (s, 1H, ArH indole), 7.18 (t, *J* = 8.0 Hz, 1H, ArH indole), 7.03 – 6.95 (m, 2H, ArH MeOPh), 6.73 (dd, *J* = 7.9, 1.0 Hz, 1H, ArH indole), 6.10 (br s, 1H, NH), 5.02 (br s, 1H, NH), 4.28 (d, *J* = 7.3 Hz, 2H, N1-CH_2), 4.20 – 4.11 (m, 2H, O-CH_2 butyl), 3.95 (dd, *J* = 11.6, 3.9 Hz, 2H, O-CH_2 THP), 3.89 (s, 3H, O-CH_3), 3.65 – 3.52 (m, 8H, $C\underline{H_2}$-O-($C\underline{H_2}$)$_2$-O-$C\underline{H_2}$), 3.47 (d, *J* = 4.8 Hz, 2H, $C\underline{H_2}CONH$), 3.35 – 3.23 (m, 4H, O-CH_2 THP & $C\underline{H_2}NHCOO$), 2.30 (t, *J* = 6.9 Hz, 2H, $\underline{CH_2}NHCO$), 2.22 – 2.09 (m, 1H, CH THP), 1.90 (q, *J* = 4.2, 3.5 Hz, 4H, O-CH_2($C\underline{H_2}$)$_2$), 1.48 – 1.30 (m, 13H, O-$CH_2C\underline{H_2}$ THP, CH_3 *t* Bu). ^{13}C NMR (101 MHz, $CDCl_3$) δ 189.84, 172.62, 162.28, 156.07, 146.63, 137.72, 133.48, 131.00, 130.03, 126.24, 123.16, 115.34, 115.12, 113.60, 105.02, 79.55, 70.38, 70.32, 70.25, 70.20, 67.69, 67.51, 56.11, 55.51, 40.48, 39.36, 37.20, 35.86, 30.48, 29.09, 28.48, 22.45. HRMS-ESI calculated for $C_{38}H_{53}N_3NaO_9$ $[M+Na]^+$ 718.3674, found *m/z* 718.3704.

_N_-{2-[2-(2-Acetamidoethoxy)ethoxy]ethyl}-5-{[3-(4-methoxybenzoyl)-1-[(oxan-4-yl)methyl]-1_H_-indol-7-yl]oxy}pentanamide (22)

21 (15 mg, 21.9 µmol), TFA (1.1 mL) and DCM (1.1 mL) were reacted as described in the procedure for **13a**. The crude product was purified by semi-preparative RP-HPLC to yield the TFA salt of *N*□{2□[2□(2□aminoethoxy)ethoxy]ethyl}□5□{[3□(4□methoxybenzoyl)□1□[(oxan□4□yl)methyl]□1*H*□indol□7□yl]oxy}pentanamide (17 mg, 20.7 µmol, 95%) as a white solid. HRMS-ESI calculated for $C_{33}H_{46}N_3O_7$ $[M+H]^+$ 596.3330, found *m/z* 596.3286. Analytical RP-HPLC R_t = 16.28 min.

This TFA salt (3.4 mg, 4.3 µmol), DIPEA (2.3 µL, 13.0 µmol), acetic anhydride (0.45 µL, 4.8 µmol) and DCM (0.27 mL) were reacted as described in the procedure for **14**. The product was purified by semi-preparative RP-HPLC and passed through an Amberlyst A21 ion exchange resin to remove TFA, yielding **22** (2.67 mg, 4.2 µmol, 96%) as a white solid. HRMS-ESI calculated for $C_{35}H_{47}N_3NaO_8$ $[M+Na]^+$ 660.3255, found *m/z* 660.3193. Analytical RP-HPLC R_t = 17.97 min.

6-(2-{4-[(_E_)-2-[2,2-Difluoro-4-(thiophen-2-yl)-1λ4,3-diaza-2λ4-boratricyclo[7.3.0.0^{3,7}]dodeca-1(12),4,6,8,10-pentaen-12-yl]ethenyl]phenoxy}acetamido)-_N_-(2-{2-[2-(5-{[3-(4-methoxybenzoyl)-1-[(oxan-4-yl)methyl]-1_H_-indol-7-yl]oxy}pentanamido)ethoxy]ethoxy}ethyl)hexanamide (23)

The TFA salt of *N*□{2□[2□(2□aminoethoxy)ethoxy]ethyl}□5□{[3□(4□methoxybenzoyl)□1□[(oxan□4□yl)methyl]□1*H*□indol□7□yl]oxy}pentanamide (as prepared for **22**) (5.88 mg, 7.1 µmol), DIPEA (3.26 µL, 18.7 µmol), BODIPY 630/650-X-OSu (1.25 mg, 1.89 µmol) and DMF (852 µL) were reacted as described in the procedure for **15a**. The crude product was purified by semi-preparative RP-HPLC and passed through an Amberlyst A21 ion exchange resin to remove TFA, yielding **23** (2.01 mg, 1.76 µmol, 93%) as a bright blue solid. HRMS-ESI calculated for $C_{62}H_{71}BF_2N_6NaO_{10}S$ $[M+Na]^+$ 1163.4916, found *m/z* 1163.4991. Analytical RP-HPLC R_t = 23.50 min.

***tert*-Butyl _N_-(6-{[3-(4-methoxybenzoyl)-1-[(oxan-4-yl)methyl]-1_H_-indol-7-yl]oxy}hexyl)carbamate (24)**

A solution of **9f** (22 mg, 61.4 µmol), NaH (7.4 mg, 0.18 mmol) and *tert*□butyl *N*□(6□bromohexyl)carbamate (prepared according to a literature procedure [63]; 26 mg, 92.1 µmol) in DMF (2.7 mL) was reacted as described in the procedure for **16a**. The crude product was purified using flash silica column chromatography (1:1 hexane:EA) to yield the desired **24**

(27 mg, 47.8 µmol, 79%), as a brown solid (R_f 0.31, 1:1 hexane:EA). ^{1}H NMR (400 MHz, $CDCl_3$) δ 7.96 (dd, *J* = 8.1, 0.8 Hz, 1H, ArH indole), 7.86 – 7.78 (m, 2H, ArH MeOPh), 7.40 (s, 1H, ArH indole), 7.18 (t, *J* = 8.0 Hz, 1H, ArH indole), 7.02 – 6.95 (m, 2H, ArH MeOPh), 6.73 (dd, *J* = 7.9, 0.9 Hz, 1H, ArH indole), 4.56 (br s, 1H, NH), 4.28 (d, *J* = 7.3 Hz, 2H, N1-CH_2), 4.12 (t, *J* = 6.5 Hz, 2H, O-CH_2 hexyl), 4.02 – 3.91 (m, 2H, O-CH_2 THP), 3.89 (s, 3H, O-CH_3), 3.29 (td, *J* = 11.7, 2.5 Hz, 2H, O-CH_2 THP), 3.13 (t, *J* = 7.0 Hz, 2H, NHC$\underline{H_2}$), 2.23 – 2.09 (m, 1H, CH THP), 1.94 – 1.81 (m, 2H, O-$CH_2C\underline{H_2}$ hexyl), 1.61 – 1.23 (m, 19H, $(CH_2)_3$, O-$CH_2C\underline{H_2}$ THP & *t* Bu CH_3). ^{13}C NMR (101 MHz, $CDCl_3$) δ 189.86, 162.32, 156.15, 146.76, 137.66, 133.55, 131.07, 130.06, 126.31, 123.22, 115.46, 115.14, 113.64, 105.05, 79.32, 68.03, 67.57, 56.12, 55.56, 40.71, 37.27, 30.54, 30.28, 29.56, 28.55, 26.72, 26.19. HRMS-ESI calculated for $C_{33}H_{44}N_2NaO_6$ $[M+Na]^+$ 587.3092, found *m/z* 587.3057.

_N_-(6-{[3-(4-Methoxybenzoyl)-1-[(oxan-4-yl)methyl]-1*H*-indol-7-yl]oxy}hexyl)acetamide (25)

24 (14 mg, 25.7 µmol) TFA (1 mL) and DCM (1 mL) were reacted as described in the procedure for **13a**. The crude product was purified by semi-preparative RP-HPLC to yield the TFA salt of 6-{[3-(4-methoxybenzoyl)-1-[(oxan-4-yl)methyl]-1*H*-indol-7-yl]oxy}hexan-1-amine (16 mg, 23.7 µmol, 92%) as a white solid. HRMS-ESI calculated for $C_{28}H_{37}N_2O_4$ $[M+H]^+$ 465.2748, found *m/z* 465.2710. Analytical RP-HPLC R_t = 16.79 min. This TFA salt (3.2 mg, 4.6 µmol), DIPEA (2.5 µL, 14.4 µmol), andacetic anhydride (0.5 µL, 5.3 µmol) in DCM (297 µL) were treated as in the procedure for **14**. The product was purified by semi-preparative RP-HPLC and passed through an Amberlyst A21 ion exchange resin to remove TFA, yielding **25** (2.3 mg, 4.6 µmol, 98%) as a white solid. HRMS-ESI calculated for $C_{30}H_{38}N_2NaO_5$ $[M+Na]^+$ 529.2673, found *m/z* 529.2661. Analytical RP-HPLC R_t = 20.0 min.

6-(2-{4-[(*E*)-2-[2,2-Difluoro-4-(thiophen-2-yl)-1λ4,3-diaza-2λ4-boratricyclo[7.3.0.0^{3,7}]dodeca-1(12),4,6,8,10-pentaen-12-yl]ethenyl]phenoxy}acetamido)-_N_-(6-{[3-(4-methoxybenzoyl)-1-[(oxan-4-yl)methyl]-1*H*-indol-7-yl]oxy}hexyl)hexanamide (26)

The TFA salt of 6-{[3-(4-methoxybenzoyl)-1-[(oxan-4-yl)methyl]-1*H*-indol-7-yl]oxy}hexan-1-amine (as prepared for **25**) (6.05 mg, 8.73 µmol), DIPEA (3.90 µL, 22.4 µmol),BODIPY 630/650-X-OSu (1.25 mg, 1.89 µmol) and DMF (862 µL)were reacted as described in the procedure for **15a**. The crude product was purified by semi-preparative RP-HPLC and passed through an Amberlyst A21 ion exchange resin to remove TFA, yielding **26** (1.46 mg, 1.45

μmol, 77%) as a bright blue solid. HRMS-ESI calculated for $C_{57}H_{62}BF_2N_5NaO_7S$ $[M+Na]^+$ 1032.4333, found *m/z* 1032.4411. Analytical RP-HPLC R_t = 24.73 min.

Pharmacology

Radioligand binding assays

Competition binding assays were carried out on membranes prepared from HEK (human embryonic kidney) 293 cells and protein concentrations were quantified using the DC Protein Assay Kit (Bio-Rad, Hercules, CA) as previously described [64]. These cells were stably transfected with either hCB_1 or hCB_2 receptors as previously described [43, 44]. Membranes were resuspended in binding buffer (50 mM HEPES, 1 mM $MgCl_2$, 1 mM $CaCl_2$, 0.2% [w/v] fatty acid free bovine serum albumin [FAF BSA; MP Biomedicals, Auckland, New Zealand], pH 7.4) to give a final assay concentration of 10 μg/well for hCB_2 or 7.5 μg/well for hCB_1. Compounds (10 mM in DMSO) were diluted with binding buffer containing EtOH to match CP55,940 (5-(1,1-dimethylheptyl)-2-[5-hydroxy-2-(3-hydroxypropyl)cyclohexyl]phenol) (Cayman Chemical, Michigan, USA) vehicle and serial dilutions were prepared using binding buffer containing the requisite amount of EtOH and DMSO to maintain vehicle levels throughout the dilution series. For CP55,940 control points, a stock aliquot in EtOH was diluted with binding buffer containing DMSO to match compound vehicle. All compounds were prepared at 4 × the required assay concentration and 50 μL added to a v-bottom 96-well plate and made up to a total volume of 200 μL with [^{3}H]CP55,940 (PerkinElmer) and membrane. Similarly, [^{3}H]CP55,940 was prepared at 10 nM, with 50 μL added to each well to give a final concentration of 2.5 nM. For vehicle control points, binding buffer containing matched concentrations of EtOH and DMSO was used in place of ligand or CP55,940. The v-bottom plates containing hCB_2 or hCB_1 membranes, [^{3}H]CP55,940 and ligand (or CP55,940 or vehicle) were incubated at 30°C for 1 h.

GF/C 96-well harvest plates (PerkinElmer) were soaked in 50 μL/well of 0.1% polyethylenimine for 1 h, then washed with 200 μL/well of ice-cold wash buffer (50 mM HEPES pH 7.4, 500 mM NaCl, 0.1% FAF BSA). The contents of the v-bottom plates were filtered through the harvest plates, followed by a 200 μL/well wash of the v-bottom plates with ice-cold wash buffer. The harvest plates were promptly washed three times with 200 μL/well of ice-cold wash buffer and dried overnight at 24°C. Scintillation fluid (50 μL/well) (IRGASAFE PLUS, PerkinElmer) was added to the harvest plates and incubated for 30 mins in darkness, after which the harvest plates were read for 2 min/well in a MicroBeta TriLux (PerkinElmer). Binding experiments were performed a minimum of three times in triplicate.

Data was analysed with GraphPad Prism 7 (GraphPad Software, Inc., San Diego, CA, USA) and competition binding curves fit by nonlinear regression using one site competition binding. Dissociation constants (K_i) of compounds were determined using [^{3}H]CP55,940 K_d = 2 nM (hCB_1) or 3 nM (hCB_2). K_i values are expressed as mean ± standard error of the mean (SEM). In cases where less than 50% displacement of [^{3}H]CP55,940 was observed with 10 μM compound, affinity of the compound was deemed too low to be able to generate an accurate competition binding curve. Therefore, a one sample t-test ($P < 0.05$) was used to determine if there was significant difference between displacement in the absence (vehicle normalised to 0%) and presence of compound (with CP55,940 normalised to 100%), in which case the ligand was determined to have a K_i >10 μM, otherwise it was determined to show no significant binding.

cAMP Assays

Function of compounds at hCB_2 and hCB_1 receptor was determined using a bioluminescence resonance energy transfer (BRET) assay measuring forskolin-stimulated cellular cAMP in the appropriate HEK 293 cells transfected with a plasmid that encodes for the cAMP sensor YFP-Epac-RLuc (CAMYEL) as previously described [44]. One or two days prior to transfection, HEK 3HA-hCB_1 pEF4A, HEK 3HA-hCB_2 S4 low or HEK wild type cells, generated as previously described [43, 44] were seeded in 10 cm sterile tissue culture dishes. Cells were transfected with 5 μg of pcDNA3L-His-CAMYEL plasmid (ATCC, Manassas, VA, USA) using 30 μg of linear PEI (molecular weight 25 kDa; Polysciences, Warrington, PA, USA) in 150 mM NaCl. After 24 h, transfected cells were plated in poly-D-lysine (PDL) (0.05 mg mL^{-1} in PBS; Sigma-Aldrich, St Louis, MO, USA) treated 96-Well Solid White Flat Bottom Polystyrene TC-Treated Microplates (Corning) at a density of 60-80,000 cells/well in Dulbecco's Modified Eagle's medium (DMEM) supplemented with 10% fetal bovine serum (FBS). After 16 h, cells were serum-starved in Hank's balanced salt solution (HBSS) containing 1 mg mL^{-1} FAF BSA, pH 7.4 for 30 mins. Cells were then treated with 7.5 μM coelenterazine-h (Nanolight Technology) for 5 mins, followed by addition of ligand or matched vehicle in HBSS plus 1mg mL^{-1} FAF BSA and 5 μM forskolin (Tocris, Bristol, UK). A LUMIstar plate reader (BMG) was used to immediately measure emission signals at 37 °C following ligand addition, which were simultaneously detected at 460/25 nM (Renilla luciferase, RLuc) and 535/25 nM (yellow fluorescent protein, YFP). The inverse BRET ratio of emission at 460/535 nm is presented in the raw data, and hence an increase in ratio

correlates to an increase in cAMP production. Assays were carried out a minimum of three times (except where stated) in duplicate.

Data analysis was performed using GraphPad Prism, with dose response curves fit by nonlinear regression. AUC analysis was achieved using values normalised to the vehicle (0%) or forskolin (100%) values for individual experiments and E_{max} was determined as a percentage of the normalised forskolin values. A t-test ($P < 0.05$) was used to determine if there was a significant difference in response for compounds at 10 µM in HEK-hCB_2 or -hCB_1 cells in the presence or absence of CP 55,940 and in WT HEK cells to determine receptor mediated signalling.

Molecular modelling

The CB_2 receptor homology model was generated using MODELLER 9.19 [65] using the structure of the antagonist-bound CB_1 receptor (PDB ID: 5TGZ) [51] as a template, based on a modified sequence alignment between hCB_1 and hCB_2 receptors from the T-Coffee server [66]. Three dimensional models of ligands were generated using Avogadro 1.2 [67] and minimised using the universal force field (UFF). Ligand docking was performed using GOLD v5.5 (CCDC Software) [68] centred on Ser285 extending for a distance of up to 15 Å and visualised in PyMOL (The PyMOL Molecular Graphics System, Version 1.8.6.0 Schrödinger, LLC.).

CONFLICT OF INTEREST

The authors certify that there is no conflict of interest with any financial organisation regarding the material discussed in the manuscript.

AUTHOR CONTRIBUTION

A.V. and A.C. were involved in the study design presented in this manuscript. A.C. carried out the chemical synthesis. Biological testing was designed by M.G. and carried out by A.C. and C.M. Molecular modelling was carried out by A.C. and J.T. The manuscript and all associated documents were produced by A.C. and A.V. with the assistance of C.M., M.G., S.H. and J.T.

ACKNOWLEDGMENTS

This work was supported by the University of Otago and the Maurice Wilkins Centre for Molecular Biodiscovery. A.C. is supported by a University of Otago Doctoral Scholarship.

SUPPLEMENTARY INFORMATION

Supplementary Material associated with this article can be found at XXXXX.

REFERENCES

[1] V. Katritch, V. Cherezov, R.C. Stevens, Structure-function of the G protein-coupled receptor superfamily, Annu Rev Pharmacol Toxicol, 53 (2013) 531-556.
[2] I. Katona, T.F. Freund, Multiple Functions of Endocannabinoid Signaling in the Brain, in: S.E. Hyman (Ed.) Annual Review of Neuroscience, Vol 35, 2012, pp. 529-558.
[3] R. Mechoulam, L.A. Parker, The endocannabinoid system and the brain, Annu Rev Psychol, 64 (2013) 21-47.
[4] S. Galiegue, S. Mary, J. Marchand, D. Dussossoy, D. Carriere, P. Carayon, M. Bouaboula, D. Shire, G. Le Fur, P. Casellas, Expression of central and peripheral cannabinoid receptors in human immune tissues and leukocyte subpopulations, Eur J Biochem, 232 (1995) 54-61.
[5] A.V. Savonenko, T. Melnikova, Y. Wang, H. Ravert, Y. Gao, J. Koppel, D. Lee, O. Pletnikova, E. Cho, N. Sayyida, A. Hiatt, J. Troncoso, P. Davies, R.F. Dannals, M.G. Pomper, A.G. Horti, Cannabinoid CB2 Receptors in a Mouse Model of A beta Amyloidosis: Immunohistochemical Analysis and Suitability as a PET Biomarker of Neuroinflammation, Plos One, 10 (2015) e0129618.
[6] M. Zhang, B.R. Martin, M.W. Adler, R.K. Razdan, J.I. Jallo, R.F. Tuma, Cannabinoid CB(2) receptor activation decreases cerebral infarction in a mouse focal ischemia/reperfusion model, J Cereb Blood Flow Metab, 27 (2007) 1387-1396.
[7] H. Xu, C.L. Cheng, M. Chen, A. Manivannan, L. Cabay, R.G. Pertwee, A. Coutts, J.V. Forrester, Anti-inflammatory property of the cannabinoid receptor-2-selective agonist JWH-133 in a rodent model of autoimmune uveoretinitis, J Leukoc Biol, 82 (2007) 532-541.
[8] P. Pacher, G. Kunos, Modulating the endocannabinoid system in human health and disease-successes and failures, FEBS J, 280 (2013) 1918-1943.
[9] A. Bettiga, M. Aureli, G. Colciago, V. Murdica, M. Moschini, R. Lucianò, D. Canals, Y. Hannun, P. Hedlund, G. Lavorgna, R. Colombo, R. Bassi, M. Samarani, F. Montorsi, A. Salonia, F. Benigni, Bladder cancer cell growth and motility implicate cannabinoid 2 receptor-mediated modifications of sphingolipids metabolism, Sci Rep, 7 (2017) 42157.
[10] Y. Gomez-Galvez, C. Palomo-Garo, J. Fernandez-Ruiz, C. Garcia, Potential of the cannabinoid CB2 receptor as a pharmacological target against inflammation in Parkinson's disease, Prog Neuropsychopharmacol Biol Psychiatry, 64 (2016) 200-208.
[11] S. Steffens, P. Pacher, Targeting cannabinoid receptor CB2 in cardiovascular disorders: promises and controversies, Br J Pharmacol, 167 (2012) 313-323.
[12] M.A. Storr, C.M. Keenan, H. Zhang, K.D. Patel, A. Makriyannis, K.A. Sharkey, Activation of the cannabinoid 2 receptor (CB2) protects against experimental colitis, Inflamm Bowel Dis, 15 (2009) 1678-1685.
[13] A. Cooper, S. Singh, S. Hook, J.D.A. Tyndall, A.J. Vernall, Chemical Tools for Studying Lipid-Binding Class A G Protein-Coupled Receptors, Pharmacol Rev, 69 (2017) 316-353.
[14] L.A. Stoddart, L.E. Kilpatrick, S.J. Briddon, S.J. Hill, Probing the pharmacology of G protein-coupled receptors with fluorescent ligands, Neuropharmacology, 98 (2015) 48-57.

[15] L.A. Stoddart, A.J. Vernall, J.L. Denman, S.J. Briddon, B. Kellam, S.J. Hill, Fragment Screening at Adenosine-A3 Receptors in Living Cells Using a Fluorescence-Based Binding Assay, Chem Biol, 19 (2012) 1105-1115.
[16] F. Ciruela, V. Fernandez-Duenas, K.A. Jacobson, Lighting up G protein-coupled purinergic receptors with engineered fluorescent ligands, Neuropharmacology, 98 (2015) 58-67.
[17] J. Joubert, S.V. Dyk, S.F. Malan, Small Molecule Fluorescent Ligands as Central Nervous System Imaging Probes, Mini Rev Med Chem, 13 (2013) 682-696.
[18] A.J. Vernall, L.A. Stoddart, S.J. Briddon, H.W. Ng, C.A. Laughton, S.W. Doughty, S.J. Hill, B. Kellam, Conversion of a non-selective adenosine receptor antagonist into A3-selective high affinity fluorescent probes using peptide-based linkers, Org Biomol Chem, 11 (2013) 5673-5682.
[19] Z. Wu, P. Shao, S. Zhang, M. Bai, Targeted zwitterionic near infrared fluorescent probe for improved imaging of type 2 cannabinoid receptors, J Biomed Opt, 19 (2014) 36006.
[20] S. Zhang, P. Shao, M. Bai, In vivo type 2 cannabinoid receptor-targeted tumor optical imaging using a near infrared fluorescent probe, Bioconjug Chem, 24 (2013) 1907-1916.
[21] R.R. Petrov, M.E. Ferrini, Z. Jaffar, C.M. Thompson, K. Roberts, P. Diaz, Design and evaluation of a novel fluorescent CB2 ligand as probe for receptor visualization in immune cells, Bioorganic Med Chem Lett, 21 (2011) 5859-5862.
[22] M. Sexton, G. Woodruff, E.A. Horne, Y.H. Lin, G.G. Muccioli, M. Bai, E. Stern, D.J. Bornhop, N. Stella, NIR-mbc94, a fluorescent ligand that binds to endogenous CB2 receptors and is amenable to high-throughput screening, Chem Biol, 18 (2011) 563-568.
[23] X. Ling, S. Zhang, P. Shao, W. Li, L. Yang, Y. Ding, C. Xu, N. Stella, M. Bai, A novel near-infrared fluorescence imaging probe that preferentially binds to cannabinoid receptors CB2R over CB1R, Biomaterials, 57 (2015) 169-178.
[24] Z. Wu, P. Shao, S. Zhang, X. Ling, M. Bai, Molecular imaging of human tumor cells that naturally overexpress type 2 cannabinoid receptors using a quinolone-based near-infrared fluorescent probe, J Biomed Opt, 19 (2014) 76016.
[25] S. Zhang, P. Shao, X. Ling, L. Yang, W. Hou, S.H. Thorne, W. Beaino, C.J. Anderson, Y. Ding, M. Bai, In vivo inflammation imaging using a CB2R-targeted near infrared fluorescent probe, Am J Nucl Med Mol Imaging, 5 (2015) 246-258.
[26] M.R. Bell, T.E. D'Ambra, V. Kumar, M.A. Eissenstat, J.L. Herrmann, J.R. Wetzel, D. Rosi, R.E. Philion, S.J. Daum, Antinociceptive (aminoalkyl)indoles, J Med Chem, 34 (1991) 1099-1110.
[27] T.E. D'Ambra, K.G. Estep, M.R. Bell, M.A. Eissenstat, K.A. Josef, S.J. Ward, D.A. Haycock, E.R. Baizman, F.M. Casiano, Conformationally restrained analogs of pravadoline: nanomolar potent, enantioselective, (aminoalkyl)indole agonists of the cannabinoid receptor, J Med Chem, 35 (1992) 124-135.
[28] V.M. Showalter, D.R. Compton, B.R. Martin, M.E. Abood, Evaluation of binding in a transfected cell line expressing a peripheral cannabinoid receptor (CB2): identification of cannabinoid receptor subtype selective ligands, J Pharmacol Exp Ther, 278 (1996) 989-999.
[29] M.M. Aung, G. Griffin, J.W. Huffman, M. Wu, C. Keel, B. Yang, V.M. Showalter, M.E. Abood, B.R. Martin, Influence of the N-1 alkyl chain length of cannabimimetic indoles upon CB(1) and CB(2) receptor binding, Drug Alcohol Depend, 60 (2000) 133-140.
[30] R.A. Ross, H.C. Brockie, L.A. Stevenson, V.L. Murphy, F. Templeton, A. Makriyannis, R.G. Pertwee, Agonist-inverse agonist characterization at CB1 and CB2 cannabinoid receptors of L759633, L759656, and AM630, Br J Pharmacol, 126 (1999) 665-672.
[31] E. Cichero, A. Ligresti, M. Allara, V. di Marzo, Z. Lazzati, P. D'Ursi, A. Marabotti, L. Milanesi, A. Spallarossa, A. Ranise, P. Fossa, Homology modeling in tandem with 3D-QSAR analyses: a computational approach to depict the agonist binding site of the human CB2 receptor, Eur J Med Chem, 46 (2011) 4489-4505.
[32] Y. Shi, Y.-H. Duan, Y.-Y. Ji, Z.-L. Wang, Y.-R. Wu, H. Gunosewoyo, X.-Y. Xie, J.-Z. Chen, F. Yang, J. Li, J. Tang, X. Xie, L.-F. Yu, Amidoalkylindoles as Potent and Selective Cannabinoid Type 2 Receptor Agonists with in Vivo Efficacy in a Mouse Model of Multiple Sclerosis, J Med Chem, 60 (2017) 7067-7083.

[33] J.M. Frost, M.J. Dart, K.R. Tietje, T.R. Garrison, G.K. Grayson, A.V. Daza, O.F. El-Kouhen, L.N. Miller, L. Li, B.B. Yao, G.C. Hsieh, M. Pai, C.Z. Zhu, P. Chandran, M.D. Meyer, Indol-3-yl-tetramethylcyclopropyl ketones: effects of indole ring substitution on CB2 cannabinoid receptor activity, J Med Chem, 51 (2008) 1904-1912.
[34] S. Pasquini, C. Mugnaini, A. Ligresti, A. Tafi, S. Brogi, C. Falciani, V. Pedani, N. Pesco, F. Guida, L. Luongo, K. Varani, P.A. Borea, S. Maione, V. Di Marzo, F. Corelli, Design, synthesis, and pharmacological characterization of indol-3-ylacetamides, indol-3-yloxoacetamides, and indol-3-ylcarboxamides: potent and selective CB2 cannabinoid receptor inverse agonists, J Med Chem, 55 (2012) 5391-5402.
[35] A.S. Yates, S.W. Doughty, D.A. Kendall, B. Kellam, Chemical modification of the naphthoyl 3-position of JWH-015: in search of a fluorescent probe to the cannabinoid CB2 receptor, Bioorganic Med Chem Lett, 15 (2005) 3758-3762.
[36] J.M. Frost, M.J. Dart, K.R. Tietje, T.R. Garrison, G.K. Grayson, A.V. Daza, O.F. El-Kouhen, B.B. Yao, G.C. Hsieh, M. Pai, C.Z. Zhu, P. Chandran, M.D. Meyer, Indol-3-ylcycloalkyl ketones: effects of N1 substituted indole side chain variations on CB(2) cannabinoid receptor activity, J Med Chem, 53 (2010) 295-315.
[37] T. Vasiljevik, L.N. Franks, B.M. Ford, J.T. Douglas, P.L. Prather, W.E. Fantegrossi, T.E. Prisinzano, Design, synthesis, and biological evaluation of aminoalkylindole derivatives as cannabinoid receptor ligands with potential for treatment of alcohol abuse, J Med Chem, 56 (2013) 4537-4550.
[38] M.A. Eissenstat, M.R. Bell, T.E. D'Ambra, E.J. Alexander, S.J. Daum, J.H. Ackerman, M.D. Gruett, V. Kumar, K.G. Estep, E.M. Olefirowicz, J.R. Wetzel, M.D. Alexander, J.D. Weaver, D.A. Haycock, D.A. Luttinger, F.M. Casiano, S.M. Chippari, J.E. Kuster, J.I. Stevenson, S.J. Ward, Aminoalkylindoles: structure-activity relationships of novel cannabinoid mimetics, J Med Chem, 38 (1995) 3094-3105.
[39] T.S. Jiang, G.W. Wang, Synthesis of 3-acylindoles by palladium-catalyzed acylation of free (N-H) indoles with nitriles, Org Lett, 15 (2013) 788-791.
[40] Y. Ma, J. You, F. Song, Facile access to 3-acylindoles through palladium-catalyzed addition of indoles to nitriles: the one-pot synthesis of indenoindolones, Chemistry, 19 (2013) 1189-1193.
[41] A.J. Vernall, L.A. Stoddart, S.J. Briddon, S.J. Hill, B. Kellam, Highly potent and selective fluorescent antagonists of the human adenosine A(3) receptor based on the 1,2,4-triazolo[4,3-a]quinoxalin-1-one scaffold, J Med Chem, 55 (2012) 1771-1782.
[42] L.A. Stoddart, A.J. Vernall, S.J. Briddon, B. Kellam, S.J. Hill, Direct visualisation of internalization of the adenosine A3 receptor and localization with arrestin3 using a fluorescent agonist, Neuropharmacology, 98 (2015) 68-77.
[43] N.L. Grimsey, C.E. Goodfellow, M. Dragunow, M. Glass, Cannabinoid receptor 2 undergoes Rab5-mediated internalization and recycles via a Rab11-dependent pathway, Biochim Biophys Acta, 1813 (2011) 1554-1560.
[44] E.E. Cawston, W.J. Redmond, C.M. Breen, N.L. Grimsey, M. Connor, M. Glass, Real-time characterization of cannabinoid receptor 1 (CB1) allosteric modulators reveals novel mechanism of action, Br J Pharmacol, 170 (2013) 893-907.
[45] M. Soethoudt, U. Grether, J. Fingerle, T.W. Grim, F. Fezza, L. de Petrocellis, C. Ullmer, B. Rothenhäusler, C. Perret, N. van Gils, D. Finlay, C. MacDonald, A. Chicca, M.D. Gens, J. Stuart, H. de Vries, N. Mastrangelo, L. Xia, G. Alachouzos, M.P. Baggelaar, A. Martella, E.D. Mock, H. Deng, L.H. Heitman, M. Connor, V. Di Marzo, J. Gertsch, A.H. Lichtman, M. Maccarrone, P. Pacher, M. Glass, M. van der Stelt, Cannabinoid CB2 receptor ligand profiling reveals biased signalling and off-target activity, Nat. Commun., 8 (2017) 13958.
[46] Y. Liu, Y. Yang, R. Ward, S. An, X.-X. Guo, W. Li, T.-R. Xu, Biased signalling: the instinctive skill of the cell in the selection of appropriate signalling pathways, Biochem. J., 470 (2015) 155-167.
[47] M.S. Ibsen, M. Connor, M. Glass, Cannabinoid CB1 and CB2 Receptor Signaling and Bias, Cannabis Cannabinoid Res, 2 (2017) 48-60.
[48] T. Nevalainen, Recent Development of CB2 Selective and Peripheral CB1/CB2 Cannabinoid Receptor Ligands, Curr Med Chem, 21 (2014) 187-203.

[49] E. Ghosh, P. Kumari, D. Jaiman, A.K. Shukla, Methodological advances: the unsung heroes of the GPCR structural revolution, Nat Rev Mol Cell Biol, 16 (2015) 69-81.
[50] J. Shonberg, R.C. Kling, P. Gmeiner, S. Lober, GPCR crystal structures: Medicinal chemistry in the pocket, Bioorg Med Chem, 23 (2015) 3880-3906.
[51] T. Hua, K. Vemuri, M. Pu, L. Qu, G.W. Han, Y. Wu, S. Zhao, W. Shui, S. Li, A. Korde, R.B. Laprairie, E.L. Stahl, J.-H. Ho, N. Zvonok, H. Zhou, I. Kufareva, B. Wu, Q. Zhao, M.A. Hanson, L.M. Bohn, A. Makriyannis, R.C. Stevens, Z.-J. Liu, Crystal Structure of the Human Cannabinoid Receptor CB_1, Cell, 167 (2016) 750-762.
[52] Z. Shao, J. Yin, K. Chapman, M. Grzemska, L. Clark, J. Wang, D.M. Rosenbaum, High-resolution crystal structure of the human CB1 cannabinoid receptor, Nature, 540 (2016) 602-606.
[53] T. Hua, K. Vemuri, S.P. Nikas, R.B. Laprairie, Y. Wu, L. Qu, M. Pu, A. Korde, S. Jiang, J.-H. Ho, G.W. Han, K. Ding, X. Li, H. Liu, M.A. Hanson, S. Zhao, L.M. Bohn, A. Makriyannis, R.C. Stevens, Z.-J. Liu, Crystal structures of agonist-bound human cannabinoid receptor CB1, Nature, 547 (2017) 468-471.
[54] G. Ragusa, M. Gómez-Cañas, P. Morales, C. Rodríguez-Cueto, M.R. Pazos, B. Asproni, E. Cichero, P. Fossa, G.A. Pinna, N. Jagerovic, J. Fernández-Ruiz, G. Murineddu, New pyridazinone-4-carboxamides as new cannabinoid receptor type-2 inverse agonists: Synthesis, pharmacological data and molecular docking, European Journal of Medicinal Chemistry, 127 (2017) 398-412.
[55] A. Dore, B. Asproni, A. Scampuddu, S. Gessi, G. Murineddu, E. Cichero, P. Fossa, S. Merighi, S. Bencivenni, G.A. Pinna, Synthesis, molecular modeling and SAR study of novel pyrazolo[5,1-f][1,6]naphthyridines as CB2 receptor antagonists/inverse agonists, Bioorg Med Chem, 24 (2016) 5291-5301.
[56] V. Deiana, M. Gómez-Cañas, M.R. Pazos, J. Fernández-Ruiz, B. Asproni, E. Cichero, P. Fossa, E. Muñoz, F. Deligia, G. Murineddu, M. García-Arencibia, G.A. Pinna, Tricyclic pyrazoles. Part 8. Synthesis, biological evaluation and modelling of tricyclic pyrazole carboxamides as potential CB2 receptor ligands with antagonist/inverse agonist properties, European Journal of Medicinal Chemistry, 112 (2016) 66-80.
[57] D.P. Hurst, A. Grossfield, D.L. Lynch, S. Feller, T.D. Romo, K. Gawrisch, M.C. Pitman, P.H. Reggio, A lipid pathway for ligand binding is necessary for a cannabinoid G protein-coupled receptor, J Biol Chem, 285 (2010) 17954-17964.
[58] J. Jakowiecki, S. Filipek, Hydrophobic Ligand Entry and Exit Pathways of the CB1 Cannabinoid Receptor, J Chem Inf Model, 56 (2016) 2457-2466.
[59] L. Martin-Couce, M. Martin-Fontecha, O. Palomares, L. Mestre, A. Cordomi, M. Hernangomez, S. Palma, L. Pardo, C. Guaza, M.L. Lopez-Rodriguez, S. Ortega-Gutierrez, Chemical probes for the recognition of cannabinoid receptors in native systems, Angew Chem Int Ed Engl, 51 (2012) 6896-6899.
[60] B. Milani, E. Alessio, G. Mestroni, A. Sommazzi, F. Garbassi, E. Zangrando, N. Bresciani-Pahor, L. Randaccio, Synthesis and characterization of monochelated carboxylatopalladium(II) complexes with nitrogen-donor chelating ligands. Crystal structures of diacetato(1,10-phenanthroline)- and diacetato(2,9-dimethyl-1,10-phenanthroline)-palladium(II), J Chem Soc Dalton Trans, 0 (1994) 1903-1911.
[61] M.L. Bolognesi, N. Calonghi, C. Mangano, L. Masotti, C. Melchiorre, Parallel Synthesis and Cytotoxicity Evaluation of a Polyamine-Quinone Conjugates Library, J Med Chem, 51 (2008) 5463-5467.
[62] H.Y. Song, M.H. Ngai, Z.Y. Song, P.A. MacAry, J. Hobley, M.J. Lear, Practical synthesis of maleimides and coumarin-linked probes for protein and antibody labelling via reduction of native disulfides, Org Biomol Chem, 7 (2009) 3400-3406.
[63] L.M. Manus, D.J. Mastarone, E.A. Waters, X.-Q. Zhang, E.A. Schultz-Sikma, K.W. MacRenaris, D. Ho, T.J. Meade, Gd(III)-Nanodiamond Conjugates for MRI Contrast Enhancement, Nano Letters, 10 (2010) 484-489.
[64] J.M. McPartland, C. MacDonald, M. Young, P.S. Grant, D.P. Furkert, M. Glass, Affinity and Efficacy Studies of Tetrahydrocannabinolic Acid A at Cannabinoid Receptor Types One and Two, Cannabis Cannabinoid Res, 2 (2017) 87-95.

[65] A. Sali, T.L. Blundell, Comparative protein modelling by satisfaction of spatial restraints, J Mol Biol, 234 (1993) 779-815.
[66] C. Notredame, D.G. Higgins, J. Heringa, T-Coffee: A novel method for fast and accurate multiple sequence alignment, J Mol Biol, 302 (2000) 205-217.
[67] M.D. Hanwell, D.E. Curtis, D.C. Lonie, T. Vandermeersch, E. Zurek, G.R. Hutchison, Avogadro: an advanced semantic chemical editor, visualization, and analysis platform, J Cheminform, 4 (2012) 17.
[68] G. Jones, P. Willett, R.C. Glen, A.R. Leach, R. Taylor, Development and validation of a genetic algorithm for flexible docking, J Mol Biol, 267 (1997) 727-748.

SUPPLEMENTARY MATERIAL

Supplementary Table 1. Affinity of fluorescent conjugates for hCB_2 and hCB_1 receptors.

Compound	K_i hCB_2 (nM ± SEM) [a]	K_i hCB_1 (nM ± SEM) [a]
15a	no binding [b]	n.d. [c]
15c	no binding	n.d.
15b	>10000	n.d.
15d	>10000	n.d.
15e	>10000	n.d.
15f	>10000	n.d.
15g	>10000	n.d.
23	>10000	>10000
26	>10000	>10000

[a] K_i obtained by radioligand binding assays, using 2.5 nM [^{3}H]CP55,940 and transfected HEK cells. SEM = standard error of the mean. Data is from three individual experiments each performed in triplicate. Low affinity compounds that passed D'Agostino & Pearson normality test and showed significant competition with [^{3}H]CP55,940 (as determined by a one sample t-test) were determined to have a K_i value >10000 nM. [b] no significant binding was detected, where compounds showed no significant competition with [^{3}H]CP55,940 as determined by a one sample t-test. [c] n.d. = value was not determined.

Supplementary Table 2: Forskolin stimulated cAMP response in wild type HEK293 cells.

	% response in WT HEK293 cells	
Compound	10 µM ± SEM	1 µM ± SEM
9a	105.2 ± 5.9	101.9 ± 1.8
9c	118.7 ± 3.8 *	101.9 ± 3.2
9d	105.1 ± 4.0	105.9 ± 2.6
9e	109.6 ± 7.7	105.5 ± 3.5
9f	135.3 ± 4.0 *	104.3 ± 2.5
9g	108.1 ± 3.2	95.0 ± 5.0
11c	100.1 ± 6.2	98.8 ± 3.7
11d	102.8 ± 1.8	104.5 ± 3.3
16a	127.6 ± 4.9 *	95.0 ± 3.7
16b	133.9 ± 4.7 *	105.4 ± 2.5
19	160.6 ± 2.6 *	124.3 ± 2.4 *
20	129.1 ± 3.5 *	105.6 ± 3.6
25	128.0 ± 2.7 *	114.8 ± 7.1 *
SR144528	94.5 ± 1.6	99.8 ± 2.2
WIN55,212-2	102.6 ± 2.1	96.1 ± 1.0
CP-55,940	98.0 ± 4.0	99.2 ± 2.7

Assay carried out in wild type HEK 293 cells measuring forskolin-stimulated cAMP. Data is normalised, so that forskolin only response is 100% and vehicle only response is 0%. SEM = standard error of the mean. Data is the mean of three individual experiments each performed in duplicate. A one sample t-test was used to determine if values were significantly different from forskolin only response, and where values are significantly different, they are marked with *.

Representative ^{1}H and ^{13}C NMR spectra of Compound 24

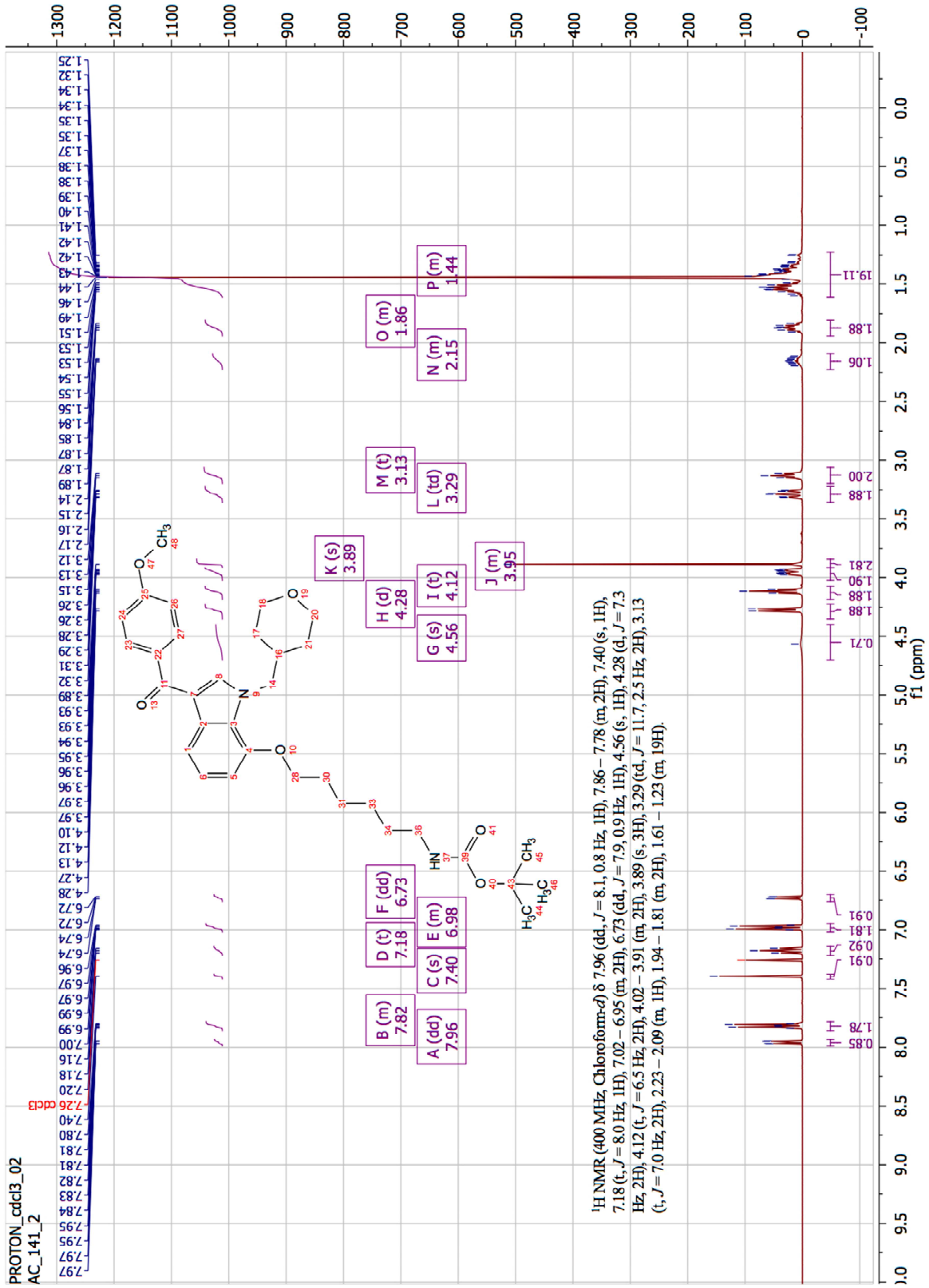

^{1}H NMR (400 MHz, Chloroform-*d*) δ 7.96 (dd, *J* = 8.1, 0.8 Hz, 1H), 7.86 – 7.78 (m, 2H), 7.40 (s, 1H), 7.18 (t, *J* = 8.0 Hz, 1H), 7.02 – 6.95 (m, 2H), 6.73 (dd, *J* = 7.9, 0.9 Hz, 1H), 4.56 (s, 1H), 4.28 (d, *J* = 7.3 Hz, 2H), 4.12 (t, *J* = 6.5 Hz, 2H), 4.02 – 3.91 (m, 2H), 3.89 (s, 3H), 3.29 (td, *J* = 11.7, 2.5 Hz, 2H), 3.13 (t, *J* = 7.0 Hz, 2H), 2.23 – 2.09 (m, 1H), 1.94 – 1.81 (m, 2H), 1.61 – 1.23 (m, 19H).

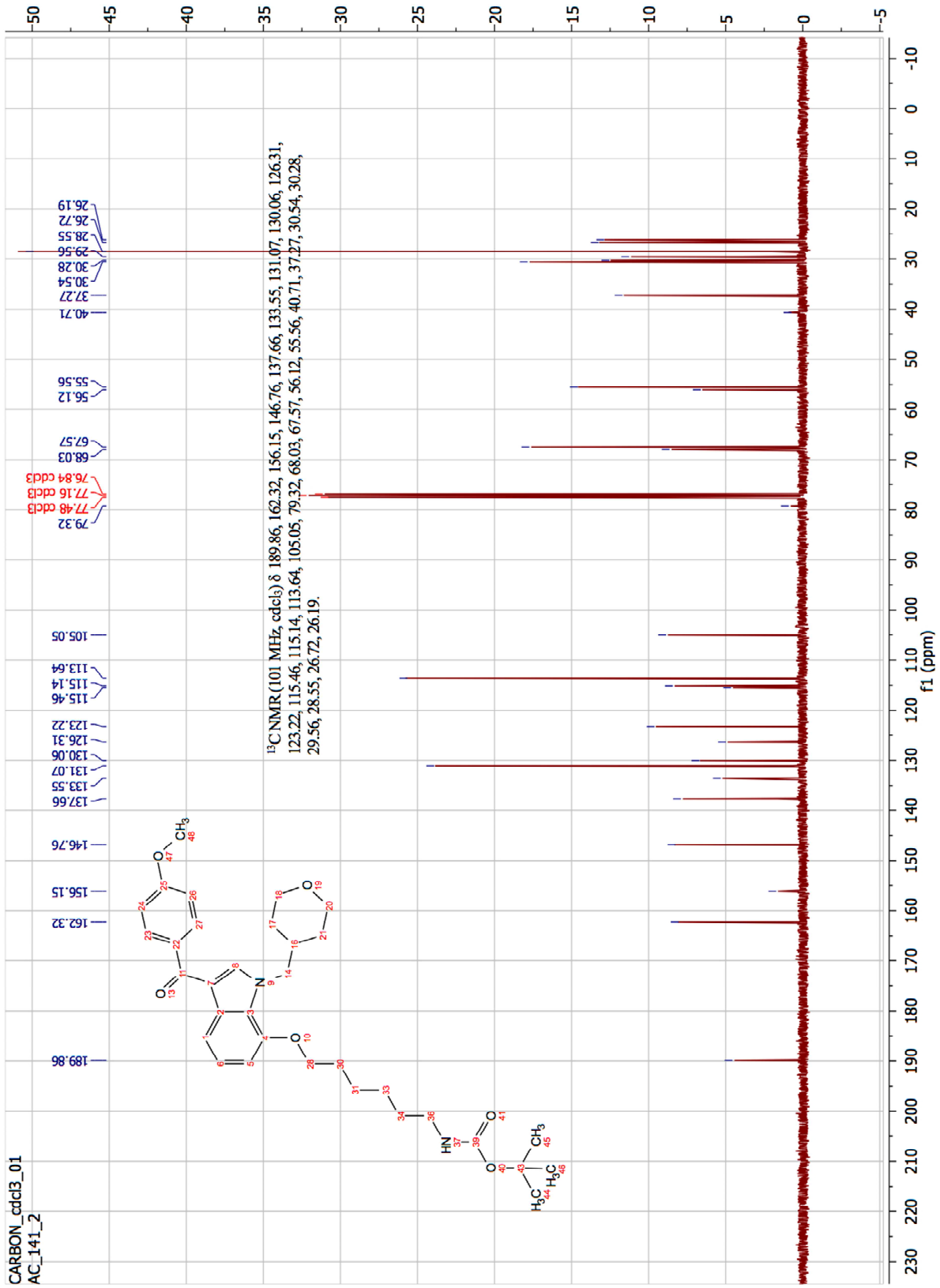
CARBON_cdcl3_01
AC_141_2
^{13}C NMR (101 MHz, cdcl$_3$) δ 189.86, 162.32, 156.15, 146.76, 137.66, 133.55, 131.07, 130.06, 126.31, 123.22, 115.46, 115.14, 113.64, 105.05, 79.32, 68.03, 67.57, 56.12, 55.56, 40.71, 37.27, 30.54, 30.28, 29.56, 28.55, 26.72, 26.19.
f1 (ppm)

Highlights

- A C7-long linker aminoalkyl indole is a promising lead for a fluorescent probe.
- A new high affinity, selective CB2 receptor inverse agonist was discovered.
- Aminoalkyl indoles modified at C5 predominantly acted as agonists at CB2 receptor.
- Aminoalkyl indoles modified at C7 predominantly acted as inverse agonists.